UNIVERSITY OF KRAGUJEVAC

FACULTY OF ENGINEERING
&
FACULTY OF MEDICINE
UNIVERSITY OF KRAGUJEVAC

Lemana Spahić

MULTISCALE MODEL FOR THROMBOSIS / ATHEROSCLEROTIC PLAQUE FORMATION AND PROGRESSION

Doctoral dissertation

Kragujevac, 2024.

Author
Name and surname: Lemana Spahic
Date and place of birth: 30.09.1996. Žepče (Bosnia and Herzegovina)
Current employment: Early Stage Researcher, BioIRC Kragujevac
Doctoral Dissertation
Title: Multiscale model for thrombosis/atherosclerotic plaque formation and progression
No. of pages: 134
No. of images: 40
No. of bibliographic data: 175
Institution and place of work: Research and Development Center for Bioengineering BioIRC, Kragujevac, Serbia
Scientific area (UDK): bioengineering
Mentor: Prof. Dr. Nenad Filipovic, Professor, Faculty of Engineering, University of Kragujevac
Topic Application Date:
18.10.2023.
Decision number and date of acceptance of the doctoral dissertation topic:
IV-07-640/4 from 16.9.2024.

Acknowledgements

When I think about gratitude, I think about all the incredible people who have been a part of this journey and contributed to its success. First and foremost, I would like to express my sincere thanks to my mentor, Prof. Dr. Nenad Filipović, for his invaluable guidance, unwavering support, and patience throughout this process. His ability to listen to my ideas and engage in productive discussions over the past two years has been instrumental in shaping this dissertation and my professional growth.

I am deeply grateful to Prof. Dimitrios Fotiadis and Prof. Giancarlo Pennati for their hospitality and support durring my secondments at University of Ioannina and Politecnico di Milano. Some of the greatest milestones of my research happened exactly at Ioannina and Milano and I will forever keep fond memories about my stay there.

I am deeply grateful to the entire team at BioIRC and the University of Kragujevac for their exceptional support during my time here. Your encouragement and collaboration created an environment where I could thrive both academically and personally. To my office colleagues, who quickly became dear friends, thank you for making me feel welcome and an integral part of the team. Your company turned countless hours of work into a truly enjoyable experience. I sincerely hope that this is not the end of our journey together but a foundation for future collaborations.

A special acknowledgment goes to my fellow Early Stage Researchers (ESRs) from the MSCA DECODE project. Sharing this journey with you has been a privilege and an inspiration. The challenges we overcame together, the shared experiences across countries, and the memories we created have left an indelible mark on my life. You have made this experience truly enriching and unforgettable.

A special thank you to my mother, whose unwavering love and support have been my anchor throughout my life. Mom, your sacrifices, wisdom, and strength have been the greatest source of inspiration for me. You have taught me the value of resilience, perseverance, and kindness, and I owe so much of who I am today to you. Thank you for believing in me, even when I doubted myself, and for always being there to lift me up.

To my family—my grandma, my uncle, and my little brother Aldin—thank you for being my pillars of strength. Your constant encouragement, care, and love have been a source of comfort and motivation. Aldin, your enthusiasm and curiosity were a constant reminder to approach life with a sense of wonder and determination.

Side by side or miles apart, sisters will always be connected by the heart! Thank you Džana for being there for me throughout this adventure.

Finally, I would like to thank everyone who, in one way or another, contributed to this project and my development as a researcher. To all the friends, mentors, and collaborators who made this journey memorable and impactful, I am forever grateful.

Mom, grandma, uncle, Aldin,

This one is for you!

Abstract

Cardiovascular diseases, particularly atherosclerosis, remain leading causes of morbidity and mortality worldwide, necessitating innovative approaches for early detection, risk stratification, and management. This research explores the application of advanced computational techniques—artificial intelligence (AI) and agent-based modeling (ABM)—to address the complexities of atherosclerosis progression. AI, leveraging machine learning and deep learning algorithms, has demonstrated significant potential in analyzing large-scale datasets, including electronic health records, medical imaging, and genetic profiles, to predict disease onset and progression with greater accuracy than traditional methods. Concurrently, ABM offers insights into the intricate biological interactions within the cardiovascular system by simulating the behaviors of individual agents, such as cells and tissues, in response to various stimuli. However, both methodologies present limitations, including challenges related to data quality, model interpretability, and the complexity of biological systems.

This research underscores the need for interdisciplinary collaboration between computational scientists, clinicians, and engineers to refine these models and facilitate their integration into clinical practice. Sensitivity analysis was conducted on the developed ABM model and a virtual population was created from the data in order to develop as surrogate model based on AI. The dataset captured a landscape of patient-specific variability and provided significant variation for the model to learn. The surrogate model for atherosclerotic plaque progression was based on artificial neural networks and deep learning and performed with 90.9% accuracy and congruency with the ABM indicating its strong potential to be used in practice.

By addressing their inherent limitations, AI and ABM hold the potential to revolutionize cardiovascular medicine, leading to more personalized and effective treatments. Future research directions include improving data integration, enhancing model transparency, and conducting real-world validation studies to translate computational insights into meaningful clinical outcomes. The findings of this study contribute to the growing body of evidence supporting the role of ABM andAI surrogate modeling in advancing our understanding of cardiovascular diseases. The potential of ABM modeling backed with decreasing of computational resources necessary and enhanced speed of decission making ensured by surrogate modeling offers promising pathways for better patient care and disease management.

Keywords: atherosclerosis, plaque progression, multiscale modeling, agent-based modeling, artificial intelligence

Saжetak istraživanja

Кардиоваскуларне болести, нарочито атеросклероза, и даље су водећи узроци морбидитета и морталитета широм света, што захтева иновативне приступе за рано откривање, стратификацију ризика и управљање болестима. Ово истраживање истражује примену напредних рачунарских техника—вештачке интелигенције (AI) и моделирања заснованог на агентима (ABM)—у решавању комплексности прогресије атеросклерозе. Вештачка интелигенција, користећи алгоритме машинског и дубоког учења, показала је значајан потенцијал у анализи великих скупова података, укључујући електронске здравствене записе, медицинске слике и генетске профиле, за прецизније предвиђање појаве и прогресије болести од традиционалних метода. Истовремено, ABM пружа увид у сложене биолошке интеракције унутар кардиоваскуларног система симулирајући понашање појединачних агената, попут ћелија и ткива, као одговор на различите стимулусе. Међутим, обе методологије имају ограничења, укључујући изазове везане за квалитет података, интерпретабилност модела и сложеност биолошких система.

Ово истраживање истиче потребу за интердисциплинарном сарадњом између рачунарских научника, клиничара и инжењера ради унапређења ових модела и њихове интеграције у клиничку праксу. Спроведена је анализа осетљивости на развијеном ABM моделу, а из података је креирана виртуелна популација ради развоја сурогат модела заснованог на вештачкој интелигенцији. Скуп података је обухватио спектар варијабилности специфичне за пацијенте и обезбедио значајну варијацију за учење модела. Сурогат модел за прогресију атеросклеротичних плакова заснован је на вештачким неуронским мрежама и дубоком учењу и постигао је тачност од 90,9% и усклађеност са ABM, што указује на његов велики потенцијал за практичну примену.

Уз превазилажење урођених ограничења, AI и ABM имају потенцијал да револуционишу кардиоваскуларну медицину, водећи ка персонализованијим и ефикаснијим третманима. Будући правци истраживања укључују унапређење интеграције података, побољшање транспарентности модела и спровођење студија валидизације у стварном свету ради претварања рачунарских увида у значајне клиничке резултате. Налази овог истраживања доприносе растућој бази доказа који подржавају улогу ABM и AI сурогат моделирања у унапређењу нашег разумевања кардиоваскуларних болести. Потенцијал ABM моделирања, подржан смањењем потребних рачунарских ресурса и убрзањем доношења одлука захваљујући сурогат моделирању, нуди обећавајуће путеве за бољу негу пацијената и управљање болестима.

Кључне речи: атеросклероза, прогресија плака, вишескално моделирање, моделирање засновано на агентима, вештачка интелигенција

Contents

List of figures

List of Tables

1. Introduction

Atherosclerosis is a chronic, progressive disease characterized by the buildup of plaques within the arterial walls, leading to reduced blood flow and increasing the risk of severe cardiovascular events such as heart attack, stroke, and peripheral artery disease. As a leading cause of morbidity and mortality worldwide, atherosclerosis is responsible for a significant proportion of deaths related to cardiovascular disease (CVD), which remains the leading global cause of death. Despite advances in prevention, diagnosis, and treatment, the burden of atherosclerosis continues to rise, driven by factors such as aging populations, sedentary lifestyles, and an increase in metabolic disorders, including obesity, diabetes, and hypertension.

The pathophysiology of atherosclerosis is complex, involving a combination of endothelial dysfunction, lipid accumulation, inflammatory processes, and cellular responses within the arterial wall. These interactions result in the formation and growth of atheromatous plaques, which can become unstable, leading to plaque rupture and thrombosis. Early detection and accurate risk stratification are critical for preventing the progression of the disease and reducing the likelihood of life-threatening complications.

However, conventional diagnostic methods, such as clinical risk scores and medical imaging techniques, often fall short in identifying subtle or early-stage disease, making it difficult to intervene before significant damage occurs. Additionally, the multifactorial nature of atherosclerosis, with contributions from genetic, environmental, and lifestyle factors, presents a substantial challenge for personalized treatment approaches. In light of these challenges, there is a growing need for novel methodologies that can capture the complexity of the disease and enhance our ability to predict its progression.

1.1. Subject and aim of this dissertation

The subject of this doctoral dissertation is the development of an advanced model for predicting the progression of atherosclerotic plaque in peripheral arteries, utilizing sophisticated computational methods such as Artificial Intelligence (AI), agent-based modeling (ABM), and finite element analysis (FEA). Atherosclerosis in peripheral arteries is a major contributor to peripheral artery disease (PAD), a serious global health concern that can lead to severe complications, including chronic pain, tissue ischemia, and, in advanced cases, gangrene or limb amputation. Moreover, PAD is closely associated with systemic atherosclerosis, significantly increasing the risk of major cardiovascular events such as heart attacks and strokes. The ability to accurately predict plaque progression and intervene early is therefore crucial for improving patient outcomes.

The primary goal of this research is to develop a predictive application that models the behavior of atherosclerotic plaque in arteries. This tool will integrate AI, ABM, and FEA to provide a powerful platform for clinicians and researchers to predict disease progression and manage high-risk patients. The application will be embedded within the DECODE platform, a comprehensive computational project aimed at advancing the diagnosis and treatment of cardiovascular diseases. This research focuses on creating a data-driven model that simulates the biological, mechanical, and hemodynamic factors influencing plaque progression, thereby enhancing our ability to predict its trajectory in arteries.

Atherosclerosis, characterized by the buildup of lipid-rich plaques within arterial walls, restricts blood flow and poses a significant risk for cardiovascular complications.

Peripheral artery disease affects the arteries of the legs and arms, leading to conditions such as claudication, where muscle pain is caused by insufficient blood flow during exercise, and in severe cases, critical limb ischemia and the potential for limb amputation. Despite the availability of diagnostic tools such as ultrasound, CT angiography, and magnetic resonance imaging (MRI), current clinical methods fall short in predicting how plaques will evolve over time. This gap underscores the need for advanced models that leverage cutting-edge technologies to improve predictions.

In combination with ABM, which provides detailed simulations of cellular and molecular interactions during plaque formation, AI adds a layer of predictive power by learning from vast datasets and making high-accuracy predictions about future plaque behavior. The integration of AI into this modeling framework is crucial because it allows for real-time analysis and prediction based on continuously updated patient data, enabling personalized treatment strategies. AI will not only assist in risk stratification but also guide therapeutic decisions, potentially identifying the optimal intervention points to prevent adverse outcomes such as plaque rupture or total arterial occlusion.

ABM offers a complementary approach by simulating the complex biological processes at play in atherosclerosis, such as the interactions between endothelial cells, smooth muscle cells, and inflammatory cells in the arterial walls. By creating a virtual environment where these "agents" interact over time, ABM allows researchers to model the dynamic progression of plaques in response to both biological stimuli (e.g., inflammation, lipid deposition) and mechanical forces (e.g., blood flow-induced shear stress). This agent-based approach is particularly valuable for exploring "what-if" scenarios, where different intervention strategies can be tested to determine their effect on plaque progression.

This interdisciplinary approach not only enhances the precision of predictions but also provides a personalized aspect to the treatment of atherosclerosis. For instance, AI can continuously learn from new patient data, improving its predictions over time, while ABM and FEA simulate the biological and mechanical factors at play. Such a tool has the potential to significantly improve clinical decision-making by offering tailored predictions of plaque growth and rupture risk, leading to earlier and more effective treatments.

1.2. Starting hypotheses

The main hypotheses of the doctoral dissertation, derived from the research goal, the candidate's previous research activities, and the results of other authors in the field of research, consist of the following assumptions:

- It is possible to create artificial intelligence networks for predicting the behavior of relevant parameters for plaque progression.
- It is possible to create an ABM (agent-based modeling) model for modeling plaque progression and the interaction of drugs delivered directly into the artery.
- It is possible to create an application for displaying a 3D model of the peripheral artery and the plaque within it.
- It is possible to create a module as a part of DECODE platform API for real deformations within the ABM, thereby achieving realistic behavior of the artery and atherosclerotic plaque as deformable bodies.

1.3. Thesis structure

In **Chapter 1**, the subject and objectives of the dissertation are defined, including the initial hypotheses and the contributions of the dissertation.

Chapter 2 explains the anatomy of the cardiovascular system, covering blood vessels and the structure of arteries, with a particular focus on peripheral arteries. It also discusses the function and mechanics of blood flow through the cardiovascular system. Atherosclerosis is introduced as a significant health concern. The causes, progression, and complications of atherosclerosis are discussed, highlighting the importance of understanding its impact on cardiovascular health.

Chapter 3 delves into artery biomechanics, explaining the mechanical forces acting on arterial walls and their role in the development and progression of atherosclerosis. The interaction between arterial structure and plaque formation is emphasized. Subsequently, the diagnostic methods for atherosclerosis, including imaging techniques such as ultrasound, angiography, and magnetic resonance imaging, are explored. The role of these technologies in early detection and ongoing monitoring of plaque progression is discussed as well as current treatment methods for atherosclerosis, both surgical and pharmacological, are reviewed. The effectiveness of different interventions is evaluated, with an emphasis on the need for improved treatment approaches. Bioengineering applications in cardiovascular medicine, highlighting the role of computational models in understanding atherosclerosis are presented next. The chapter discusses the use of Finite Element Analysis (FEA) in predicting plaque behavior and disease progression. Agent-Based Modeling (ABM) is introduced as a novel method for simulating the progression of atherosclerosis. The state-of-the-art in ABM applications for cardiovascular diseases is reviewed, with a focus on its potential to improve patient outcomes. Subsequently, applications of Artificial Intelligence (AI) in cardiovascular medicine, explaining how AI-based decision support systems are transforming diagnosis and treatment. The role of AI in analyzing complex datasets and improving clinical decision-making is explored.

Chapter 4 presents experimental research on atherosclerotic plaque progression, describing the integration of ABM and FEA models. This chapter explains the coupling of computational fluid dynamics with ABM for a more comprehensive understanding of plaque dynamics. Sensitivity analysis of ABM parameters is conducted to evaluate the robustness and reliability of the model in predicting plaque progression under different conditions. Finally a surrogate model is developed to streamline computational analysis, reducing the time and resources needed for predicting plaque progression while maintaining accuracy. The process of dataset curation is detailed, outlining the methods used to collect, retrieve, and preprocess data for model training and validation, development and implementation of the Artificial Neural Network (ANN) model, designed to predict plaque progression based on patient-specific data detailed and performance of the ANN model evaluated. A comparative analysis of the developed models with existing research in the field, assessing the improvements and contributions of this work to cardiovascular medicine is presented. Finally, the integration into DECODE cloud platform via an API is explained.

Chapter 7 presents the conclusions of the dissertation, summarizing the research findings, contributions to science and medicine, and directions for future research.

The final chapter contains the list of references.

The final chapter is followed by the candidate's biography and mandatory statements.

2. Cardiovascular system

The cardiovascular system, composed of the heart and an extensive network of blood vessels, functions as the body's primary transport mechanism, delivering oxygen and essential nutrients to tissues and removing metabolic waste products (Figure 1. Human cardiovascular systemFigure 1) (Bădilă et al., 2017). This system is fundamental to maintaining homeostasis and ensuring the proper functioning of organs and tissues. A comprehensive understanding of the physiology and biomechanics of the cardiovascular system is crucial for elucidating the mechanisms underlying cardiovascular diseases, particularly thrombosis and atherosclerosis. These conditions are major contributors to morbidity and mortality worldwide, necessitating detailed investigation and innovative therapeutic approaches (Cameron et al., 2020).

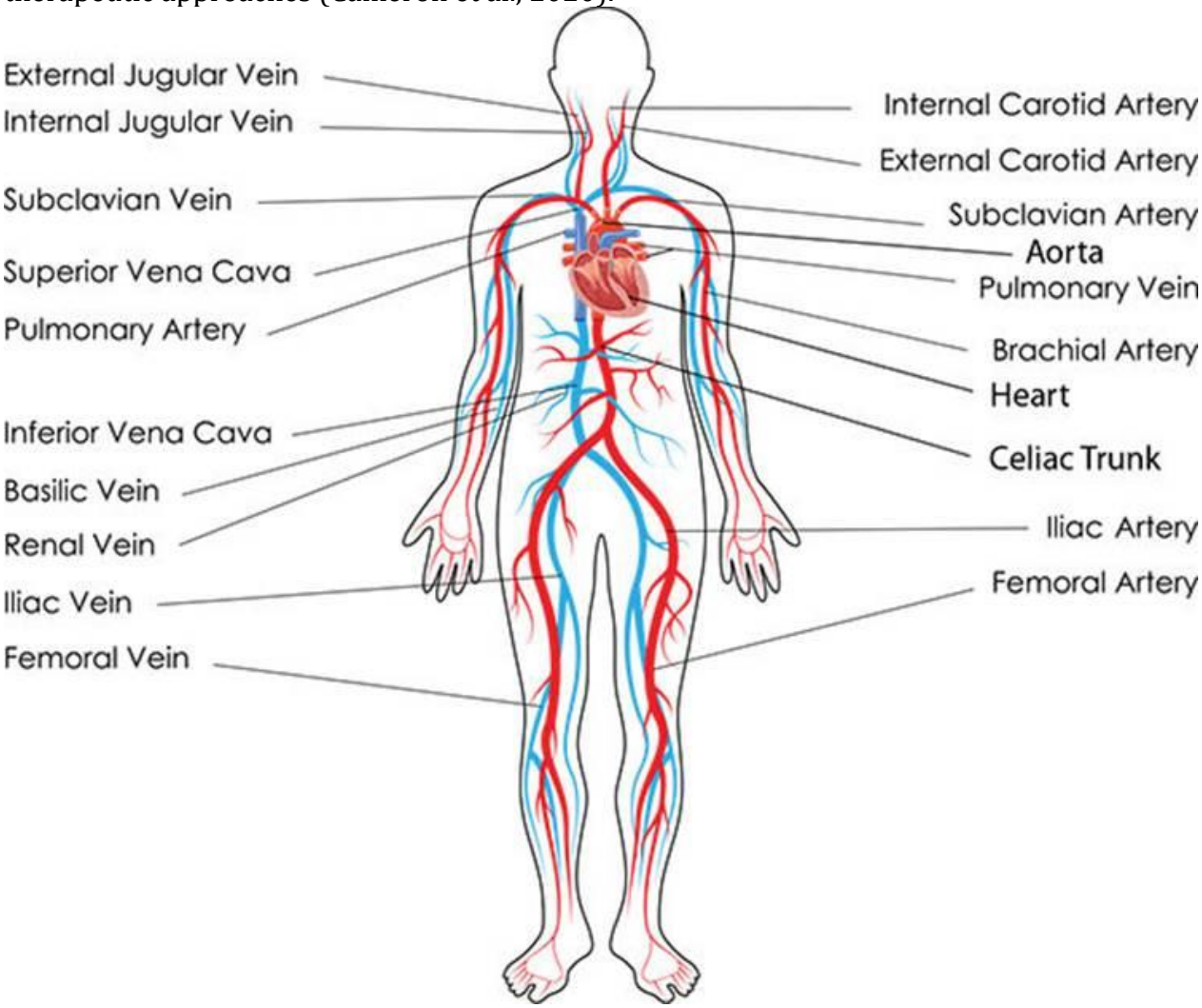

Figure 1. Human cardiovascular system (Online resource 1)

The heart serves as the „pump“ of the cardiovascular system and is divided into four chambers: two atria and two ventricles. These chambers are separated by septa, with the interatrial septum dividing the atria and the interventricular septum separating the ventricles. The chambers work in a highly coordinated manner to ensure the unidirectional flow of blood (Figure 2).

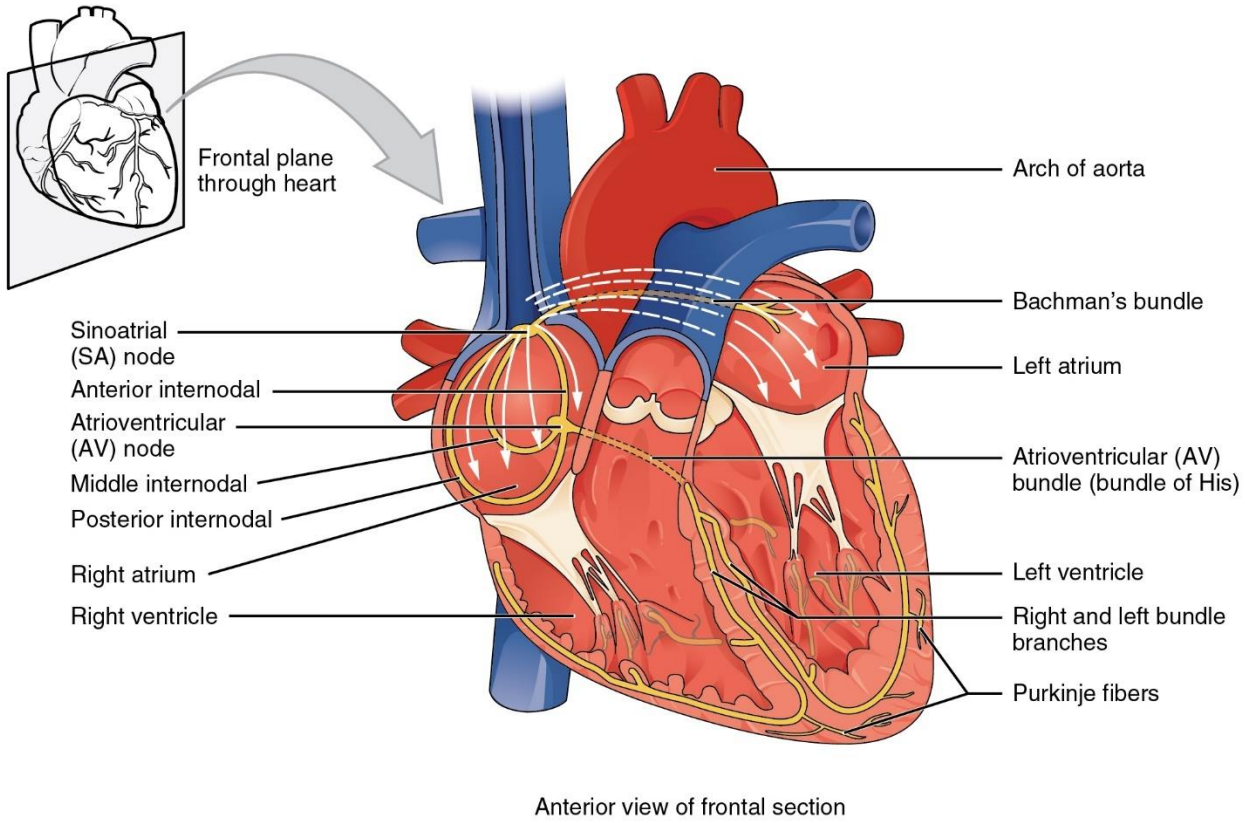

Figure 2. Heart physiology (Online resource 2)

The right atrium is the upper right chamber that receives deoxygenated blood from the body through two large veins: the superior vena cava and the inferior vena cava. The superior vena cava drains blood from the upper part of the body, including the head and arms, while the inferior vena cava carries blood from the lower regions. The right atrium also receives blood from the coronary sinus, which drains deoxygenated blood from the heart's own circulation (Hall and Hall, 2020). Blood then flows from the right atrium into the right ventricle through the tricuspid valve, which prevents backflow during ventricular contraction. The right ventricle, with its relatively thin walls, pumps blood into the pulmonary circulation through the pulmonary valve and into the pulmonary artery. This artery branches into left and right pulmonary arteries that carry deoxygenated blood to the lungs for gas exchange. In the lungs, blood travels through capillaries surrounding the alveoli where carbon dioxide is exchanged for oxygen. This oxygen-rich blood then returns to the heart via four pulmonary veins, entering the left atrium. Unlike other veins in the body, pulmonary veins carry oxygenated blood. The left atrium receives oxygenated blood from the lungs. This blood then passes through the mitral valve, which prevents backflow, into the left ventricle. The mitral valve, also known as the bicuspid valve, has two cusps and is structurally more robust than the tricuspid valve due to the higher pressures in the left side of the heart. The left ventricle, with its thick muscular walls, is the most powerful chamber of the heart. It must generate sufficient force to propel blood through the systemic circulation. Blood is ejected from the left ventricle into the aorta through the aortic valve. The aorta is the largest artery in the body and distributes oxygenated blood to all parts of the body via the systemic circulation. The heart valves ensure unidirectional blood flow and prevent backflow during the cardiac cycle. The tricuspid and mitral valves, located between the atria and ventricles, are known as atrioventricular valves. The pulmonary and aortic valves, located at the exits

of the right and left ventricles respectively, are known as semilunar valves. These valves open and close in response to pressure changes during the cardiac cycle, maintaining efficient circulation.
The cardiac cycle comprises two main phases: diastole and systole. During diastole, the heart muscle relaxes, and the chambers fill with blood. The atrioventricular valves are open, allowing blood to flow from the atria to the ventricles. During systole, the heart muscle contracts, the atrioventricular valves close to prevent backflow, and the semilunar valves open to allow blood to be ejected into the pulmonary artery and aorta. The heart's ability to contract rhythmically is regulated by its intrinsic electrical conduction system. The sinoatrial (SA) node, located in the right atrium, acts as the natural pacemaker, generating electrical impulses that spread through the atria, causing them to contract. The impulses then reach the atrioventricular (AV) node, which delays the signal before transmitting it to the ventricles via the bundle of His and Purkinje fibers. This delay ensures that the atria have time to fully contract and empty their blood into the ventricles before ventricular contraction begins (Hall and Hall, 2020).

2.1. Blood vessels

The blood vessels are classified into three primary types: arteries, veins, and capillaries (Figure 3). Arteries carry the blood away from the heart and are characterized by thick, elastic walls that can withstand high pressure. Veins return blood to the heart and have thinner walls and valves that prevent backflow, facilitating the low-pressure return of blood. Capillaries are microscopic vessels where the exchange of gases, nutrients, and waste products occurs between the blood and tissues (Silverthorn, 2020).

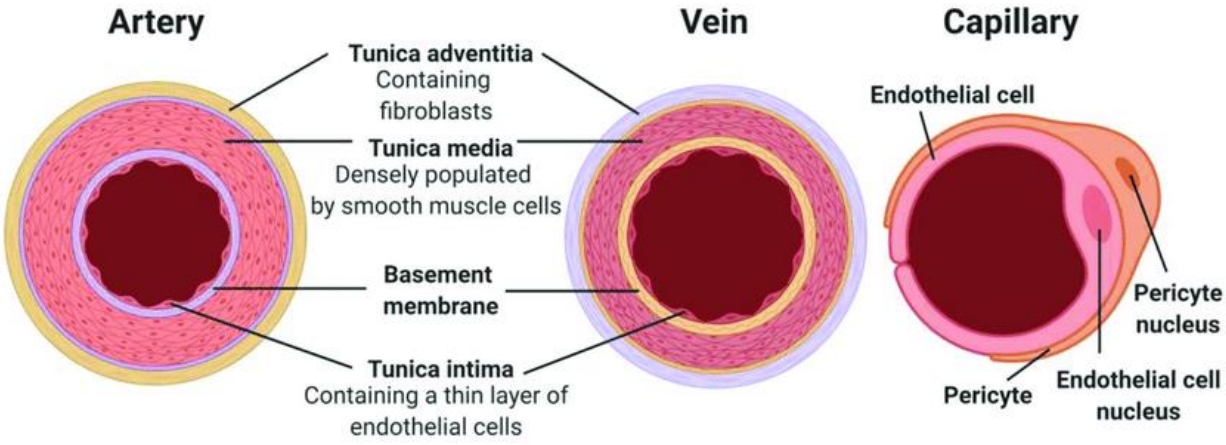

Figure 3. Artery, vein and capilary structure(Jouda et al., 2022)

Arteries are blood vessels that carry blood away from the heart. They are characterized by their thick, elastic walls, which are designed to withstand and accommodate the high pressure generated by the heart's pumping action. The walls of arteries consist of three layers: the tunica intima, tunica media, and tunica adventitia.

Tunica intima is the innermost layer is composed of a single layer of endothelial cells that provides a smooth surface for blood flow and is crucial for vascular homeostasis. It consists of the epithelium, the innermost layer composed of a single layer of flattened endothelial cells that form a smooth lining that reduces friction as blood flows through the vessel followed by a subendothelial layer that consists of loose connective tissue that

provides structural support and the internal elastic lamina, a well-defined layer of elastic fibers that provides flexibility and allows the vessel to stretch and recoil.

Tunica Media is the middle layer that is the thickest and contains smooth muscle cells and elastic fibers. This layer is responsible for the contractility and elasticity of the artery, allowing it to expand and recoil with each heartbeat. It consists of smooth muscle cells arranged in concentric layers that control the diameter of the artery through contraction and relaxation, which regulates blood pressure and flow. Elastic fibers of tunica media are interspersed among the smooth muscle cells and provide the artery with the ability to stretch and recoil with the pulsatile flow of blood followed by the external elastic lamina present in larger arteries for additional elasticity.

Tunica adventita, also known as the tunica externa is the outer layer composed of connective tissue that provides structural support and protection to the artery. Its outermost layer is made up of connective tissue, primarily collagen fibers, which anchor the artery to surrounding tissues and provide structural integrity. Vasa vasorum are small blood vessels that supply blood to the walls of large arteries and nervi vasorum are nerves that innervate the blood vessel wall, particularly influencing the smooth muscle tone (Silverthorn, 2020).

Arteries can be categorized into several types based on their size, structure, and function, each playing a unique role in maintaining hemodynamic stability. Elastic arteries are the largest arteries in the body, including the aorta and its major branches, such as the brachiocephalic, common carotid, and subclavian arteries. These arteries have a substantial amount of elastic tissue in their walls, particularly in the tunica media, which allows them to stretch and recoil with each heartbeat. This elasticity is vital for dampening the pulsatile nature of blood flow generated by the heart and ensuring a smooth, continuous flow of blood throughout the arterial system. Key functions of elastic arteries include acting as a pressure reservoir by expanding to accommodate the surge of blood while, during diastole, they recoil, maintaining pressure and propelling blood forward, followed by pressure dampening by smoothing out the pressure variations from the heart, providing a more consistent blood flow to the smaller arteries and arterioles.

The brachiocephalic, common carotid, and subclavian arteries are responsible for delivering blood to the head, neck, and upper limbs, playing a crucial role in maintaining adequate circulation to these vital areas. Each of these arteries has distinct anatomical features, specific functions, and important clinical relevance. The brachiocephalic artery, also known as the brachiocephalic trunk, is one of the three major branches that originate from the aortic arch. It is unique in that it is the only one of these branches to bifurcate, providing a critical blood supply pathway to the right side of the head and neck and the right upper limb. The brachiocephalic artery travels upward until it divides into the right common carotid artery and the right subclavian artery. This bifurcation occurs at the level of the right sternoclavicular joint. The common carotid arteries are vital for supplying blood to the head and neck. There are two common carotid arteries, the right common carotid artery, which originates from the brachiocephalic artery, and the left common carotid artery, which directly branches off the aortic arch. The subclavian arteries are major arteries that supply blood to the upper limbs. The right subclavian artery branches off from the brachiocephalic artery, while the left subclavian artery directly originates from the aortic arch.

Muscular arteries are medium-sized arteries that distribute blood to specific organs and tissues. Examples include the radial, femoral, and coronary arteries. Unlike elastic arteries, muscular arteries have a thicker tunica media composed mainly of smooth muscle cells, which gives them greater control over blood flow through vasoconstriction and vasodilation. Their key functions include blood distribution as they direct blood to various parts of the body based on the body's needs and regulation of blood flow and pressure as their muscular walls can contract or relax to regulate the amount of blood flowing to different tissues, maintaining systemic blood pressure.

The coronary arteries are a unique subset of muscular arteries with the crucial task of supplying blood to the heart muscle, or myocardium. Their structure and function are finely adapted to meet the heart's high metabolic demands, ensuring that the myocardium receives a continuous and adequate supply of oxygen and nutrients. Given the heart's role as the central pump of the circulatory system, maintaining the health and functionality of the coronary arteries is essential for overall cardiovascular health. The coronary arteries are strategically positioned to optimize blood delivery to the heart muscle (Figure 4). They originate from the base of the aorta, just above the aortic valve, ensuring they receive the freshest, most oxygen-rich blood immediately after it is pumped from the left ventricle. The left coronary artery (LCA) quickly bifurcates into two major branches, the left anterior descending (LAD) artery that travels down the front of the heart, supplying blood to the front and bottom of the left ventricle and the front of the septum, the circumflex artery that encircles the heart muscle, providing blood to the outer side and back of the heart. The right coronary artery (RCA) runs along the right side of the heart and primarily supplies the right atrium, right ventricle, and parts of the bottom portion of both the left ventricle and the septum and branches into the posterior descending artery (PDA) which supplies the back of the heart. The coronary arteries are integral to the heart's performance. By providing a continuous supply of oxygen and essential nutrients, they ensure the myocardium maintains its vigorous contractile function. This is especially critical during periods of increased physical activity when the heart's demand for oxygen escalates (Silverthorn, 2020).

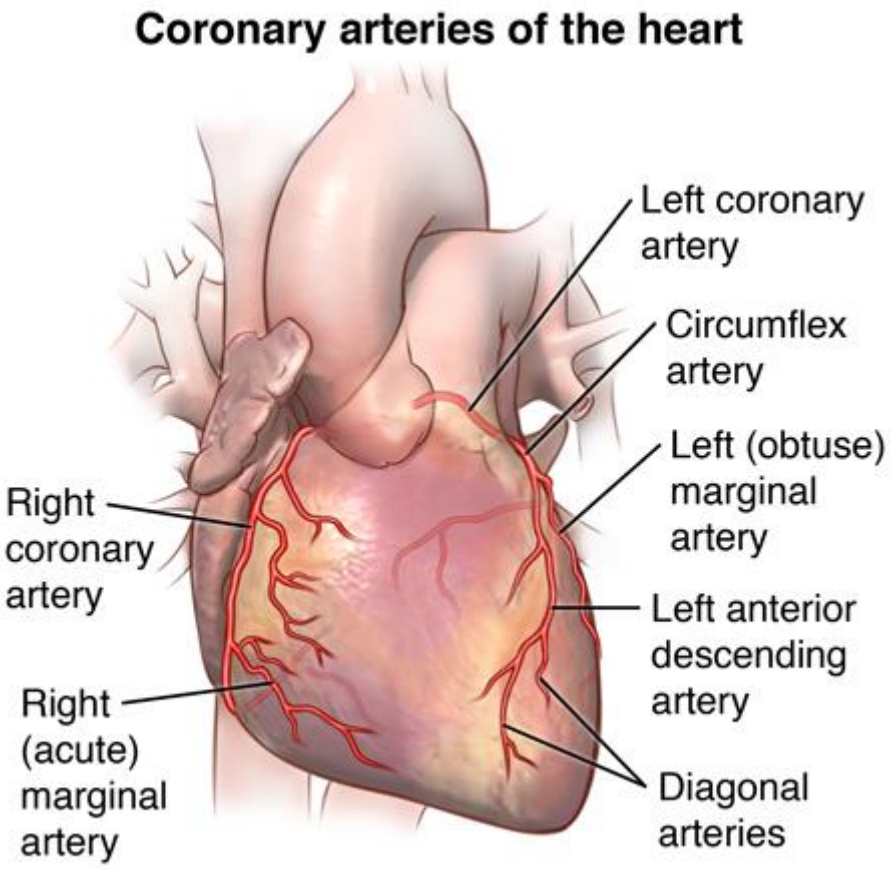

Figure 4. Coronary arteries (Online resources 3)

Peripheral arteries encompass all arteries outside the heart and brain, with a primary role in supplying blood to the limbs and peripheral organs. These arteries are crucial for maintaining the health and functionality of various tissues throughout the body. Key examples of peripheral arteries include the femoral, popliteal, and iliac arteries, each of which plays a vital role in the vascular system. Peripheral arteries are characterized by their extensive branching and distribution, ensuring comprehensive blood supply to the extremities and peripheral organs. The femoral artery is a major blood vessel in the thigh and the main arterial supply to the lower limb. It continues from the external iliac artery and branches into the deep femoral artery, which supplies blood to the deep structures of the thigh. The femoral artery continues with the popliteal artery which runs through the popliteal fossa (behind the knee) and branches into the anterior and posterior tibial arteries, supplying blood to the lower leg and foot. The common iliac arteries branch from the aorta and further divide into the internal and external iliac arteries. The internal iliac arteries supply the pelvic organs, while the external iliac arteries continue as the femoral arteries to supply the lower limbs.
Peripheral arteries are essential for delivering oxygenated blood to tissues throughout the body, supporting various physiological functions necessary for maintaining homeostasis and overall health.

Arteries branch into smaller vessels known as arterioles, which regulate blood flow into capillary beds through the contraction and relaxation of smooth muscle cells. This process is crucial for controlling blood pressure and directing blood flow to specific tissues based

on their metabolic needs. They have a thin tunica media composed of one or two layers of smooth muscle cells.

2.2. Atherosclerosis

Atherosclerosis of the coronary arteries is a chronic, progressive condition characterized by the buildup of plaque within the arterial walls. Coronary artery disease (CAD), more specifically coronary atherosclerosis (CATS), is one of the leading causes of death worldwide, accounting for approximately 17.9 million deaths annually (Su et al., 2023). It is a condition marked by the accumulation of plaque on the artery wall, which is made up of fat, cholesterol, calcium, and other components. This causes arteries to gradually narrow, eventually occluding and preventing blood flow (Libby et al., 2011) (Figure 5).

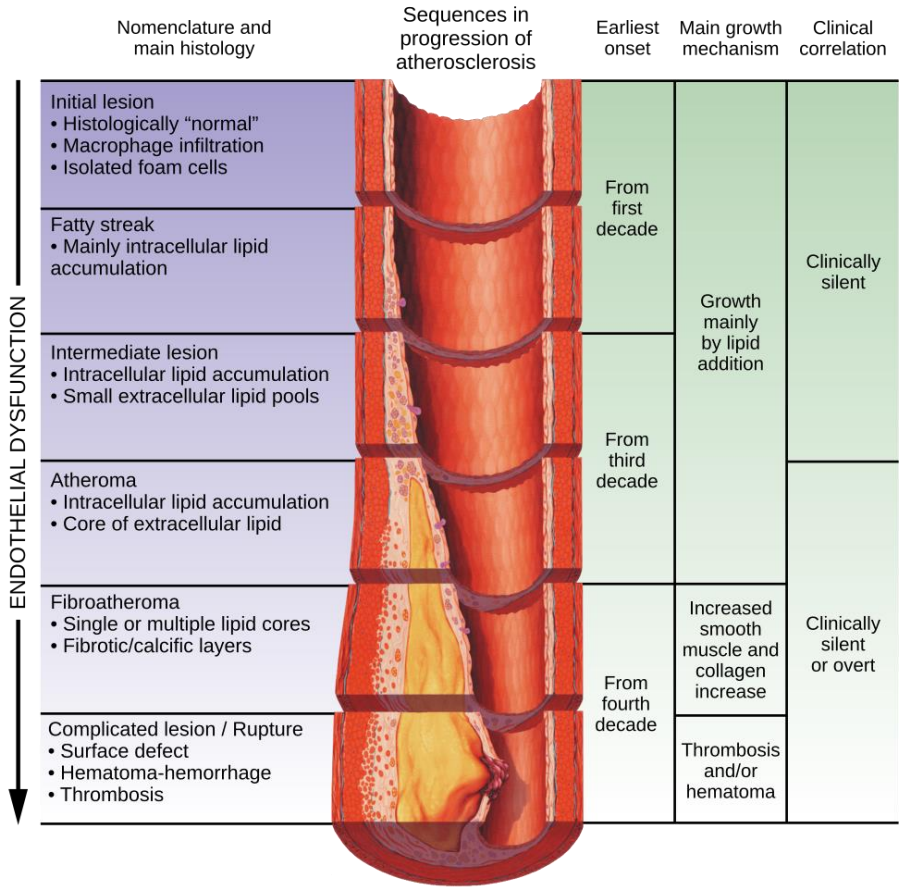

Figure 5. Atherosclerotic progression and thickening of the artery (Hirahatake et al., 2021)

The most prevalent signs and symptoms of CAD are chest pain and discomfort, which are medically known as angina (Shao et al., 2020). Excessive plaque buildup in the arteries, which obstructs blood flow to the heart and the rest of the body, causes the angina. Reduced oxygen and nutrition delivery as a result of this insufficient blood flow runs the risk of causing tissue damage and, in extreme circumstances, even death (Ahmed, 2016). Obesity, physical inactivity, an unhealthy diet, smoking, a family history of CAD or heart disease, and comorbidities such as diabetes, high blood pressure, and elevated blood cholesterol levels are all risk factors contributing to coronary artery disease (Yusuf et al., 2020). The significance of early detection and prevention techniques is emphasized by

the fact that many of these characteristics can be altered by alterations in lifestyle and medical treatment (Arnett et al., 2019). Aside from causing partial or total blockage of arteries, plaque can separate from the artery wall and flow into the bloodstream, resulting in an acute thrombotic event (Bentzon et al., 2014). This can lead to a heart attack or a stroke, which both have high morbidity and death rates (Benjamin et al., 2018). It is essential to comprehend the relevance of factors influencing the evolution of atherosclerotic lesions in order to properly treat and prevent future cardiac events. Inflammation, endothelial dysfunction, and oxidative stress are a few of the mechanisms that have been linked to the development of atherosclerosis in studies (Higashi, 2022). It has been demonstrated that pharmaceutical therapies that target these processes, such as statins and antihypertensive drugs, lower the incidence of CAD-related events (Bertrand et al., 2016). In addition, crucial elements of CAD management and prevention include stress management, regular physical activity, a heart-healthy diet, and quitting smoking (Westland et al., 2020). These adjustments can enhance cardiovascular health overall, lower the risk of future cardiac events, and slow the development of atherosclerosis. Successful treatment and prevention of coronary artery disease depend on an understanding of the variables influencing the development of atherosclerotic plaques. It is possible to lessen the overall burden of CAD and enhance patient outcomes by focusing on modifiable risk factors and the underlying processes of atherosclerosis. It is well known that atherosclerosis occurs because of an interplay of a variety of factors. The correlations of these factors to atherosclerosis is explored computationally in order to aid physicians in treating the exact cause of CATS, however research has found that most commonly several factors influence characteristics and hence optimal treatment strategy in the case of arterial plaque (Lechner et al., 2019). For this reason, it is crucial to apply a multiscale approach to analysis of risk factors leading to CATS, starting from cells that make up the coronary arteries, through tissues to the entire organism and its environment (Devinder et al., 2020). Pinpointing the most significant combination of risk factors for CATS development and treatment prognosis would enable physicians to target the disease with optimal treatment strategy and enable better patient outcomes.

The development of atherosclerotic plaques in the coronary arteries typically progresses through the following stages (Rafieian-Kopaei et al., 2014) (Figure 6):

- endothelial dysfunction
- lipid accumulation and foam cell formation
- plaque progression
- plaque destabilization and rupture
- thrombus formation and occlusion

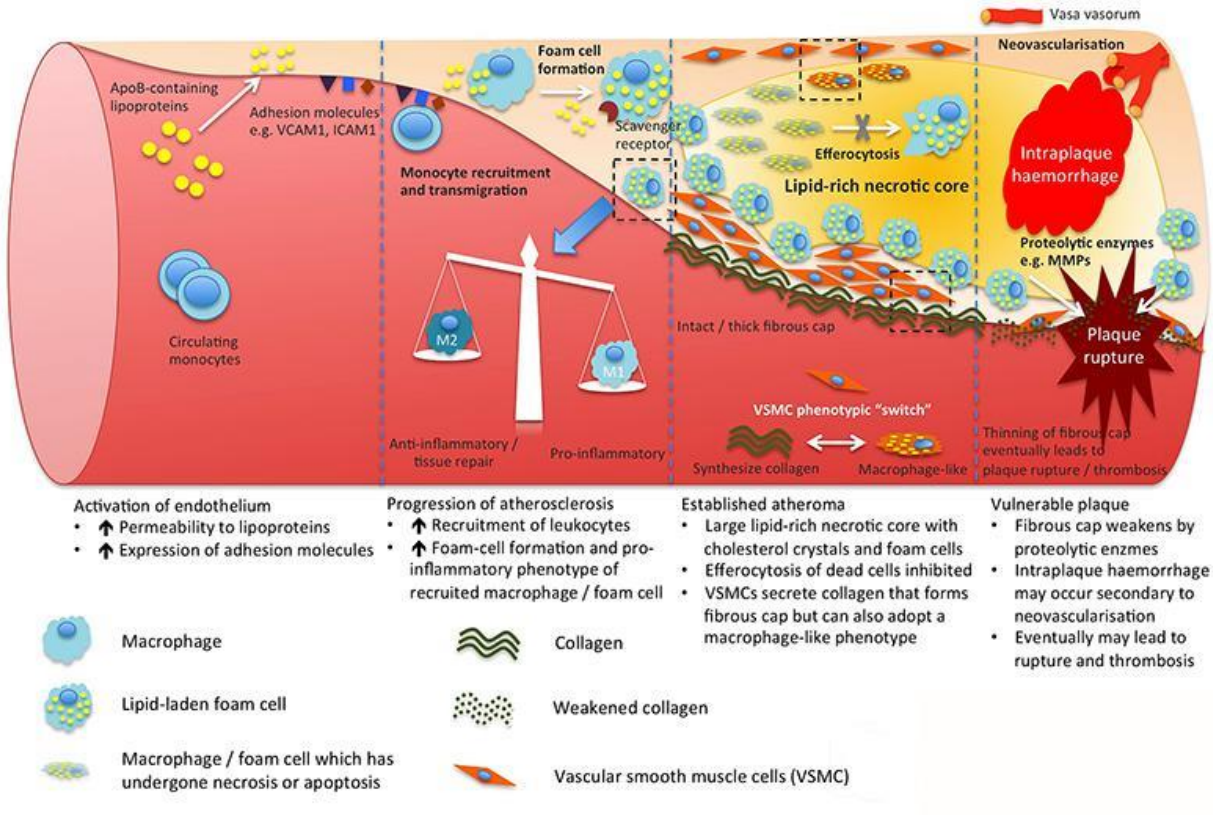

Figure 6. Atherosclerosis progression (Bardin, 2022)

The initial step in atherosclerosis is endothelial injury, which can be caused by factors such as hypertension, smoking, hyperlipidemia, and diabetes. This injury leads to increased permeability and adhesion of leukocytes to the endothelium. Low-density lipoprotein (LDL) cholesterol penetrates the damaged endothelium and accumulates in the intima. Oxidized LDL (oxLDL) is particularly atherogenic and triggers an inflammatory response. Monocytes adhere to the endothelium, migrate into the intima, and differentiate into macrophages. These macrophages ingest oxLDL and transform into foam cells, creating fatty streaks. Smooth muscle cells migrate from the media to the intima, proliferate, and produce extracellular matrix components such as collagen and elastin. This leads to the formation of a fibrous cap over the lipid core, forming a stable plaque. Plaques can become unstable due to continuous inflammation and enzymatic degradation of the fibrous cap. If the cap ruptures, it exposes the underlying thrombogenic material, leading to platelet aggregation and thrombus formation. Thrombus formation can partially or completely occlude the coronary artery, leading to acute coronary syndromes such as unstable angina, non-ST-segment elevation myocardial infarction (NSTEMI), or ST-segment elevation myocardial infarction (STEMI) (Rafieian-Kopaei et al., 2014).

Atherosclerosis of the peripheral arteries, often referred to as peripheral artery disease (PAD), is a chronic condition characterized by the accumulation of plaques within the arterial walls, leading to narrowed and hardened arteries that impair blood flow to the limbs. This condition primarily affects the arteries that supply the legs and can result in significant morbidity. A comprehensive understanding of the pathophysiology, clinical manifestations, diagnostic approaches, and treatment strategies for peripheral artery atherosclerosis is essential for effective management and prevention of severe

complications. Same as with CATS, PAD involves complex interactions among lipid metabolism, endothelial dysfunction, inflammatory responses, and genetic predispositions following the same pattern of plaque progression with the difference of the effect of thrombus formation, where in PAD it can partially or completely occlude the artery, leading to critical limb ischemia or acute limb ischemia, which can cause severe tissue damage (Signorelli et al., 2020).

2.3. Artery biomechanics

The mechanical properties of arteries are determined by their composition and structure, allowing them to perform essential functions in the cardiovascular system. Understanding artery biomechanics is crucial for diagnosing and managing cardiovascular diseases such as hypertension, atherosclerosis, and aneurysms. Changes in arterial compliance and stiffness are early indicators of vascular dysfunction and can predict cardiovascular risk (Carpenter et al., 2020).
Arteries are highly elastic vessels due to the presence of elastic fibers in the tunica media, particularly in large elastic arteries such as the aorta and pulmonary arteries. This elasticity allows arteries to expand and recoil in response to changes in blood pressure, converting pulsatile flow from the heart into a steady flow through smaller vessels. Arterial compliance (C) is the ability of arteries to stretch and accommodate changes in blood volume without a significant increase in pressure. It is calculated as:

$$C = \frac{\Delta V}{\Delta P} \qquad \text{Eq. 1}$$

Where:

- ΔV is change in blood volume
- ΔP is change in pressure

Distensibility refers to the ability of arteries to stretch in response to pressure changes. It is influenced by the elastic fibers in the tunica media and determines how much the artery can expand in response to each pulse of blood ejected from the heart. The distensibility coefficient (DC) is defined as:

$$DC = \frac{\Delta D}{D \times \Delta P} \qquad \text{Eq.2}$$

Where:

- ΔD is change in arterial diameter
- D is baseline arterial diameter
- ΔP is change in pressure (usually the pulse pressure)

Arteries exhibit viscoelastic behavior, meaning they demonstrate both elastic (reversible deformation) and viscous (time-dependent deformation) properties. The viscoelasticity of arteries helps them adapt to different flow conditions and resist damage from pressure fluctuations over time (Carpenter et al., 2020).

Arteries contribute significantly to hemodynamics, the study of blood flow dynamics within the cardiovascular system. Arterial pressure-volume (P-V) relationships describe how changes in arterial pressure affect arterial volume. The compliance of arteries

influences these relationships, with stiffer arteries showing less change in volume for a given change in pressure. Arteries transmit the pulsatile pressure wave generated by each heartbeat (systole) from the heart to the periphery. Pulse wave velocity (PWV) is a measure of how quickly this wave travels along the arterial tree and is influenced by arterial stiffness. Increased PWV is associated with aging and vascular disease. Arteries act as a Windkessel, or pressure reservoir, dampening the pulsatile nature of blood flow. This effect is facilitated by the elasticity of large arteries, which store energy during systole and release it during diastole to maintain continuous flow (Carpenter et al., 2020).

Arterial biomechanics plays a critical role in the initiation, progression, and clinical consequences of atherosclerosis. Mechanical forces such as shear stress and mechanical stretch influence endothelial function, arterial remodeling, and the development of atherosclerotic plaques (Carpenter et al., 2020). Understanding these biomechanical factors provides insights into disease mechanisms and informs strategies for preventing and managing cardiovascular diseases associated with atherosclerosis (Figure 7).

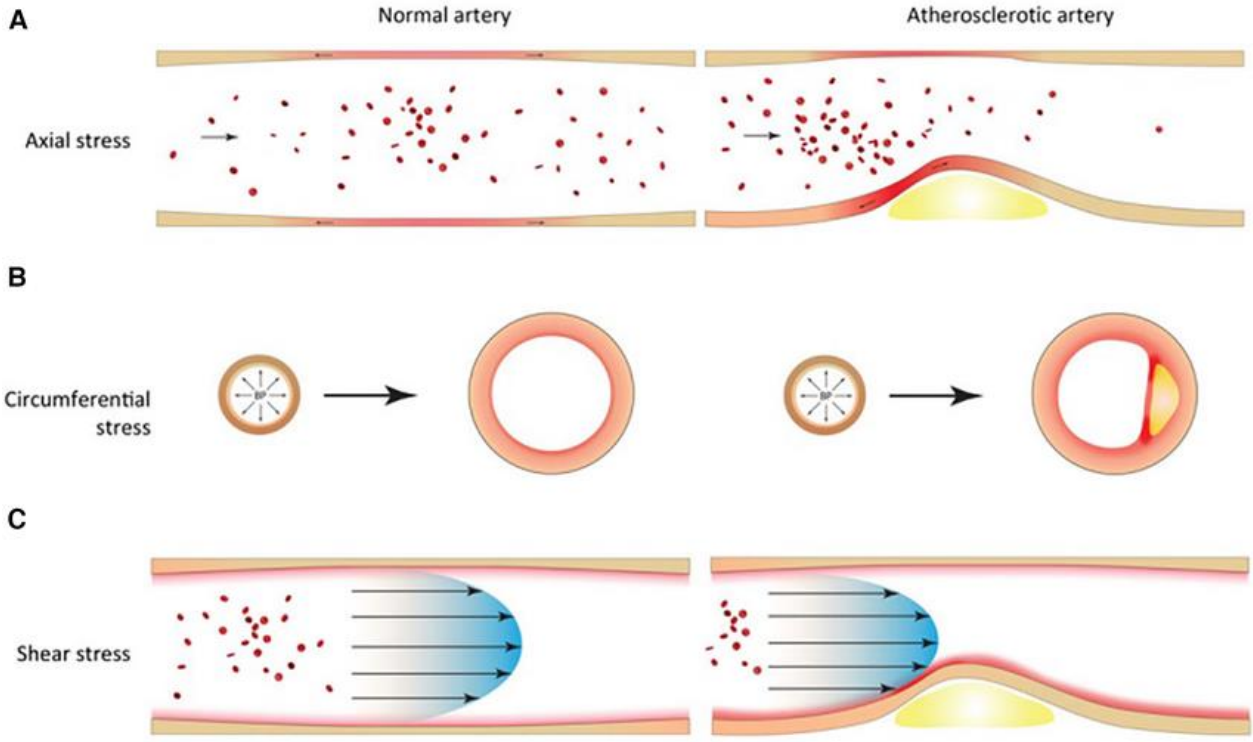

Figure 7. Aterial biomechanics (Bacigalupi et al., 2024)

Shear stress (τ) is the frictional force exerted by blood flow on the endothelial cells lining the arterial wall. It is calculated using the formula:

$$\tau = \eta \cdot \frac{du}{dy} \qquad \text{Eq. 3}$$

Where:

- η is the blod viscosity
- $\frac{du}{dy}$ is the velocity gradient perpendicular to the vessel wall (rate of change of blood flow velocity with respect to distance from the wall)

Normal, laminar blood flow generates shear stress that promotes endothelial health and function. However, disturbed or turbulent flow patterns, such as those occurring at

arterial bends or bifurcations, can lead to low and oscillatory shear stress. These disturbed flow patterns are associated with endothelial dysfunction and the initiation of atherosclerosis . While low shear stress reduces the production of nitric oxide (NO) and other protective factors by endothelial cells, promoting inflammation and leukocyte adhesion to the arterial wall, oscillatory shear stress contributes to the activation of endothelial cells, increased permeability of the endothelium, and enhanced uptake of lipids into the arterial wall (Carpenter et al., 2020).
Arterial biomechanics also involves mechanical stretch, particularly in regions where arteries experience higher pressures or pulsatile flow. Chronic exposure to increased mechanical stretch can lead to arterial remodeling, characterized by changes in arterial wall thickness, diameter, and composition. The pulsatile nature of blood flow subjects arteries to cyclic stretch during each cardiac cycle. This cyclic stretch influences vascular smooth muscle cell phenotype, extracellular matrix synthesis, and overall arterial wall structure (Carpenter et al., 2020).

2.4. Diagnosis and treatment of atherosclerosis

Diagnosis and treatment of atherosclerosis in these critical arteries are essential for preventing complications such as myocardial infarction (heart attack) and stroke. Diagnosis often begins with a thorough clinical evaluation, including assessing the patient's medical history, risk factors (e.g., smoking, hypertension, diabetes), and symptoms such as chest pain (angina) or transient neurological symptoms suggestive of stroke.
Imaging is the most accurate diagnostic modality for atherosclerosis and imaging modalities used depend on the artery affected by atherosclerosis. Coronary angiography and coronary computed tomography (CTA) are the golden standard and it’s alternative for diagnosing coronary artery atherosclerosis respectively. Coronary angiography is considered the gold standard for evaluation of coronary artery disease (CAD). It is an invasive procedure involvung insertion of a catheter into a blood vessel (typically the femoral or radial artery) followed by injecting a contrast dye to outline the coronary arteries with X-ray imaging thus providing high-resolution images that reveal the presence, location, and severity of coronary artery narrowing or blockages (stenosis). It is essential for guiding decisions on interventions such as percutaneous coronary intervention (PCI) or coronary artery bypass grafting (CABG) in patients with significant CAD. Coronary CTA has emerged as a valuable non-invasive imaging technique for evaluating coronary artery anatomy and detecting plaque buildup and stenosis. It utilizes computed tomography (CT) technology to acquire detailed, three-dimensional images of the coronary arteries without the need for invasive procedures. Coronary CTA is particularly useful for assessing patients with suspected CAD, providing comprehensive visualization of plaque characteristics and coronary artery morphology. It plays a crucial role in risk stratification and treatment planning, especially in patients with equivocal stress test results or atypical symptoms (Robert et al., 2019).
Optical cogerence tomography (OCT) is an intravascular imaging technique that uses near-infrared light to create high-resolution cross-sectional images of the arterial wall. Incorporating OCT alongside other imaging modalities enhances the diagnostic accuracy and therapeutic management of atherosclerosis, providing clinicians with comprehensive insights into arterial structure and pathology. Its ability to visualize fine details within the arterial wall makes OCT a valuable tool in both research and clinical practice for optimizing patient care and outcomes. It provides detailed visualization of arterial

morphology, including plaque characteristics such as thickness, composition (lipid-rich or fibrous), and presence of microcalcifications. It offers superior resolution compared to other imaging modalities, enabling precise assessment of plaque morphology and characteristics. This information aids in determining the vulnerability of plaques to rupture and guiding treatment strategies. Additionally, OCT helps in differentiating stable from unstable plaques, thereby assisting in risk stratification for future cardiovascular events. OCT is particularly useful during coronary interventions, such as percutaneous coronary intervention (PCI), to assess stent placement and optimize procedural outcomes. It allows clinicians to visualize stent apposition and expansion, detect edge dissections, and evaluate residual plaque burden. OCT-guided interventions contribute to improved procedural success rates and reduced complications (Prati et al., 2010, Bouma et al., 2017).

When carotid atherosclerosis is suspected, either carotid ultrasound or carotid angiography are employed as imaging strategies. Carotid ultrasound is a non-invasive imaging modality that utilizes high-frequency sound waves to assess blood flow dynamics and detect abnormalities within the carotid arteries. It is particularly effective in evaluating carotid artery stenosis, a significant risk factor for ischemic stroke. Carotid ultrasound can visualize plaque formation, measure intima-media thickness (IMT) – an early marker of atherosclerosis, and assess blood flow velocities using Doppler ultrasound. This imaging technique is invaluable for identifying patients at high risk of stroke and guiding decisions on further management, including medical therapy or surgical intervention (Polak, 2001). Similar to coronary angiography, carotid angiography involves the insertion of a catheter into a blood vessel (typically the femoral artery) and the injection of contrast dye to visualize the carotid arteries under X-ray imaging (Jackson and Meaney, 2015, Sonka et al., 2000). This invasive procedure provides detailed images of the carotid artery anatomy and allows for precise assessment of narrowing or blockages (stenosis). Carotid angiography is typically reserved for cases where non-invasive imaging results are inconclusive or when surgical intervention, such as carotid endarterectomy or carotid artery stenting, is being considered. It provides critical information for planning surgical procedures and optimizing patient outcomes in individuals with significant carotid artery disease (Pizzolato et al., 2014).

The diagnostic process for PAD typically begins with a thorough clinical assessment. Healthcare providers evaluate the patient's medical history, including risk factors such as smoking, diabetes, hypertension, hyperlipidemia, and family history of cardiovascular disease (Peach et al., 2012). Symptoms suggestive of PAD include:

- Intermittent Claudication: Pain, cramping, or fatigue in the legs during physical activity that resolves with rest.
- Rest Pain: Pain in the feet or toes that worsens at night and improves when dangling the legs over the edge of the bed.
- Non-healing Wounds: Ulcers or sores on the legs or feet that do not heal properly.
- Coolness or Pallor: Reduced temperature or color changes in the affected limb compared to the unaffected limb.

The ankle-brachial index (ABI) serves as the first tool in the diagnosis and assessment of peripheral artery disease (PAD), a condition where arteries supplying blood to the limbs become narrowed or blocked due to atherosclerosis (Crawford et al., 2016). This simple

yet effective test compares blood pressure measurements taken at the ankles and arms, offering valuable insights into the extent of arterial obstruction and consequent reduction in blood flow to the legs. During the ABI test, a healthcare provider uses a Doppler ultrasound probe to measure systolic blood pressure in both arms and both ankles. This non-invasive procedure involves applying the probe to these areas to detect and record blood flow sounds, which are indicative of arterial pressure. The ABI is calculated by dividing the highest systolic blood pressure measured at the ankle by the highest systolic blood pressure measured in either arm. A normal ABI falls within the range of 0.90 to 1.30, indicating relatively unobstructed blood flow to the lower extremities. Conversely, an ABI lower than 0.90 suggests the presence of PAD, with severity categorized as follows:

- An ABI between 0.70 and 0.90 typically indicates mild PAD, where arterial narrowing may cause intermittent claudication (leg pain during activity).
- An ABI ranging from 0.40 to 0.70 signifies moderate PAD, characterized by more pronounced symptoms and greater impairment in blood flow.
- An ABI less than 0.40 indicates severe PAD, where critical limb ischemia may occur, potentially leading to tissue damage and non-healing wounds.

Interpreting ABI results allows healthcare providers to tailor treatment plans accordingly, aiming to alleviate symptoms, prevent disease progression, and reduce the risk of complications such as limb amputation. Regular monitoring of ABI over time helps track disease progression and assess the effectiveness of therapeutic interventions, including lifestyle changes, medications, and surgical procedures aimed at improving blood flow and enhancing quality of life for individuals with PAD (Casey et al., 2019).

Advanced imaging techniques play a crucial role in the comprehensive evaluation and management of peripheral artery disease (PAD), providing detailed insights into arterial anatomy, blood flow dynamics, and the extent of arterial narrowing or occlusion. These imaging modalities are essential for confirming diagnosis, guiding treatment decisions, and assessing therapeutic outcomes. Duplex ultrasound combines traditional ultrasound with Doppler ultrasound technology to visualize blood flow in the arteries and detect abnormalities such as stenosis or occlusions. During the procedure, high-frequency sound waves are transmitted through tissues, and the echoes are captured to create images of blood vessels. Doppler ultrasound specifically measures the speed and direction of blood flow, allowing healthcare providers to assess the severity and location of arterial narrowing in real-time. Duplex ultrasound is particularly advantageous for evaluating PAD in the lower extremities, where it can accurately identify the presence of atherosclerotic plaques, measure blood flow velocities, and assess the hemodynamic significance of arterial lesions (Eiberg et al., 2010).
CTA is a non-invasive imaging technique that utilizes computed tomography CT technology to generate detailed, three-dimensional images of the arteries. It involves the intravenous injection of contrast dye, which highlights the vascular structures and enables visualization of arterial anatomy with high spatial resolution. CTA is highly effective in identifying areas of stenosis, occlusion, or plaque buildup in patients suspected of having PAD. It provides comprehensive anatomical information that helps healthcare providers plan interventions such as angioplasty or stenting, assess collateral circulation, and evaluate the suitability for surgical revascularization procedures (Fleischmann et al., 2006).

Magnetic resonance angiography (MRA) utilizes magnetic resonance imaging (MRI) technology to create detailed images of blood vessels without the use of ionizing radiation. MRA is particularly advantageous for evaluating complex arterial anatomy, including tortuous vessels or regions with calcified plaques, which may be challenging to visualize with other imaging modalities. MRA provides multiplanar images that allow for precise assessment of arterial stenosis, occlusion, and collateral circulation in patients with PAD. It is especially beneficial for individuals with contraindications to iodinated contrast agents used in CTA, such as those with renal insufficiency or allergies (Nelemans et al., 2000).
These advanced imaging modalities complement clinical evaluation and non-invasive tests like the ankle-brachial index (ABI), enhancing the accuracy of PAD diagnosis and facilitating tailored treatment strategies. By providing detailed anatomical and functional information, duplex ultrasound, CTA, and MRA enable healthcare providers to make informed decisions regarding medical management, endovascular interventions, or surgical procedures aimed at improving blood flow to the affected limbs. Regular utilization of these imaging techniques also supports longitudinal monitoring of disease progression and therapeutic efficacy, ensuring optimal care and outcomes for patients with PAD.

2.5. Biochemical and genetic testing for atherosclerosis

Biochemical and genetic testing for atherosclerosis supports a personalized approach to cardiovascular risk assessment and management (Deric et al., 2008, Paynter et al., 2016). Biochemical tests measure specific markers in the blood associated with inflammation, lipid metabolism, and endothelial dysfunction, all of which are key contributors to the development and progression of atherosclerosis (Medina-Leyte et al., 2021). A lipid profile measures levels of cholesterol, triglycerides, and lipoproteins in the blood. Elevated levels of low-density lipoprotein cholesterol (LDL-C) are a major risk factor for atherosclerosis, as LDL particles can infiltrate arterial walls and initiate plaque formation. Conversely, high levels of high-density lipoprotein cholesterol (HDL-C), often referred to as "good cholesterol," are associated with reduced cardiovascular risk. The ratio of total cholesterol to HDL-C is also informative, with higher ratios indicating increased risk (Bhatt, 2018, Toth, 2005). Markers such as C-reactive protein (CRP) and interleukin-6 (IL-6) indicate systemic inflammation, which contributes to endothelial dysfunction and promotes atherosclerosis progression. Elevated levels of CRP, in particular, have been linked to increased cardiovascular risk independent of traditional risk factors. Endothelial dysfunction precedes atherosclerosis development (Held et al., 2017). Biomarkers such as soluble adhesion molecules (e.g., sICAM-1, sVCAM-1) and endothelin-1 reflect impaired endothelial function, facilitating leukocyte adhesion, vascular smooth muscle cell proliferation, and plaque formation (Ugurlu et al., 2013).

Genetic testing assesses inherited variations that influence susceptibility to atherosclerosis and cardiovascular disease. While not routinely performed in clinical practice, genetic testing provides valuable insights into individual risk profiles and can guide personalized preventive strategies (Laan et al., 2018). Familial hypercholesterolemia FH is a genetic disorder characterized by high LDL-C levels from birth, significantly increasing the risk of premature atherosclerosis and cardiovascular events (Khera and Hegele, 2020). Genetic testing can identify mutations in genes such as LDLR (LDL receptor), APOB (apolipoprotein B), or PCSK9 (proprotein convertase

subtilisin/kexin type 9), which disrupt normal lipid metabolism and contribute to FH (Meshkov et al., 2021). Various single nucleotide polymorphisms (SNPs) associated with lipid metabolism, inflammation, and endothelial function have been linked to atherosclerosis risk. Examples include SNPs in genes encoding proteins involved in cholesterol transport (e.g., ABCA1)(Fitzgerald et al., 2010), inflammation (e.g., IL-6) (Schieffer et al., 2004), and oxidative stress pathways (Batty et al., 2022). Genetic risk scores (GRS) integrate multiple genetic variants associated with cardiovascular risk into a single score. They provide a quantitative assessment of genetic susceptibility to atherosclerosis and can stratify individuals into high, moderate, or low-risk categories. GRS are increasingly used in research and may eventually inform clinical decision-making regarding preventive therapies and lifestyle interventions (Christiansen et al., 2020).

2.6. Treatment of atherosclerosis

Effective management strategies aim to halt CATS progression, reduce plaque burden, prevent complications such as myocardial infarction and stroke, and improve overall cardiovascular health. Initially, patients are advised to make lifestyle modifications that include:

- Adopting a heart-healthy diet low in saturated fats, trans fats, and cholesterol while emphasizing fruits, vegetables, whole grains, and lean proteins can lower LDL cholesterol levels and reduce inflammation. The Mediterranean diet, rich in olive oil, nuts, and fish, has shown particular benefit in reducing cardiovascular risk.
- Engaging in regular physical activity improves cardiovascular fitness, lowers blood pressure, promotes weight loss, and enhances overall vascular health. Aerobic exercises such as brisk walking or cycling are recommended, aiming for at least 150 minutes per week.
- Quitting smoking significantly reduces cardiovascular risk by improving endothelial function, decreasing inflammation, and lowering the formation of atherosclerotic plaques.

Pharmacotherapy for CATS includes:

- Statins as first-line medications that lower LDL cholesterol levels and stabilize plaques. High-intensity statin therapy (e.g., atorvastatin, rosuvastatin) is recommended for most patients with atherosclerosis to achieve LDL-C reduction goals (Lee et al., 2018)
- Antiplatelet agents like aspirin and other antiplatelet medications (e.g., clopidogrel) reduce the risk of thrombosis and cardiovascular events in patients with established atherosclerosis. Dual antiplatelet therapy may be considered in selected high-risk patients (Patrono et al., 2017)
- Antihypertensive drugs for controlling blood pressure with medications such as ACE inhibitors, angiotensin II receptor blockers (ARBs), beta-blockers, or diuretics helps prevent plaque progression and reduces cardiovascular risk by maintaining optimal blood pressure levels (Nissen et al., 2004)
- Antithrombotic therapy for selected patients with high-risk features such as recent myocardial infarction or atrial fibrillation, anticoagulant therapy (e.g., warfarin, direct oral anticoagulants) may be recommended to prevent thrombotic events (Parker and Storey, 2021)

In cases where lifestyle adjustments and pharmacotherapy fail, interventional and surgical procedures are advised and employed. Angioplasty is a procedure to widen blocked arteries, involves inserting a catheter into the site of blockage using imaging techniques like angiography. Before using drug-coated balloons (DCB) or drug-eluting stents (DES), pre-dilation with a percutaneous transluminal angioplasty (PTA) balloon catheter is recommended (Unverdorben et al., 2009). For DCB, the PTA balloon should be 1mm smaller than the artery diameter, while for DES, it should match the artery's nominal diameter. The pressure applied should stay below the balloon's rated burst pressure. If high stenosis rates are present, a two-step pre-dilation using smaller then larger balloons is suggested. The balloon's diameter and length should match the vessel's size and lesion length respectively, with the total drug dose not exceeding 34,845ug. If residual stenosis remains above 50% after DCB use, stent placement is con-sidered. A successful procedure leaves ≤50% residual stenosis (non-stented subjects) or ≤30% (stented subjects). When deploying DES, correct stent positioning is crucial. The stent should be slowly deployed, aiming for an initial pressure that achieves a stent-to-vessel diameter ratio of about 1.1, held for 30 seconds. DES and DCB are two innovative medical technologies developed for the treatment of vascular diseases, including CAD and PAD. Both devices operate on the principle of lo-calized drug delivery to inhibit neointimal hyperplasia and restenosis, issues commonly associated with bare-metal stent implantation (Grüntzig et al., 1978, Abdullah et al., 2018, Lindquist and Schramm, 2018). DES have become a cornerstone of percutaneous coronary intervention (PCI) for the treatment of CAD since their introduction in the early 2000s (Moses et al., 2003). They are composed of a metallic scaffold coated with an antiprolif-erative drug and a polymer carrier material, designed to slowly release the drug over sev-eral weeks to. The drugs used in DES, such as paclitaxel or sirolimus, inhibit the growth of smooth muscle cells to reduce restenosis risk (Moses et al., 2003). Due to their effective-ness in the treatment of CAD, DES have also been used for PAD. Successive genera-tions of DES have aimed to improve upon earlier designs' limitations, with a focus on op-timizing drug delivery, reducing thrombosis risk, and enhancing biocompatibility (Bangalore et al., 2013). Despite initial concerns about late stent thrombosis (LST) and delayed endothelial heal-ing with first-generation DES, newer versions have demonstrated improved safety and ef-ficacy outcomes, with lower rates of LST and comparable or superior reductions in ISR (Bangalore et al., 2013). However, DES use comes with risks, including the prolonged presence of a foreign object in the artery, potentially increasing blood clot risk, and concerns about long-term safety(Cornelissen and Vogt, 2019). On the other hand, DCB, a more recent technology, consist of a balloon catheter coated with an antiproliferative drug, which is released during balloon inflation to treat vascular diseases (Byrne et al., 2014). They have been utilized primarily in PAD treatment and have shown promising results in reducing restenosis rates and improving clinical outcomes. DCB deliver their drug load during balloon inflation, with the drug typically com-bined with a carrier to facilitate transfer and retention in the arterial wall (Hossainy et al., 2008). In clinical trials, DCB have been found to be as effective as DES in treating lesions, with a lower risk of restenosis and less need for repeat procedures. DCB are especially effective in treating PAD, particularly in femoropopliteal and below-the-knee lesions and have been investigated as an alternative to DES in CAD treatment (Cornelissen et al., 2019). While DCB have several advantages over DES, such as being less invasive as they do not require permanent im-plantation, they also come with their own set of limitations. These include the potential for uneven drug coating, leading to incomplete drug delivery, and risks of complications like dissection or perforation. Both

DES and DCB represent significant advancements in the treatment of vascular diseases. They share a common goal of localized drug delivery to inhibit restenosis but each has its unique sets of advantages and disadvantages. The choice between DES and DCB may depend on the specific characteristics of the patient and the disease, including the severity and location of the lesions, the patient's risk profile, and other factors.
Comparative studies on DCB and DES in vascular disease treatment reveal no signif-icant difference in major adverse cardiovascular events at a one-year follow-up, according to Katsanos et al. (Katsanos et al., 2018). Yet, DCB were found to be associated with a lower risk of target le-sion revascularization (TLR) than DES. A two-year follow-up study by Tepe et al. also found no significant difference in the rate of primary patency, but DCB had a lower rate of clinically-driven TLR (Tepe et al., 2015). Further research indicates DCB have a lower restenosis risk and TRL than DES a year post-angioplasty, and they are more cost-effective when treating femoropopliteal artery disease due to their lower TLR and overall cost (Alfonso et al., 2018).
Alternatively, surgical revascularization and carotid endarterectomy (CEA) are employed. Surgical revascularization is a crucial intervention for patients with advanced coronary artery disease (CAD), where the buildup of atherosclerotic plaque significantly restricts blood flow to the heart muscle (Slovut et al., 2012). This procedure, known as Coronary Artery Bypass Grafting (CABG), involves creating bypass grafts using healthy blood vessels sourced from elsewhere in the body, such as the saphenous vein or internal mammary artery (Alexander and Smith, 2016). These grafts are used to bypass narrowed or blocked coronary arteries, restoring proper blood flow to the heart muscle. CEA is typically recommended for symptomatic patients with severe carotid artery stenosis (usually greater than 70%) who have experienced transient ischemic attacks (TIAs) or strokes related to carotid artery disease. CEA involves surgically removing the buildup of atherosclerotic plaque from the inner lining of the carotid artery. This plaque removal reduces the risk of stroke by restoring proper blood flow to the brain. By removing the plaque, CEA reduces the risk of embolic stroke caused by plaque rupture and thrombus formation within the carotid artery (Alexander et al., 2016).

Laser or rotational atherectomy are advanced interventional techniques employed in the treatment of peripheral artery disease and coronary artery disease when traditional methods like angioplasty or stenting may not be sufficient due to particularly dense or complex plaque formations within the arterial walls (Tomey et al., 2014). Laser atherectomy is particularly effective in cases where plaque has become calcified or otherwise resistant to traditional angioplasty techniques. It utilizes specialized catheters equipped with laser fibers to target and vaporize plaque deposits within the arteries. The procedure begins with the insertion of a catheter into the affected artery under fluoroscopic guidance. Once positioned, the laser is activated, emitting high-energy light pulses that vaporize the hardened plaque while sparing the arterial walls. The vaporized debris is removed from the bloodstream naturally. By effectively removing dense plaque, laser atherectomy improves blood flow through the treated artery, thereby alleviating symptoms such as claudication (leg pain) in PAD patients or angina in CAD patients. Compared to traditional surgical interventions, laser atherectomy minimizes trauma to the artery and surrounding tissues, which can expedite recovery times and reduce complications (Tsutsui et al., 2021). Rotational atherectomy is specifically effective in cases where plaque has become heavily calcified, making it difficult to compress with a balloon during standard angioplasty procedures. It involves the use of a specialized catheter equipped with a rotating burr at its tip. This burr, powered by a high-speed

motor, mechanically abrades and removes plaque deposits from within the arterial lumen. The procedure is performed similarly to angioplasty, with the catheter inserted through a small incision in the groin or wrist and advanced to the site of the arterial blockage under fluoroscopic guidance. By mechanically ablating calcified plaque, rotational atherectomy restores arterial patency and improves blood flow to the affected region. Often used in conjunction with balloon angioplasty and stent placement, rotational atherectomy helps prepare the vessel for optimal stent deployment by creating a smooth arterial surface (Gupta et al., 2019).

3. Bioengineering in cardiovascular medicine

3.1. Finite element analysis for atherosclerosis

Finite element modeling of atherosclerosis plays a crucial role in understanding the biomechanical behavior of arterial walls under pathological conditions (Filipovic et al., 2011, Filipovic, 2020, Filipovic et al., 2017, Filipovic et al., 2013). Computational models based on finite element analysis provide a powerful tool to simulate and analyze the complex mechanical interactions that occur within these diseased arteries (Saveljic et al., 2020, Tomasevic et al., 2024). At its core, finite element modeling of atherosclerosis involves discretizing the arterial wall into small geometric elements, each represented by a set of mathematical equations that describe its mechanical behavior. These elements are interconnected at nodes, allowing researchers to simulate the distribution of stresses and strains throughout the arterial wall under various physiological conditions (Djorovic et al., 2020). Key factors influencing the mechanical behavior of atherosclerotic plaques include plaque composition (e.g., lipid core, fibrous cap), degree of calcification, and the overall geometry of the vessel. By incorporating these factors into finite element models, researchers can predict stress concentrations within the plaque, assess the risk of plaque rupture, and evaluate the effectiveness of different therapeutic interventions (Filipovic et al., 2011, Filipovic et al., 2014, Isailovic et al., 2017). Finite element models enable researchers to explore how changes in blood flow patterns, such as those caused by stenosis (narrowing of the artery), influence plaque development and progression. By integrating fluid-structure interaction simulations, these models can provide insights into the hemodynamic forces acting on the arterial wall and their role in plaque formation (Filipovic et al., 2011, Filipovic et al., 2013). Recent advancements in computational techniques, coupled with improvements in imaging modalities like MRI and CT angiography, have enhanced the accuracy and predictive capabilities of finite element models in studying atherosclerosis. These models not only contribute to our fundamental understanding of disease mechanisms but also hold promise for personalized medicine by guiding clinicians in making informed decisions regarding patient-specific treatment strategies.

Biological systems exhibit behaviors that arise from the actions of individual cells and their interactions. Cells possess the ability to move, interact, reproduce, and undergo apoptosis. These cellular behaviors collectively influence the dynamics of multicellular biological systems. Therefore, modeling such systems necessitates accounting for intricate interactions among individual cells and environmental factors. Consequently, there is a growing trend towards conducting research at the multicellular level, employing various methodologies to model these complex biological systems. Behavior of complex multicellular systems in models is defined by representation of discrete autonomous entitites and examining their interactions on micro-level. This approach not only enhances our understanding of complex biological processes but also facilitates efficient and cost-effective virtual experiments (Johnson et al., 2018).
Two commonly utilized systems include cellular automata models (CA) and agent-based models (ABM). Both approaches employ a bottom-up methodology where global system behaviors emerge from local interactions among individual cells, each explicitly represented with defined local behavioral rules (Hwang et al., 2009). Although CA and ABM share similarities, their primary distinction lies in how they model the environment. The opperation of these models is based on a lattice system with cells occupying specific

network elements and transitioning between them (Hwang et al., 2009). Alternatively, models can exist in a continuum (lattice-free) space, allowing cells to reside anywhere within the computational domain. Here, the position of each cell is often determined by solving kinematic or dynamic equations of motion, offering ABM a potential advantage in realism over cellular automata, which impose stricter spatial constraints (Zahedmanesh and Lally, 2012). In general, both CA and ABM strategies are suitable for modeling complex behaviors such as those found in regulatory processes of the cardiovascular system, where individual cell behaviors intricately influence macroscopic outcomes that are challenging to predict straightforwardly.

3.2. ABM in cardiovascular medicine

When the behavior of complex biological systems relies heavily on interactions among multiple cells, which are themselves influenced by changes in micro-environmental factors, employing a multi-scale modeling approach becomes essential. Therefore, methodologies like CA and ABM are used for investigating various aspects of cardiovascular tissue and system regulation (Zahedmanesh & Lally, 2012).

ABM has emerged as a powerful computational tool in cardiovascular medicine, enabling researchers and clinicians to simulate and analyze the complex interactions among biological, environmental, and behavioral factors that influence cardiovascular health (Bhui and Hayenga, 2017, Blagojevic et al., 2022, Corti et al., 2019, Corti et al., 2020b, Corti et al., 2021, Corti et al., 2022, Corti et al., 2023, Tomasevic et al., 2024, Filipovic et al., 2023, Tsompou et al., 2022). By modeling individual entities, or "agents," and their interactions within a defined system, ABM provides valuable insights into the dynamics of cardiovascular diseases, particularly those related to atherosclerosis, hypertension, and heart failure (Tsompou et al., 2022). This innovative approach facilitates the exploration of scenarios that are often challenging to assess through traditional statistical methods or experimental designs. At its core, ABM is a simulation technique that allows for the representation of individual agents (e.g., cells, tissues, organs) and their behaviors in a defined environment. Each agent operates based on a set of rules and interacts with other agents and the environment according to specific protocols. This individual-based perspective captures the heterogeneity within populations and enables the modeling of complex systems where emergent behaviors arise from the interactions of simpler entities (Bhui and Hayenga., 2017).

In cardiovascular medicine, ABM can simulate various processes, such as the progression of atherosclerosis, the response of the cardiovascular system to interventions, and the impact of lifestyle factors on heart health (Hayenga, 2011, Hayenga et al., 2011). By representing individual patients or cells, ABM models can incorporate a wide range of variables, including genetic predispositions, metabolic states, and lifestyle choices, to better understand their contributions to cardiovascular disease risk and outcomes (Corti et al., 2019; Corti et al., 2020; Corti et al., 2022).
Atherosclerosis is a prime candidate for ABM due to its multifactorial nature and the interplay of various biological processes. ABM can simulate the progression of atherosclerotic plaques by modeling the behavior of individual cells, such as endothelial cells, smooth muscle cells, and macrophages, within the arterial wall (Corti et al., 2019; Tomasevic et al., 2024). Each cell type can have specific rules governing its behavior,

including proliferation, migration, apoptosis, and response to inflammatory stimuli. For instance, an ABM approach can capture how lipid accumulation, oxidative stress, and inflammatory responses contribute to plaque formation and stability. By simulating the interactions between lipid particles and arterial wall cells, researchers can observe how different conditions, such as hyperlipidemia or hypertension, influence the development of atherosclerosis over time. These models can also explore how therapeutic interventions, such as statins or anti-inflammatory agents, affect plaque dynamics and overall cardiovascular risk (Bhui et al., 2017; Blagojevic et al., 2022; Corti et al., 2019; Corti et al., 2020; Corti et al., 2022; Tomasevic et al., 2024; Filipovic et al., 2023; Tsompou et al., 2022)..

ABM is also valuable for modeling cardiovascular responses to various stimuli, including pharmacological interventions, exercise, or dietary changes. For instance, an ABM can simulate the effects of a lifestyle intervention, such as increased physical activity, on the cardiovascular system. By modeling individual agents that represent patients with varying levels of baseline fitness and health status, researchers can assess how different exercise regimens impact cardiovascular health, including changes in blood pressure, heart rate, and overall fitness. ABM can also be used to evaluate the effects of medical treatments on patient outcomes. By incorporating clinical data and treatment protocols, ABM can simulate how different patients respond to specific therapies based on their unique profiles. This personalized approach allows for the exploration of tailored treatment strategies, identifying patients who more prone to benefiting from tailored interventions and under what circumstances.

3.3. State-of-the art in ABM for atherosclerosis

For instance, (Pappalardo et al., 2008) introduced a 2D agent-based model aimed at simulating early-stage atherosclerosis and the subsequent immune system response. Their model comprehensively represented the critical entities and interactions involved in immune processes that regulate atherogenesis. In a subsequent study (Pappalardo et al., 2008), they explored the heightened risk of atherosclerosis due to short-term elevations in LDL concentration, assessing whether reducing LDL levels could mitigate this risk. Curtin and Zhou (2014) (Curtin and Zhou, 2014) developed a 2D ABM for simulation of restenosis in blood vessels occuring after angioplasty and bare-metal stent implantation. Their research highlighted how different vessel geometries and stent placements influence restenosis development, using realistic pathologic geometries and modeling atherosclerotic plaque as an inert entity. Olivares et al. (2017) (Olivares et al., 2017) advanced this approach with a 3D ABM to simulate early foam cell formation in the intima. They focused on dynamic interactions involving LDL oxidation, persistence of oxidized LDL, and macrophage transformation into foam cells.

In addition to discrete methods like CA and ABM, robust numerical methods such as finite element modeling (FEM) can be integrated into hybrid frameworks. FEM offers advantages in quantification of arterial wall stress and wall shear stress (WSS) role exploration in atherosclerosis pathogenesis, linking mechanotransduction at the cellular level. Diseases associated with pathogenesis incorporate the release of specific chemicals in the endothelium, permeability of low-density lipoprotein, cellular and extracellular functions, proliferation of smooth muscle cell, and the dynamics of extracellular matrix (ECM) (Chatzizisis et al., 2007).

Zahedmanesh and colleagues developed an innovative hybrid biological modeling framework that integrates a 2D agent-based model (ABM) in continuum space with a finite element model (FEM) (Zahedmanesh & Lally, 2012). The FEM component was employed to quantitatively assess von Mises stresses, crucial for evaluating arterial damage following stent deployment. Meanwhile, the ABM in their work focused on simulating the migration, proliferation, and degradation of ECM, as well as its synthesis within the arterial wall due to restenosis as quantified by the FE analysis. Previously, this modeling framework successfully elucidated vascularization patterns in tissue-engineered blood vessels, revealing insights into how scaffold compliance and loading regimes influence the growth of vascular smooth muscle cells and their role in intimal hyperplasia development (Zahedmanesh & Lally, 2012).
Garbey and collaborators developed another hybrid computational framework that integrates Partial Differential Equations (PDE) with ABM to study vascular adaptation post-acute interventions (Garbey et al., 2015). PDEs accurately describe continuum mechanics, calculating hemodynamic forces and stress-strain relationships defining the vascular environment. In contrast, the fixed grid ABM comprehensively models discrete cellular elements within the tissue, tracking cell dynamics including proliferation, apoptosis, and ECM production or degradation. This computational approach was further refined to relax assumptions, particularly regarding cellular motion which ideally should be computed in a continuum space rather than on a discrete grid. This advancement allows for a more realistic simulation of biological laws governing cellular behavior and the active role of membrane interfaces between vascular layers (Garbey et al., 2019).

Current multiscale models of atherosclerosis capture the complex interplay between hemodynamics and arterial wall remodeling during plaque development and atherogenesis (Bhui & Hayenga, 2017; Corti et al., 2019; Corti et al., 2020). These frameworks are based on coupled stochastic ABM for cellular dynamics and a hemodynamics module for blood flow computation. Bhui and Hayenga (2017) incorporated a molecular module to describe transport processes of inflammatory cytokines and LDL within arterial walls, applied to a 3D idealized coronary artery model to investigate the role of wall shear stress (WSS) in leukocyte trans-endothelial migration (TEM) and plaque progression. Computational fluid dynamics (CFD) simulations computed the WSS profile, used for initializing the ABM process. During plaque growth, changes in luminal geometry simulated by ABM are coupled with CFD to calculate hemodynamics in current vascular geometry and update WSS distribution.

In their implementation, a 3D ABM model featured a uniform arterial wall layer covered by endothelial cells and leukocytes as active agents. Behavioral rules governed endothelial adhesion, TEM, and other cellular processes, with leukocyte adhesion probability influenced by WSS, circulating cytokines, and leukocyte concentration. TEM was defined relative to arterial stiffness, while LDL transport and accumulation in the arterial wall depended on WSS and systemic LDL concentration, modeled according to Fick's law. Rules governing LDL oxidation and phagocytosis by monocyte-derived foam cells were applied, incorporating Glagov's remodeling theory which preserves lumen area during initial atherosclerosis phases through compensatory outward remodeling (Glagov et al., 1987).

3.4. Applications of AI in medicine

AI in healthcare is a rapidly evolving field, offering promising solutions to some of the most pressing challenges in this sector. However, the integration of AI into healthcare also raises various ethical, legal, and social issues. Consequently, there is a growing need for comprehensive regulations to govern the use of AI in healthcare (Shearer et al., 2021). In the changing world of artificial intelligence, the European Union stands as a predecessor of balance between innovation and the safeguarding of fundamental rights. The EU's regulatory framework for AI is carefully crafted, embodying a risk-based approach that distinguishes between high-risk and low-risk AI applications. High-risk AI systems, given their profound impact on safety and fundamental rights, have stringent requirements imposed onto them. These encompass robust data governance to ensure data quality and representativeness, comprehensive documentation for traceability, and explicit transparency to inform users about the AI's capabilities and limitations. The essence of human oversight is not lost, mechanisms are designed in a manner that allows human intervention, ensuring that AI operates within the bounds of safety and ethics. On the other hand, low-risk AI systems enjoy a breath of freedom, with regulations that are designed to foster innovation and widespread adoption. Every high-risk AI system is subjected to a rigorous conformity assessment, and those that are deemed approved are marked with the CE marking - a certificate to their compliance with the standards of the EU. Yet, in this world of artificial intelligence, there are practices that the EU holds in prohibition, particularly those that violate fundamental rights. Social scoring and manipulative practices are banished, and the use of AI for biometric identification is stringently limited, especially in the sanctuaries of public spaces. The guardians of these regulations are the national supervisory authorities, established in each EU member state, overseen by the watchful eyes of the European Artificial Intelligence Board. This board, a congregation of representatives from each member state and the Commission, ensures the harmonious application of AI rules across the grandeur of the EU. In the pursuit of innovation and excellence, the EU nurtures a dynamic AI ecosystem. Small and medium-sized enterprises and startups, the leaders of innovation, are supported with special provisions, ensuring that the blossoms of their creativity enriches the AI landscape. The EU's outlook is not limited to its borders, it extends globally, aiming to shape international norms and standards for AI. It is a dance of diplomacy and technology, facilitating international data flows while upholding the sanctity of data protection. Public engagement and ethical considerations are the soul of the EU's AI regulation. Both public and a variety of stakeholders, are involved in the process of AI development and governance. In this narrative, the EU stands not as a solitary entity but as a collective, where innovation, ethics, and public welfare are intertwined in the artificial intelligence (Krishnan Ganapathy, 2021).

The European Union's Artificial Intelligence Act is a comprehensive document that delineates the regulatory landscape for AI applications, with a particular focus on high-risk systems. It carefully outlines the Parliament's position on various AI applications, underscoring the imperative for stringent regulations to mitigate associated risks. Biometric categorization systems and predictive policing emerge as focal points of regulatory scrutiny. The Parliament advocates for a prohibition on biometric systems that utilize sensitive characteristics, such as gender, race, and ethnicity. Similarly, predictive policing systems, especially those rooted in profiling, location, or past criminal behavior, are earmarked for stringent oversight. The document elaborates on the expanded definition of high-risk AI systems, encapsulating those that pose a 'significant risk' to

health, safety, fundamental rights, or the environment. AI applications deployed in political campaigns and by very large online platforms, as defined under the Digital Services Act, are categorised as high-risk, warranting enhanced regulatory oversight. The Act also addresses general-purpose AI and foundation models, imposing obligations on providers to safeguard fundamental rights and democracy. Generative AI models, exemplified by systems like ChatGPT, are subjected to stringent transparency obligations, ensuring accountability and ethical deployment. In the realm of governance and enforcement, the Act empowers national authorities with unprecedented access to both trained and training models of AI systems. It proposes the establishment of an AI Office to facilitate the harmonised application of the AI Act across member states. The Act underscores its commitment to fostering innovation and research, with a pronounced emphasis on the development and deployment of free and open-source AI. High-risk AI systems are subjected to a new regulatory regime, encompassing ex-ante conformity assessment and mandatory registration in an EU-wide database. These systems must adhere to stringent requirements spanning risk management, testing, technical robustness, data training and governance, transparency, human oversight, and cybersecurity (Novelli et al., 2023).

United Kingdom´s National Health Services, the NHS, which offers free health care, is at a key point when it comes to regulations associated with AI. Recent advancements, especially in machine learning and deep learning, have led to algorithms that can perform tasks comparable to doctors, such as diagnostics and managing complex treatments. The NHS's extensive data on citizens' health throughout their lives positions it to be a leader in healthcare AI. The NHS collects a vast amount of patient data daily, which is invaluable for training AI systems. However, this raises significant ethical and legal concerns, particularly regarding potential misuse. Public trust in how the NHS handles patient data is crucial, and incidents like the unauthorized use of data from 1.6 million patients by the Royal Free NHS Trust for AI development have raised concerns. Ensuring explicit patient consent for the use of their data in AI is essential. However, the actual use of AI in the NHS is still limited, primarily due to the lack of comprehensive policy guidance (Hart, 2024).

In response to the growing importance of AI, the UK government published a code of conduct in 2018. This code outlines expectations for AI development in the NHS, focusing on proper data handling, algorithmic transparency, and accountability. It aims to provide a policy framework for creating safe and effective AI applications in healthcare. However, this code is still in the initial consultation stage, indicating ongoing development. The need for real-life data in machine learning presents ethical dilemmas, especially when patient data are used beyond their original collection purpose. Public trust could be eroded if such incidents recur, potentially leading patients to refuse to share their information. The introduction of a national data opt-out program in 2018 has given patients more control over their data, but maintaining trust and ethical standards remains a challenge (Piel et al., 2018).

As seen in the example of NHS, AI is making significant inroads into the field of medicine, promising enhancements in early detection, diagnosis, innovative therapies, personalised medicine, and disease surveillance. The rapid development and widespread application of AI present both opportunities and challenges, especially in domains previously considered exclusive to human expertise. The swift evolution of AI technologies poses a challenge for European legislators striving to keep legislation relevant and updated. Initial attempts to impose legal standards and limitations on AI applications have primarily involved soft law, including codes of conduct, recommendations, and declarations issued

by EU institutions. A central concern for legislators and stakeholders is the unintelligibility of AI systems. The explicability of AI, encompassing the traceability and explainability of AI outputs, is crucial to safeguarding individual and collective rights. The AI4People Scientific Committee established the explicability principle in 2018, emphasizing the importance of intelligibility and accountability in AI systems (Prakash et al., 2022).

AI systems used in healthcare would be categorized as High-risk AI systems in terms of the EU AI Act. High-risk AI systems are those that could potentially impact people's safety or their fundamental rights. In the context of healthcare, AI applications could potentially fall under the category of high-risk AI systems, especially if they are used as a safety component of a product or are governed by EU health and safety harmonisation legislation. Such applications would be subject to stringent regulations to ensure safety and compliance with ethical standards. The AI Act aims to mitigate the risks associated with AI applications, ensuring that they are developed and used in ways that are safe, ethical, and respect fundamental human rights (Prakash et al., 2022).

3.4.1. Decision Support Systems in Healthcare

Decision Support Systems (DSS) in healthcare are integral tools that assist clinicians and healthcare professionals in making informed and accurate decisions. These systems leverage a combination of technologies, data, and algorithms to provide insights and recommendations, enhancing the quality and efficiency of healthcare delivery. Healthcare DSS integrates a vast array of data sources, including Electronic Health Records (EHRs), laboratory results, and medical imaging data. For instance, Kawamoto et al. (2005) demonstrated that the integration of clinical data into DSS significantly improves clinical practice and patient outcomes. These systems utilize advanced algorithms and artificial intelligence to analyze complex datasets, offering personalized recommendations for patient care. Clinical Decision Support (CDS) systems, a subset of DSS, are particularly notable for their role in diagnosis and treatment. They analyze patient-specific data to provide evidence-based recommendations. A study by Osheroff et al. (2012) highlighted the role of CDS in reducing medical errors, improving healthcare quality, and reducing costs. However, the implementation of DSS in healthcare is not without challenges.

Ethical and privacy concerns are paramount, underscoring the intricate balance between technological advancement and ethical considerations. The ethical implications of using DSS were analyzed by Ammenwerth et al (Ammenwerth and Rigby, 2016). shedding light on a spectrum of concerns that are as diverse as they are complex. One of the primary concerns, as mentioned by both the EU AI act and the UK regulation is data privacy. With DSS integrating vast amounts of sensitive patient data, the risk of unauthorized access and data breaches is a significant concern. Patients' confidential information, including medical histories, diagnoses, and treatment plans, must be safeguarded with the utmost integrity. The systems must comply with legal frameworks like the Health Insurance Portability and Accountability Act (HIPAA) in the U.S. or the General Data Protection Regulation (GDPR) in Europe, which impose stringent measures to protect patient data. In addition to privacy, security is another important aspect. The infrastructure supporting DSS must be fortified against potential cyber-attacks and unauthorized access. The integrity of the data and the systems is crucial not just for the privacy of the individuals but also for the accuracy and reliability of the decision support provided. A breach could not only compromise privacy but also the quality of healthcare delivery. The potential for bias in algorithmic recommendations is also a pressing ethical issue. Algorithms are

designed and trained by humans, and can inadvertently inherit biases present in the training data or the designers. This can lead to skewed or unfair recommendations, impacting certain patient groups disproportionately. It underscores the need for transparency, fairness, and accountability in the design and implementation of algorithms in DSS. The issue of informed consent also looms large. Patients must be adequately informed about how their data will be used and must have the autonomy to consent or decline. The transparency in the usage of data and the decisions made by DSS is integral to building trust and ensuring ethical standards (Ammenwerth et al., 2018).

3.4.2. AI in Diagnosis and Treatment

Artificial intelligence continues to revolutionize the field of medical diagnosis, with advancements in machine learning, particularly deep learning, leading the charge. These technologies have proven instrumental in enhancing the accuracy, speed, and efficiency of diagnosing a variety of medical conditions. The integration of AI in healthcare has been a subject of ongoing research and development over the past few years (Jiang et al., 2017). AI systems, particularly machine learning (ML) and deep learning (DL) algorithms, have demonstrated unprecedented capabilities in diagnosing diseases, sometimes outperforming human clinicians (Esteva et al., 2019).

In addition to clinical DSS, application of AI and DSS extends towards management and maintenance of medical equipment. As medical equipment stands at the forefront of medical decision making it is of utmost importance to ensure its performance and accuracy. The European Commission has stipulated the importance of this by introduction of post-market surveillance as mandatory in the new medical device regulation (MDR) introduced in 2017 and put in force in 2022 (Badnjević and Vuković, 2020, Badnjević and Pokvić, 2020, Badnjević et al., 2022, Badnjevic et al., 2023).

Post-market surveillance of medical devices (Badnjević et al., 2015) has been proven useful in case studies conducted in Bosnia and Herzegovina where a large number of medical devices has been deemed inaccurate on the basis of performance inspection (Gurbeta et al., 2018a, Gurbeta and Badnjević, 2017, Gurbeta et al., 2016a, Gurbeta et al., 2015, Gurbeta et al., 2017, Gurbeta et al., 2018b, Gurbeta et al., 2016b). As a result of performing post-market surveillance, a vast amount of data was collected and the team from Verlab has decided to utilize it and design algorithms capable of predicting medical device failure on the basis of their performance throughout the years (Hadžić et al., 2020, Hrvat et al., 2020, Spahić et al., 2020). Transcending the diagnostic challenges and ensuring safe and reliable measurements made by medical devices, the following paragraphs will briefly describe the applications of AI as DSS for aiding in diagnosis, treatment and prognosis of the leading causes of mortality and co-morbidity worldwide.

In oncology, AI models have been developed to predict cancer development, progression and treatment planning (Nuhić et al., 2020, Spahić and Ćordić, 2020). AI algorithms analyze complex data sets, including genomic, proteomic, and imaging data, to identify the most effective treatment strategies (Hafizović et al., 2021, Mujkić et al., 2022). By integrating and analyzing vast and complex genomic data, AI identifies specific gene mutations and pathways associated with individual cancers. This genomic insight facilitates the development and administration of targeted therapies, enhancing treatment efficacy while minimizing adverse effects. Zhang et al. (2019) (Zhang et al., 2019) illustrated how AI could predict gene mutations from imaging data, leading to personalized treatment strategies for lung cancer patients. AI also empowers clinicians to

personalize chemotherapy regimens by predicting individual patient responses to various drugs. Algorithms analyze clinical, genomic, and proteomic data to identify optimal drug combinations and dosages, minimizing toxicity and enhancing treatment outcomes.

AI has been instrumental in diagnosing respiratory diseases like asthma (Stokes et al., 2021), chronic obstructive pulmonary disease (COPD) (Badnjevic et al., 2014, Bećirović et al., 2021), and lung cancer. AI algorithms have demonstrated accuracy in identifying malignant nodules in CT scans (Ardila et al., 2019). Moreover, AI-based systems are being employed to analyze pulmonary function tests and predict COPD exacerbations, offering valuable insights for treatment planning (Golpe et al., 2022). Machine learning models are instrumental in predicting COPD exacerbations, enhancing preventive measures and treatment planning (Bećirović et al., 2021). Deep learning algorithms analyze sputum smear microscopy images to detect Mycobacterium tuberculosis with high accuracy (Lopes and Valiati, 2017). In addition to medical imaging data, clinical data was used to predict the severity of COVID-19 clinical presentation (Badnjević et al., 2024).

AI has been prominently used for the early prediction of metabolic disorders such as lactose intolerance (Spahic et al., 2020), Addison disease (Džaferović et al., 2022) and type 2 diabetes (Alić et al., 2017). Machine learning models leverage data such as patient demographics, clinical parameters, and lifestyle factors to predict the onset of diabetes (Alic et al., 2017). AI can also be used for prediction and management of gestational diabetes, a type of diabetes that affects pregnant women. Machine learning models analyze prenatal data, including maternal age, body mass index (BMI), family history, and blood glucose levels to predict the risk of developing gestational diabetes, enabling preventive measures (Desai et al., 2024).

AI also plays a critical role in drug discovery, significantly reducing the time and resources traditionally required. Machine learning algorithms predict the pharmacological properties of various compounds, identifying potential new drugs. Machine learning models predict the biological activity of numerous compounds, facilitating the selection of promising candidates for further development. Chen et al. (2018) (Chen et al., 2018) discussed the role of AI in analyzing biological networks to identify potential drug targets and pathways, accelerating preclinical drug development. AI models can also predict potential drug targets and analyze complex biological data to develop new therapeutic agents, as evidenced in the rapid development of treatments and vaccines for diseases like COVID-19. AI is also enhancing clinical trial design, recruitment, and execution, ensuring the expedited development and approval of new drugs. Machine learning models analyze vast datasets, including electronic health records and real-world data, to identify optimal trial designs, predict patient responses, and monitor adverse effects in real-time.

AI enhances mental health treatment by providing personalized interventions and real-time monitoring. Machine learning models analyze patient data, including speech, text, and behavioral patterns, to identify mental health conditions and monitor treatment progress. AI-powered applications and chatbots provide instant, personalized therapeutic interventions, improving accessibility and effectiveness of mental health care (Iniesta et al., 2016). AI is instrumental in physical rehabilitation, offering personalized treatment plans and real-time monitoring of patient progress. AI algorithms analyze data from sensors and wearable devices to tailor rehabilitation exercises to individual patients' needs, optimizing recovery outcomes. Machine learning models also predict patient progress and adapt treatment plans accordingly, ensuring optimal rehabilitation

efficiency and effectiveness (Pobiruchin et al., 2017). AI aids in personalizing pain management strategies, ensuring patients receive effective relief tailored to their specific needs. Machine learning algorithms analyze clinical, genomic, and real-time data to predict individual responses to various pain management interventions. AI applications in mobile health technologies enable real-time monitoring and management of pain, improving patient outcomes and quality of life (Campion et al., 2016).

Integration of AI into everyday healthcare practice is a part of the fourth industrial revolution, commonly termed as Industry 4.0 (Pokvic et al., 2020). Developing computing capabilities and big data processing are effectively used to automate and expedite hospital and clinical processes thus ensuring state of the art healthcare for every patient at any time (Bećirović et al.).

3.5. State of the art in AI in cardiovascular field

Figure 8 shows the diverse aplications of artificial intelligence in the field of cardiovascular medicine.

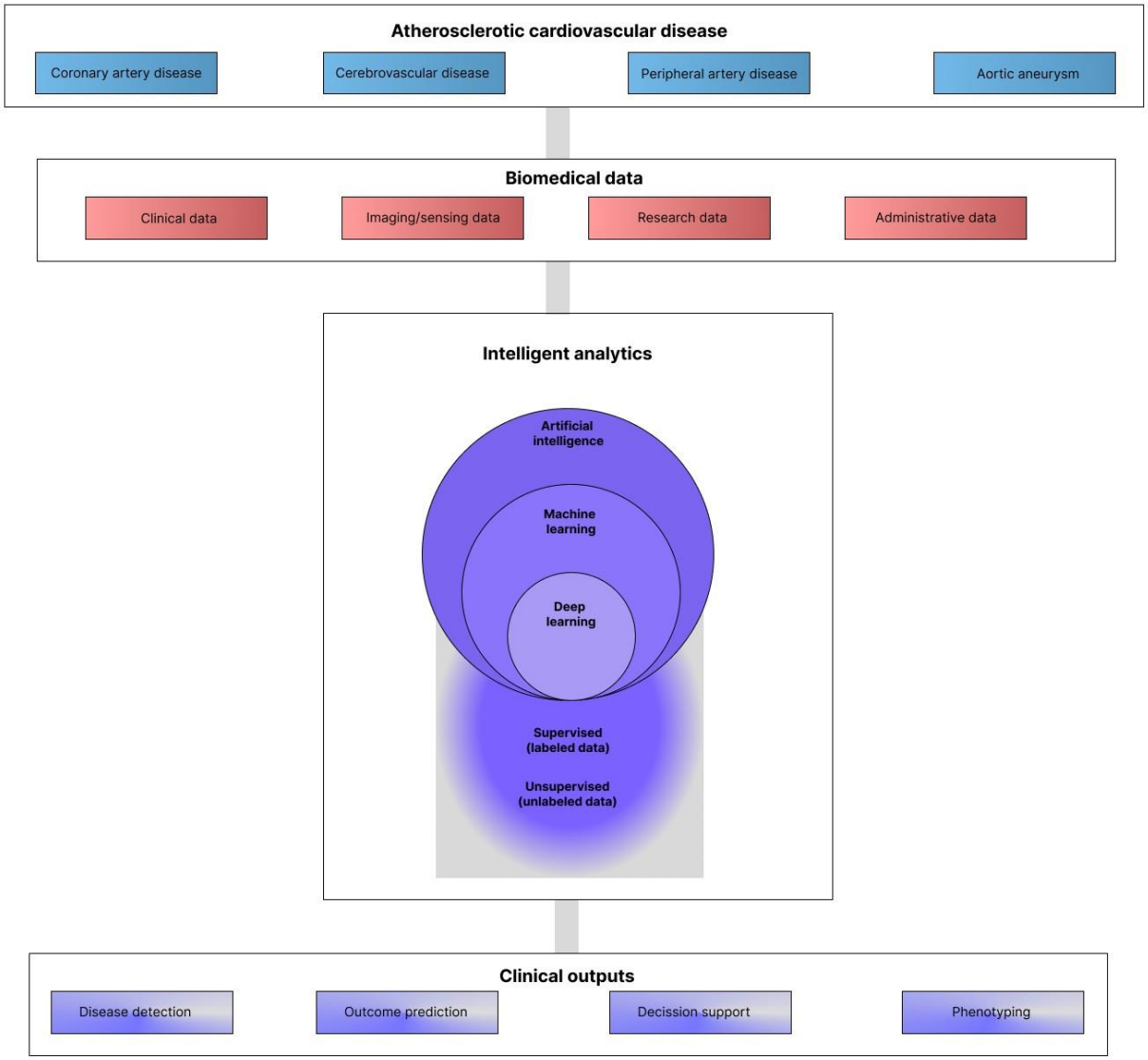

Figure 8. Fields of application of AI in cardiovascular medicine

AI has revolutionized the perception of early detection of atherosclerosis by automating image analysis and predicting plaque progression through clinical data integration (Föllmer et al., 2024, Rogers and Aikawa, 2019, Wang and Zhu, 2024). Traditional diagnostic methods often rely on manual interpretation of medical images, which can be time-consuming and prone to subjective error. In contrast, AI enables the rapid and accurate analysis of large volumes of patient data, allowing for more precise identification of atherosclerotic changes at earlier stages, when interventions can be most effective. Machine learning (ML) and deep learning (DL) algorithms have demonstrated remarkable capabilities in processing diverse and complex datasets, including electronic health records (EHRs), medical imaging, and genetic profiles (Maragna et al., 2021). These data sources collectively provide a multidimensional view of patient health, offering insights

that span both clinical parameters and detailed anatomical features. The integration of these diverse datasets through AI techniques enables a more holistic approach to diagnosing and predicting diseases such as atherosclerosis, where multiple factors converge to influence disease onset and progression (Spahić et al., 2023).

Medical Imaging plays a pivotal role in the assessment and diagnosis of atherosclerosis, particularly in visualizing plaques within the arteries (Mushenkova et al., 2020). ML and DL models, especially convolutional neural networks (CNNs), are increasingly applied to process large volumes of medical images such as coronary computed tomography angiography (CCTA), magnetic resonance imaging (MRI), and intravascular ultrasound (IVUS) (Kolossváry et al., 2017, Lee et al., 2016). These imaging modalities provide high-resolution images of the arterial walls, enabling the detection of plaques, calcifications, and vessel stenosis. CNNs can be trained to identify and classify different types of atherosclerotic plaques—such as lipid-rich, fibrous, or calcified—based on their appearance in these images (Athanasiou et al., 2014, Kunchur and Mostaço-Guidolin, 2022, Kolluru, 2018, Shibutani et al., 2021). The ability of CNNs to detect subtle features that may be missed by human observers, such as micro-calcifications or minute changes in plaque composition, allows for earlier and more accurate diagnosis of high-risk atherosclerotic lesions .

In addition to detecting plaques, AI-driven models can quantify the extent of arterial narrowing, assess the stability of plaques (distinguishing between stable and unstable plaques that are prone to rupture), and track changes in the size or composition of plaques over time (Föllmer et al., 2024). By automating the process of image analysis, AI reduces the variability that arises from manual interpretation by clinicians, ensuring more consistent and reliable diagnoses. Moreover, integrating imaging data with clinical risk factors from EHRs allows ML models to develop more robust predictions of disease progression, offering a comprehensive view of the patient's cardiovascular health(Amal et al., 2022, Sanchez-Martinez et al., 2022).

Genetic profiles add yet another layer of complexity and richness to the data that AI models can process. Genetic factors play a significant role in determining an individual's predisposition to atherosclerosis. Genome-wide association studies (GWAS) have identified numerous genetic variants associated with an increased risk of atherosclerotic cardiovascular disease (Holdt et al., 2013). These include variants in genes related to lipid metabolism (such as LDLR or APOB), inflammation (e.g., IL6), and vascular homeostasis (e.g., NOS3) (Butnariu et al., 2022). By integrating genetic data with clinical and imaging information, AI models can identify genetic predispositions that, in combination with lifestyle factors, contribute to an individual's overall risk of developing atherosclerosis (Krittanawong et al., 2022, Usova et al., 2021). One of the strengths of AI in this domain is its ability to handle high-dimensional data, where the number of variables (such as genetic markers) far exceeds the number of patients. Traditional statistical methods may struggle with this type of data, particularly when interactions between genetic and environmental factors are complex. However, ML algorithms, especially those using regularization techniques, can identify subtle associations between genetic variants and disease outcomes, offering insights into how specific genetic profiles influence the development and progression of atherosclerosis (Okser et al., 2014).

EHRs represent a critical source of clinical data for AI-based models, encompassing detailed patient information such as medical history, laboratory results, medications, and physician notes. Within the context of atherosclerosis, EHRs hold valuable insights on traditional cardiovascular risk factors, including cholesterol levels, blood pressure, the presence of hypertension, diabetes, smoking status, body mass index (BMI), and family history of cardiovascular disease (Carrasco-Ribelles et al., 2023). These variables are essential for assessing an individual's risk for developing atherosclerosis and its related complications, such as coronary artery disease or stroke. ML algorithms can efficiently sift through these massive datasets, uncovering correlations between patient risk factors and atherosclerosis development that might not be immediately apparent through traditional statistical methods. For instance, algorithms can detect non-linear relationships between risk factors or interactions that contribute to a heightened risk for plaque formation. Moreover, beyond risk factor stratification, EHRs also provide longitudinal data, allowing for tracking patient health over time. By analyzing trends in laboratory results or changes in medication regimens, ML models can predict future cardiovascular events or plaque progression with a high degree of accuracy. This longitudinal aspect of EHRs is particularly useful for developing personalized treatment plans, as the AI models can adjust risk estimates based on new clinical data, leading to more dynamic and individualized patient care (Carrasco-Ribelles et al., 2023). When these data sources—EHRs, imaging, and genetics—are combined, ML and DL algorithms can offer unprecedented insights into atherosclerosis risk stratification. These models can not only predict the likelihood of plaque formation but also forecast its progression and potential complications, helping clinicians tailor preventative and therapeutic strategies to the needs of each patient (Seckanovic et al., 2020). Moreover, these AI systems can adapt as more data is collected, continuously refining predictions and treatment recommendations in real-time, thus leading to more dynamic and personalized care.

AI is very useful in predicting heart failure using electronic health records and real-time cardiac monitoring data. Machine learning algorithms can analyze vast datasets, including clinical, laboratory, and imaging data, to identify early signs of heart failure, enabling proactive management (Futoma et al., 2017; Spahic et al., 2023; Seckanovic et al., 2020). A study by Weng et al. (2017) employed machine learning algorithms to predict the risk of cardiovascular disease. The study utilized electronic health data, including age, sex, ethnicity, and medication, and found that machine learning models were more accurate in predicting cardiovascular events compared to traditional statistical models. AI models, especially deep learning, are employed in the real-time detection of atrial fibrillation, a common cardiac arrhythmia. By analyzing electrocardiogram (ECG) data, AI was proven to be effective in identification of patterns indicative of atrial fibrillation with high accuracy, aiding in timely diagnosis and treatment (Hannun et al., 2019). Machine learning models can also effectively analyze coronary computed tomography angiography (CCTA) images to detect and quantify coronary plaque, thus aiding in risk stratification and treatment planning in the realm of coronary artery diseases (Spahic et al., 2023; Zreik et al., 2018). Another application of AI in the field of cardiology are ML technologies are employed for the prediction, classification, and outcome prediction of stroke. They analyze clinical data, imaging, and genetic information to classify stroke types, predict occurrences, and project recovery outcomes, significantly enhancing patient care (Hrvat et al., 2023; Monteiro et al., 2020).

4. Experimental research of atherosclerotic plaque progression

4.1. Agent Based Modeling

The dataset used for development of agent based models in this PhD thesis originates from imaging of carotid arteries with bifurcation. The initially idealized peripheral artery geometry dataset was unavailable due to experimental drawbacks. In order to ensure the reliability of the results, a more complex geometry of an artery with bifurcation was used to conduct the in silico experiments. The dataset consisted of 15 patient-specific geometries obtained by means of reconstruction from MRI. The initial geometries were incorporated into input files suitable for finite element analysis using PAK software via a data converter designed specifically for this purpose. The initial .dat files contained default set parameters for simulation.

The methodology for the agent based model adopted in this work, based on Corti et al. (2020), involves four iterative steps: 1) geometry preparation, 2) CFD simulation, 3) ABM simulation, and 4) new 3D geometry generation. Firstly, a 3D model of a healthy artery is built, followed by generation of a fluid domain mesh using PAK software. A CFD simulation is then performed in PAK to compute hemodynamics and extract Wall Shear Stress (WSS) values at the lumen interface across 2D vessel cross-sections. For each cross-section, hemodynamic-driven remodeling is simulated using an ABM that models cellular, extracellular, and lipid dynamics. The CFD simulation is responsible for calculating WSS values, while the ABM handles the remodeling of the arterial wall.

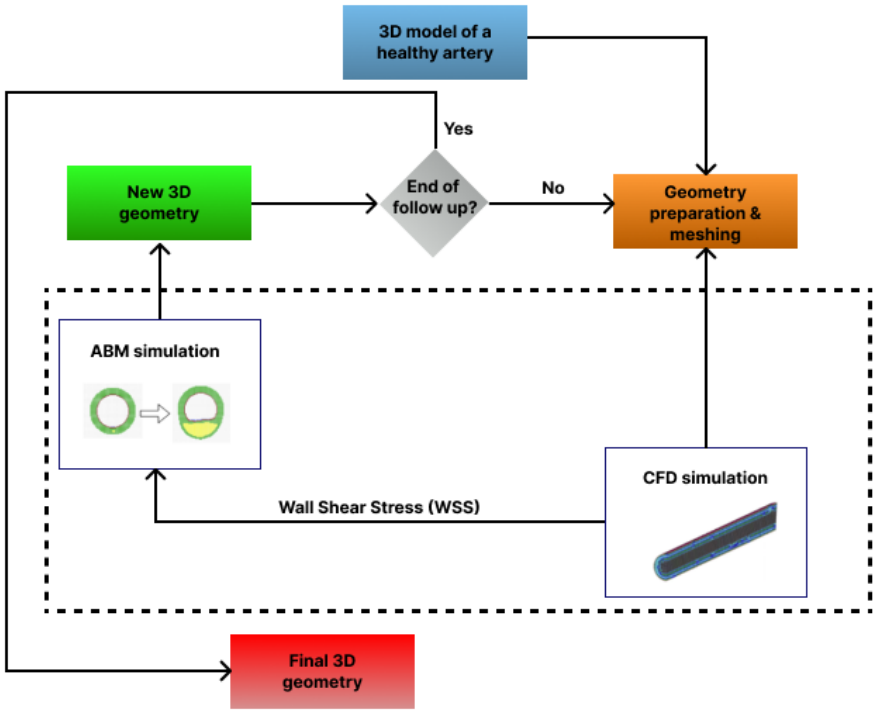

Figure 9. ABM methodology

Figure 9 outlines the workflow of the proposed framework. For each 2D cross-section, geometry changes resulting from the ABM are transferred to the fluid domain, causing a recalculation of blood flow and WSS values, which are then used to update the ABM in the next step. This coupling ensures that the WSS distribution is continuously updated as the geometry of the artery evolves. By simulating cell mitosis, ECM degradation and productin and lipid infiltration in the intima, the ABM replicats arterial wall remodeling. Various vessel structures and compositions, along with new cellular events, were incorporated into the model. The ABM used in this study was methodologically developed by Corti et al. (2020) and validated under atherogenic conditions. The coupling between the CFD and ABM modules begins by initializing the ABM with hemodynamic input.

WSS values were derived from 3D CFD simulation and eq.4 represents the calculation of endothelial dysfunction level D^i while WSS^i represents WSS at site i and WSS_o= 1Pa the WSS threshold.

$$D(WSS)^i = D^i = \begin{cases} 1 - \frac{WSS^i}{WSS_o}, \ if\ WSS^i < WSS_o \\ 0, \ otherwise \end{cases} . \qquad \text{Eq. 4}$$

WSS_o was determined based on the work of Samady et al.,(Samady et al., 2011). Each dysfunctional endothelial site i, with $D^i \neq 0$, starting a state of alteration that diffuses within the intima through isotropic diffusion, from a peak of intensity D^i with a diffusion constant φ. $A^{i,k}(D^i, d)$ represents the alteration level recorded at the k-th site and produced by the i-th endothelial site within intima, at a distance d from i (eq.5).

$$A^{i,k}(D^i, d) = A^{i,k} = D^i * e^{-\frac{1}{2}\left(\frac{d}{4\varphi t}\right)^2} . \qquad \text{Eq. 5}$$

The global inflammation level of the k-th site I^k is calculated as a sum of individual alteration states for each site k as shown in eq.6.

$$I^k = \sum_{i=1}^{N_L} A^{i,k} . \qquad \text{Eq. 6}$$

Where:

-N_L is the initial number of sites of the lumen wall

- resulting I^k that affects the agent dynamics

WSS profile was defined as atherogenic when all the WSS values at the i-th sites are larger than the designated threshold, $D^i = 0\ \forall i$ and $I^k = 0$ everywhere or if a state of inflammation I develops and the mechanisms of plaque formation are activated ($WSS^i < WSS_0$)

The physiological conditions were replicated by setting baseline probability densities for cell mitosis/apoptosis and ECM deposition/degradation rates as defined with Eq.7 and Eq.8, respectively:

$$p_{mit} = p_{apop} = \alpha_1 , \qquad \text{Eq.7}$$

$$p_{prod} = \beta * p_{deg} = \alpha_4 \,, \qquad \text{Eq.8}$$

where α_1, α_4 and β are involved in maintaining the physiological cell/ECM ratio defined for each tissue layer during initialization. (Garbey et al., 2017).

Coefficient β for the intima, media and adventitia layers were set in accordance to Garbey et al. (Garbey et al., 2017) to guarantee stable trends of ECM in each layer under baseline conditions. Eq.7 and Eq. 8 thereby trigger arterial wall remodelling, leading to the replication of healthy artery homeostasis. Inflammation level consequently increases the probability of cell mitosis and ECM production in the intima causing an increase in the number of neighboring lipids and the closeness to the lumen (Doran et al., 2008), leading to the following:

$$p_{mit} = \begin{cases} \alpha_1 \cdot (1 + \alpha_2 I^k) \; if \; n_{lip} = 0 \\ \alpha_1 \cdot (1 + \alpha_2 I^k)\big(1 + \alpha_3 n_{lip}\big)\big\{1 + \exp\big(-d^k_{lumen}\big)\big\} \; if \; n_{lip} \neq 0 \end{cases}, \qquad \text{Eq.9}$$

$$p_{prod} = \begin{cases} \alpha_4 \cdot (1 + \alpha_2 I^k) \; if \; n_{lip} = 0 \\ \alpha_4 \cdot (1 + \alpha_2 I^k)\big(1 + \alpha_3 n_{lip}\big)\big\{1 + \exp\big(-d^k_{lumen}\big)\big\} \; if \; n_{lip} \neq 0 \end{cases}, \qquad \text{Eq.10}$$

where α_2 and α_3 weight the effect of the inflammation state I^k and the influence of the neighboring lipids n_{lip}, while d^k_{lumen} is the distance between the site k and the lumen wall. The coefficients were set following the framework proposed by Corti et al.(Corti et al., 2020a).

Once the intima thickens over a given threshold (Bentzon et al., 2014), lipid dynamics is activated and lipid infiltration is calculated as the probability of a site k expressed by:

$$p_{lipid} = \alpha_5 (1 + I^k)\big\{1 + \alpha_6 \cdot \exp\big(-d^k_{lip}\big)\big\}\left(1 + \frac{n_{lip}}{\alpha_7}\right), \qquad \text{Eq.11}$$

where α_5 sets the event probability in the interval (0, 1). Lipid clustering is promoted by increasing the probability of a lipid to occupy a site k close to another lipid, whose distance is d^k_{lip} as defined in terms $\alpha_6 \cdot \exp\left(-d^k_{lip}\right)$ and $\left(1 + \frac{n_{lip}}{\alpha_7}\right)$. Only a single lipid can enter the intima at an individual time step. The terms and coefficients of Eq. 11 are set so to mimic a lipid nucleus (Otsuka et al., 2013). Once the lipids enter the intima layer, the lipid agents have to maintain their position throughout the entire simulation. Maintenance of the lipid core is ensured by defining that the agent movement is performed along the shortest path that does not include the lipid agents. In order to provide structural integrity and fidelity of the simulation the agent movement complies with the minimum energy principle at all times except in the case when the lipid agents are positioned along the shortest path. Figure 10. Tissue reorganization when K produces an element or is removed in b) the intima, c) media and d) adventitia. Figure 10 provides a schematic representation of the arterial wall (Fig. 10a), an example of generation or disposal of an agent in the intima layer (Fig. 10b), the media layer (Fig. 10c) and the adventitia layer (Fig. 10d).

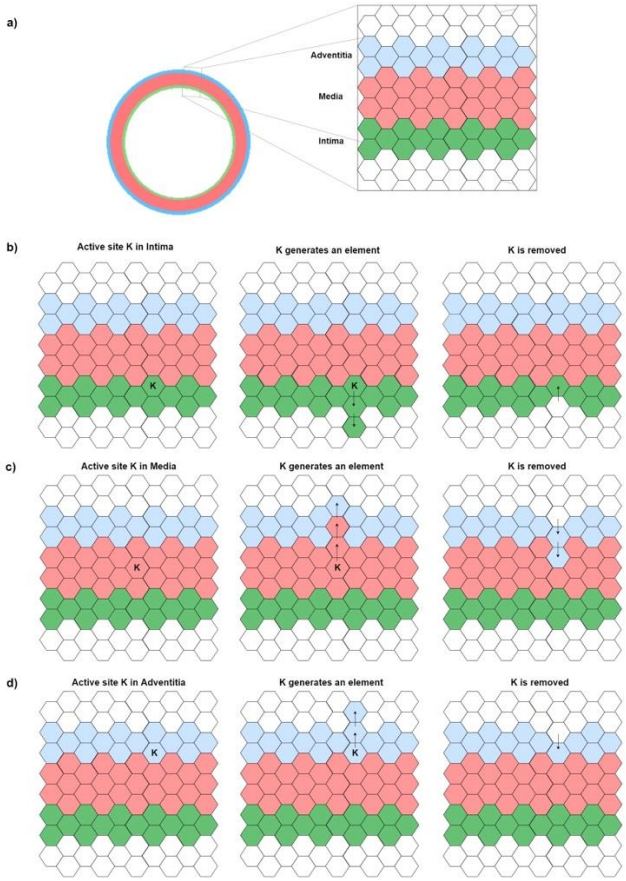

Figure 10. Tissue reorganization when K produces an element or is removed in b) the intima, c) media and d) adventitia.

A distinct 3D geometry of the vessel lumen is constructed, and the initial ABM configuration for each plane in the subsequent cycle is determined. For each ABM solution at a specific cross-section (M), the lumen and external radii, along with plaque thickness, are calculated and represented as: $R_j^i(\vartheta)$, with $j = 1,2,3$, respectively. The corresponding deviation, Δ^i, from the average configuration, $\overline{R_j(\vartheta)}$ was computed as defined in Eq. 12, and the ABM i-th output minimizing Δ was selected:

$$\Delta^i = \sum_{j=1}^{3} \int_0^{2\pi} w_j \sqrt{\left(R_j^i(\vartheta) - \overline{R_j(\vartheta)}\right)^2 d\vartheta} \ , \qquad \text{Eq.12}$$

where each j-th quantity is weighed by w_j. The same criterion was applied for all cross-sections and the 3D geometry was finally reconstructed.

Coupling FE computational fluid dynamics with ABM

Blood flow dynamics can be effectively modelled using continuum methods like the Finite Element Method (FEM). By numerically solving the Navier-Stokes equations, it is possible to obtain velocity and pressure fields, as well as the distribution of shear stresses along the vessel wall. Recent studies have demonstrated that hemodynamic parameters play a crucial role in the development of atherosclerosis, with Wall Shear Stress being one of the

key factors. WSS influences the transport of LDL from the bloodstream into the vessel wall, thereby impacting the progression of atherosclerosis.

Atherosclerosis progresses through intricate molecular interactions within the vessel wall, governed by distinct rules and involving various cellular and molecular components. The process initiates when LDL particles penetrate the vessel wall, linking the molecular dynamics of atherosclerosis to the hemodynamic characteristics of blood flow. To address the interplay between macroscopic blood flow and microscopic disease mechanisms, a hybrid model integrating FEM and an ABM was established. The ABM parameters are drawn from references outlined in the theoretical background section, while the LDL entry rate into the domain varies and is derived from FEM outputs. The distribution of axial LDL flux along the vessel is projected onto the ABM's horizontal axis, with LDL source locations evenly spaced along this axis. The entry rate at each source is scaled to the LDL flux at the corresponding FEM coordinate, while the vertical positioning of these sources is randomized. This setup provides the boundary conditions for simulating atherosclerosis progression using the ABM. Figures presented in a comparative manner in Tables 1-13 show the changes in the geometry of the artery due to remodelling driven by agent-based modelling coupled with blood flow. The results are presented for the variables wall shear stress, velocities and the ABM modulus.

Table 1. ABM results for patient specific geometry 1

Time step 1	Time step 15
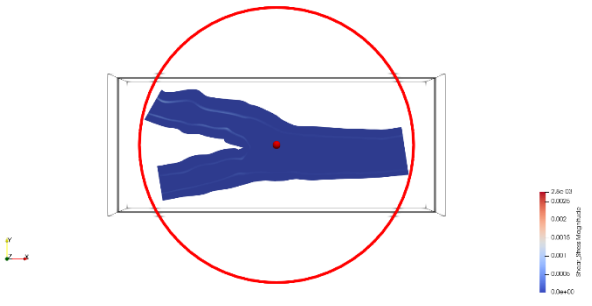	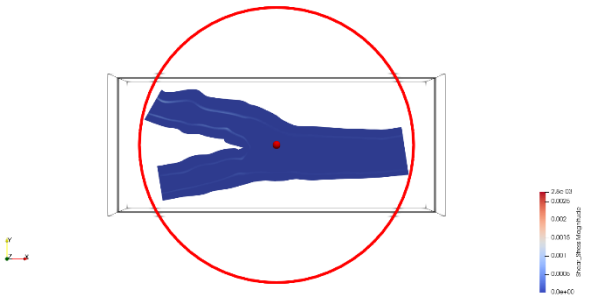
Wall shear stress (WSS)	
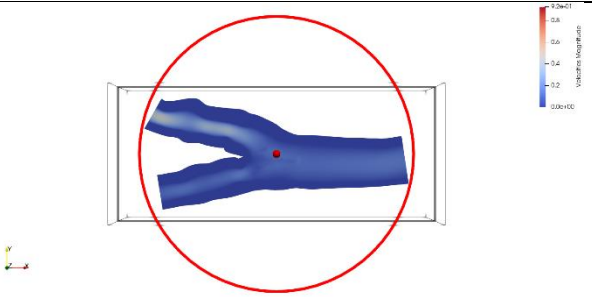	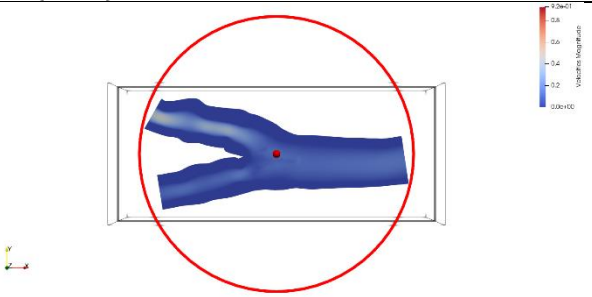
Velocities	
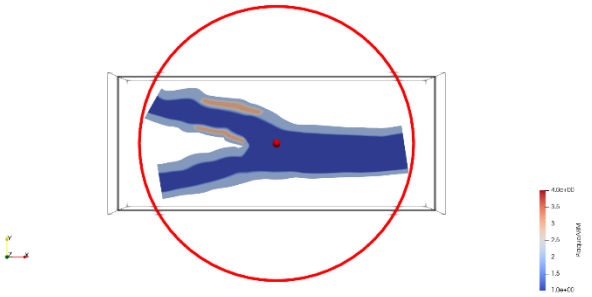	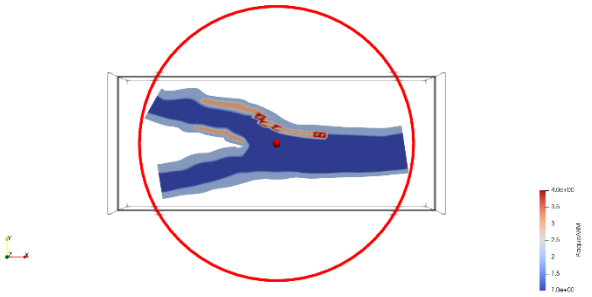
Agent based model (ABM)	

Table 2. ABM results for patient specific geometry 2

Time step 1	Time step 15
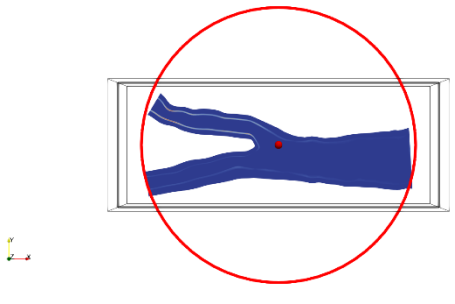	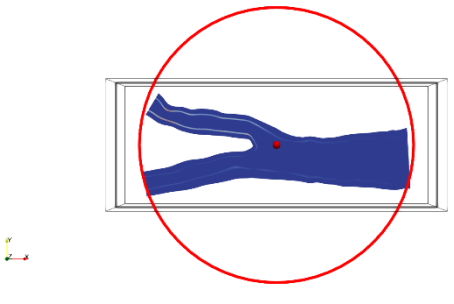
Wall shear stress (WSS)	
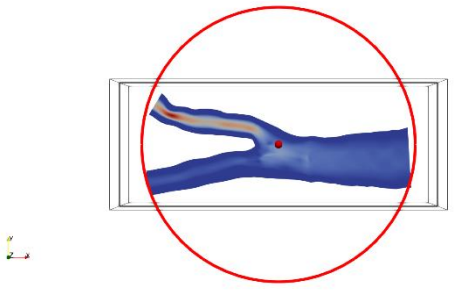	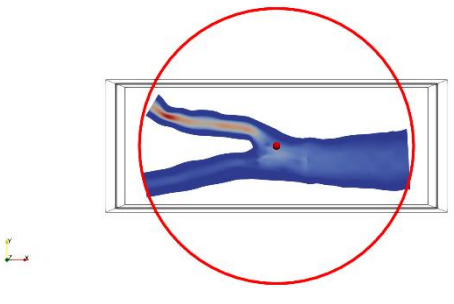
Velocities	
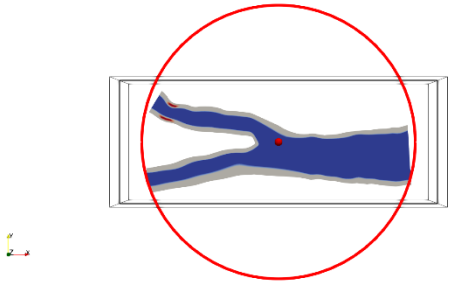	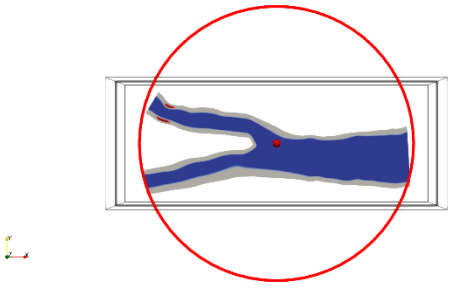
Agent based model (ABM)	

Table 3. ABM results for patient specific geometry 2

Time step 1	Time step 15
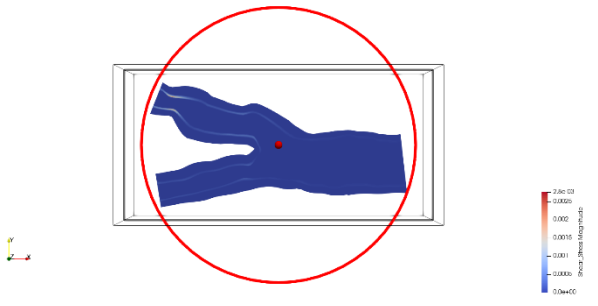	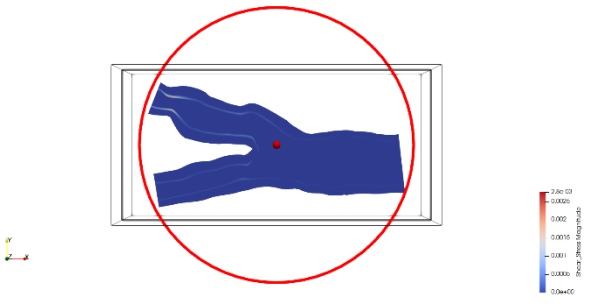
Wall shear stress (WSS)	
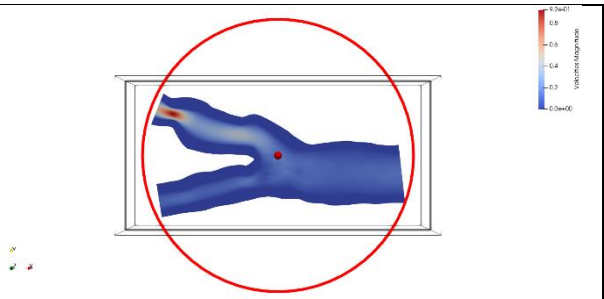	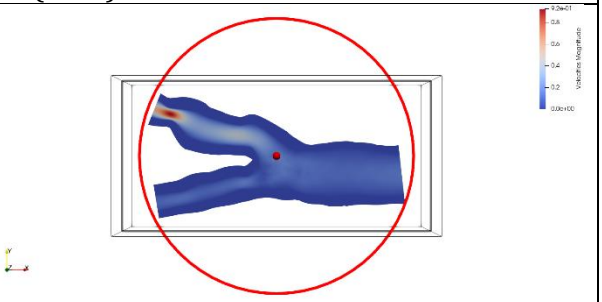
Velocities	
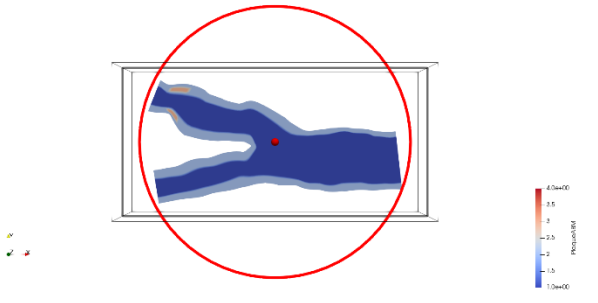	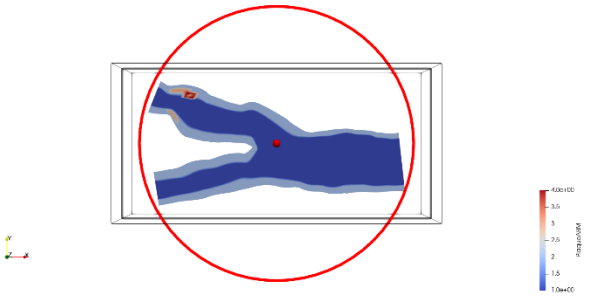
Agent based model (ABM)	

Table 4. ABM results for patient specific geometry 4

Time step 1	Time step 15
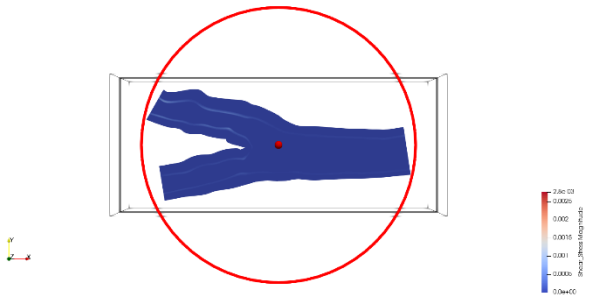	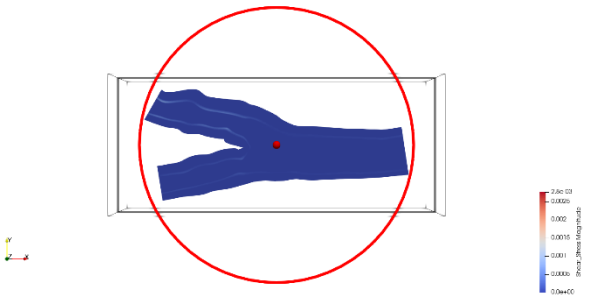
Wall shear stress (WSS)	
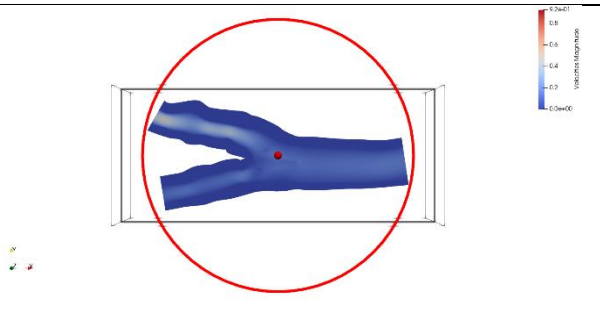	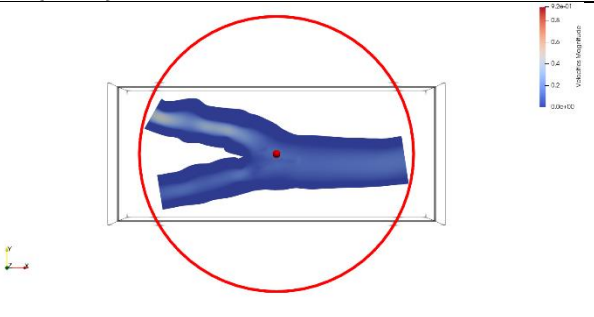
Velocities	
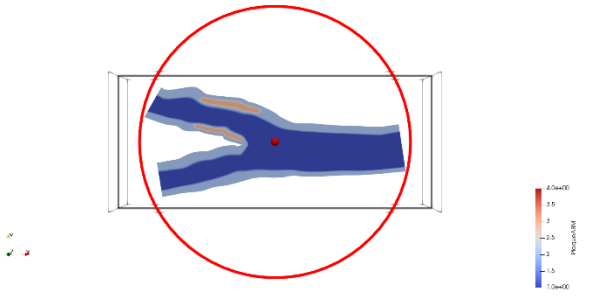	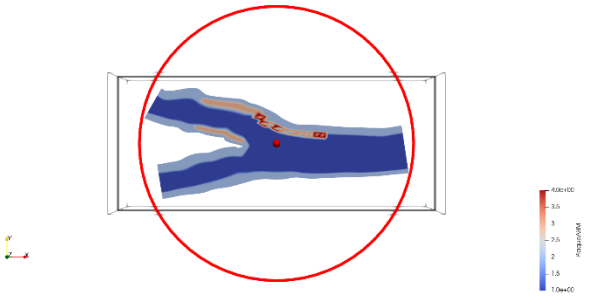
Agent based model (ABM)	

Table 5. ABM results for patient specific geometry 2

Time step 1	Time step 15
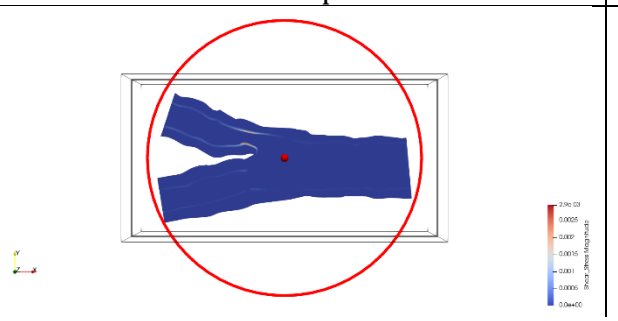	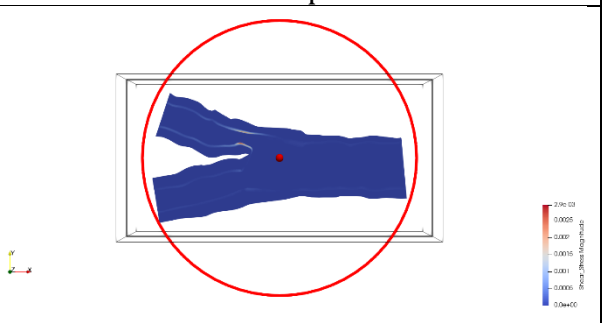
Wall shear stress (WSS)	
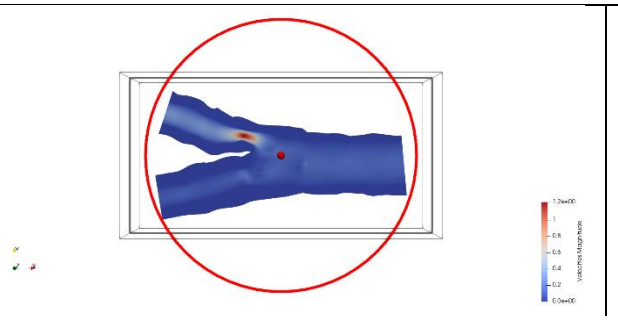	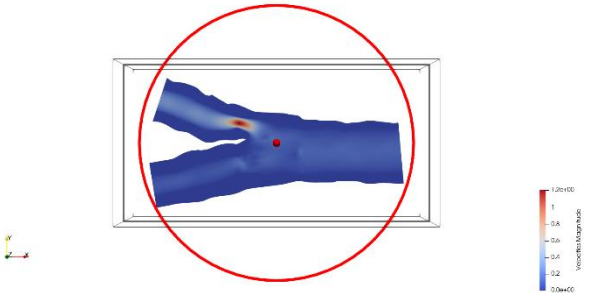
Velocities	
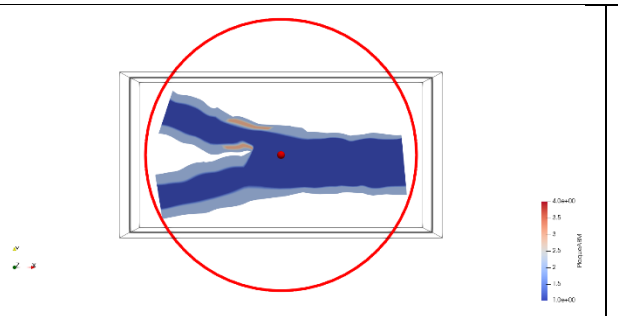	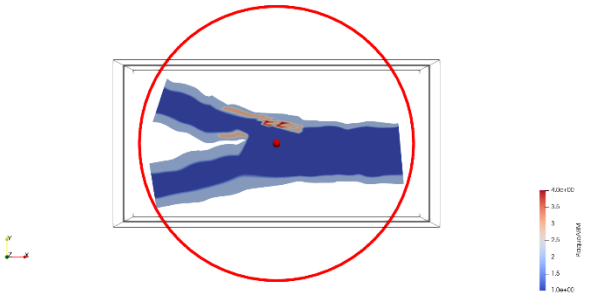
Agent based model (ABM)	

Table 6. ABM results for patient specific geometry 6

Time step 1	Time step 15
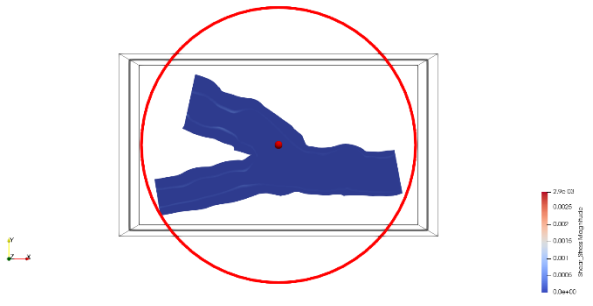	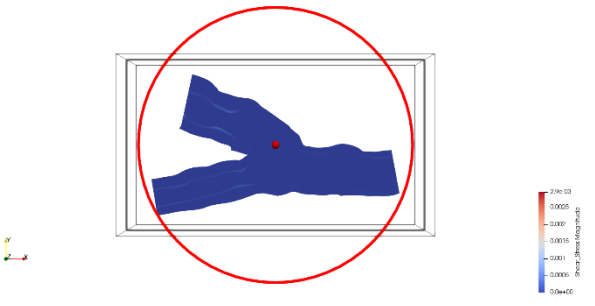
Wall shear stress (WSS)	
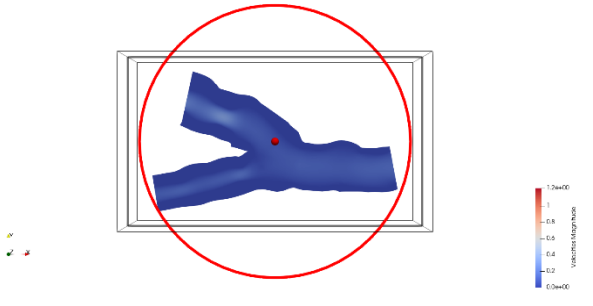	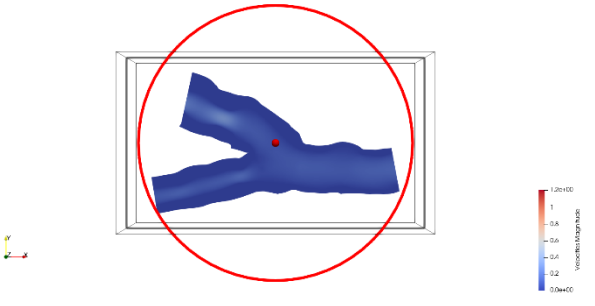
Velocities	
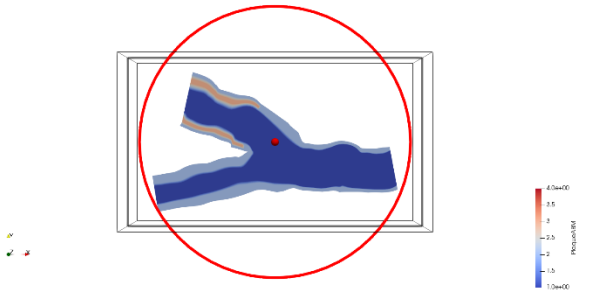	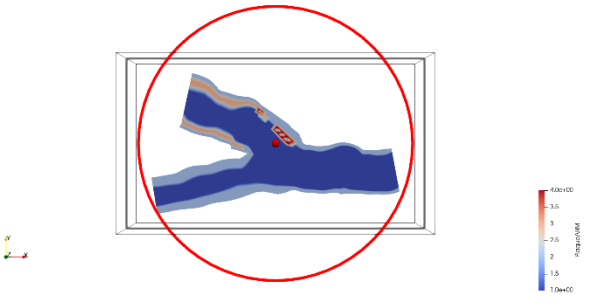
Agent based model (ABM)	

Table 7. ABM results for patient specific geometry 7

Time step 1	Time step 15
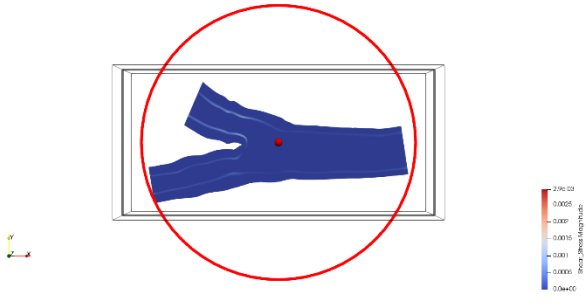	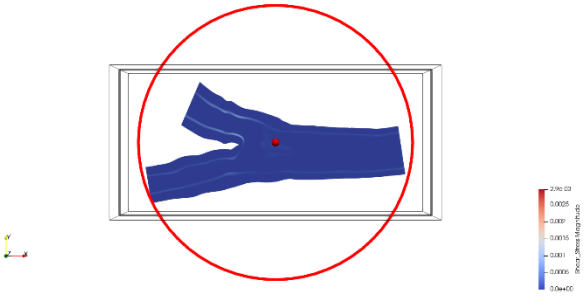
Wall shear stress (WSS)	
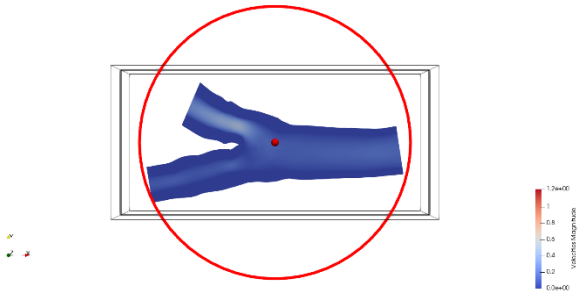	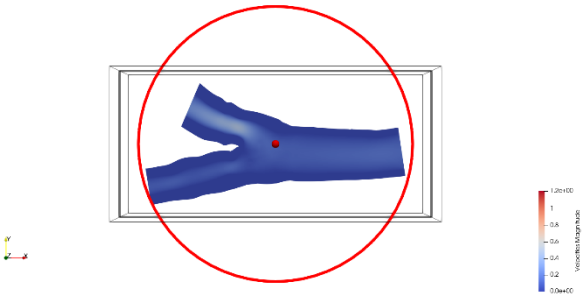
Velocities	
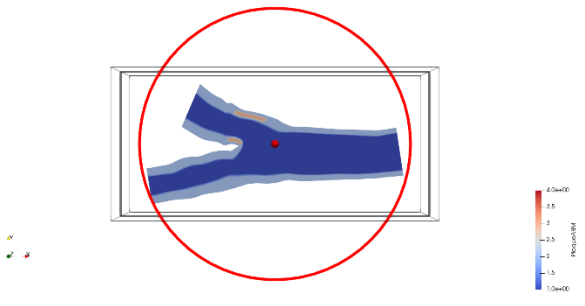	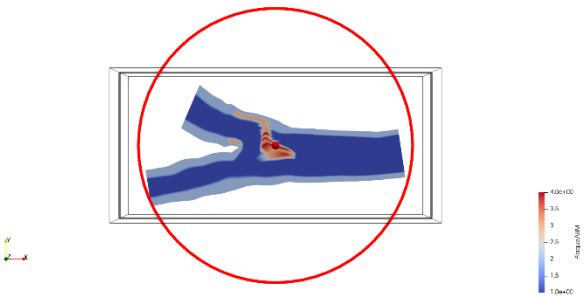
Agent based model (ABM)	

Table 8. ABM results for patient specific geometry 8

Time step 1	Time step 15
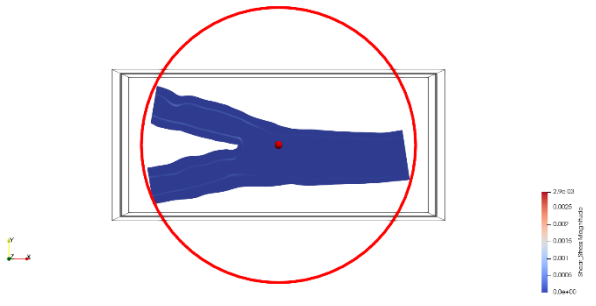	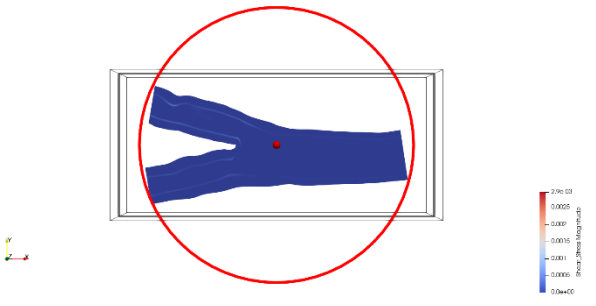
Wall shear stress (WSS)	
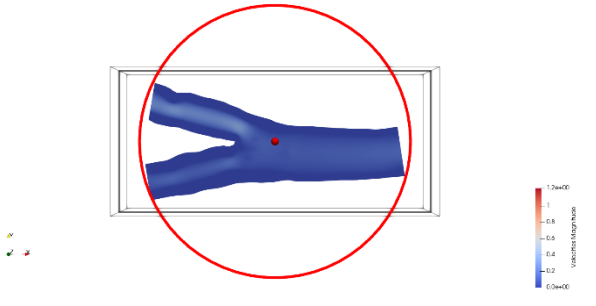	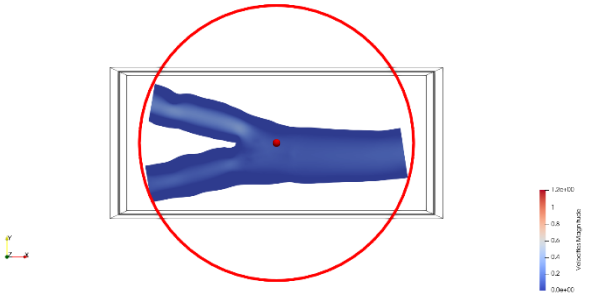
Velocities	
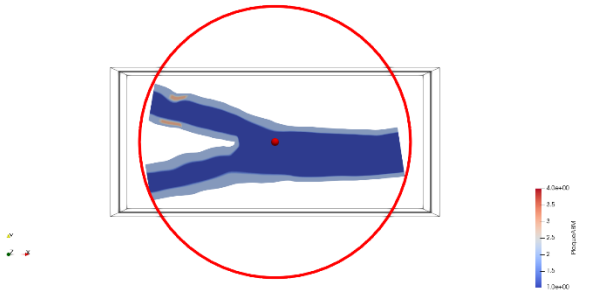	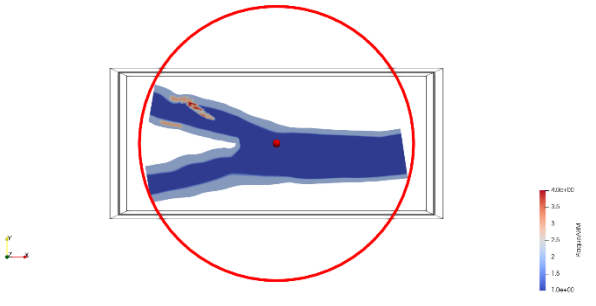
Agent based model (ABM)	

Table 9. ABM results for patient specific geometry 9

Time step 1	Time step 15
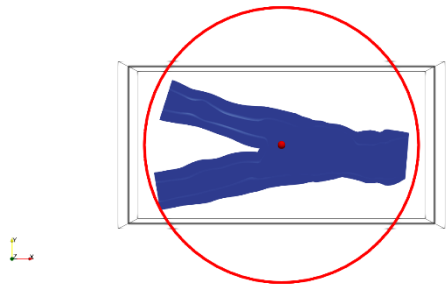	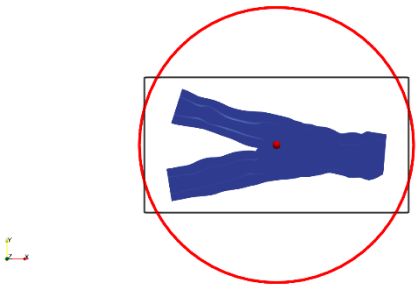
Wall shear stress (WSS)	
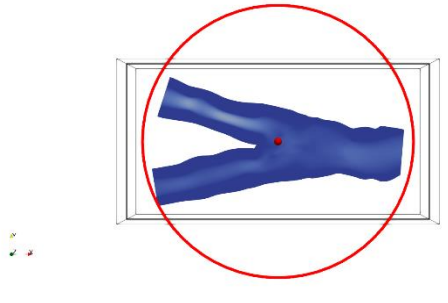	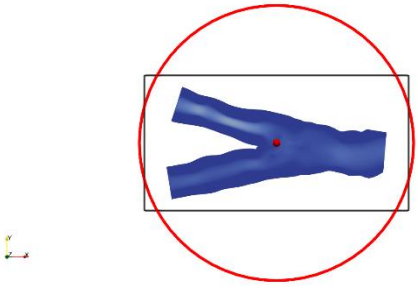
Velocities	
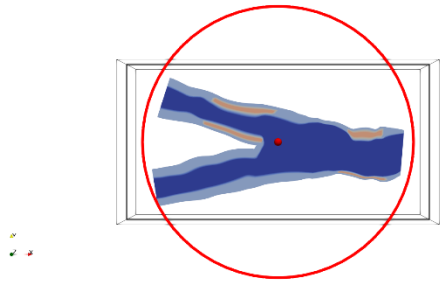	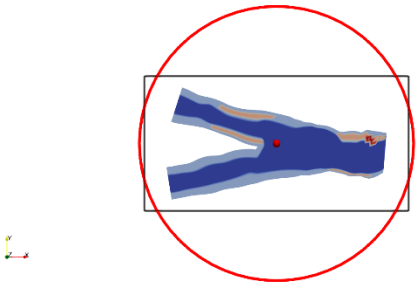
Agent based model (ABM)	

Table 10. ABM results for patient specific geometry 10

Time step 1	Time step 15
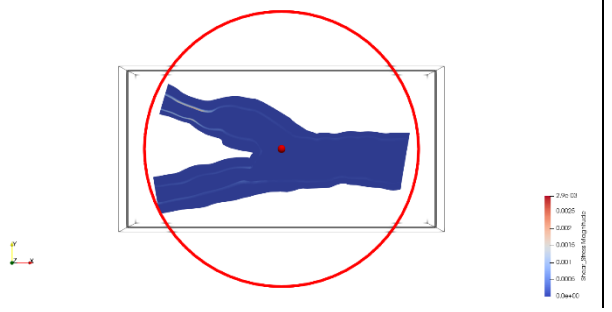	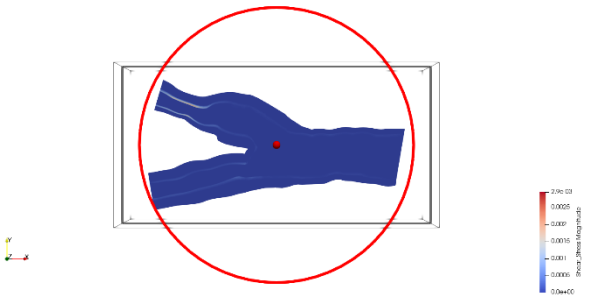
Wall shear stress (WSS)	
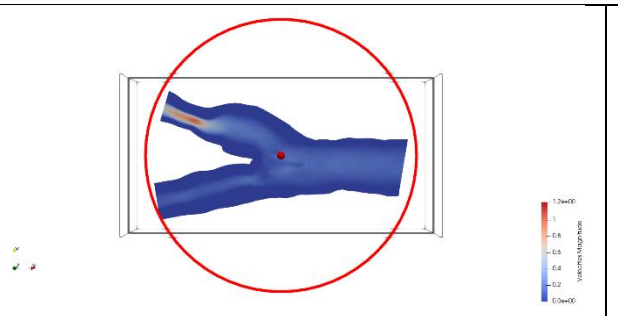	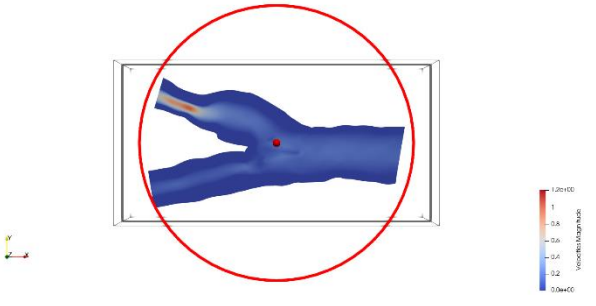
Velocities	
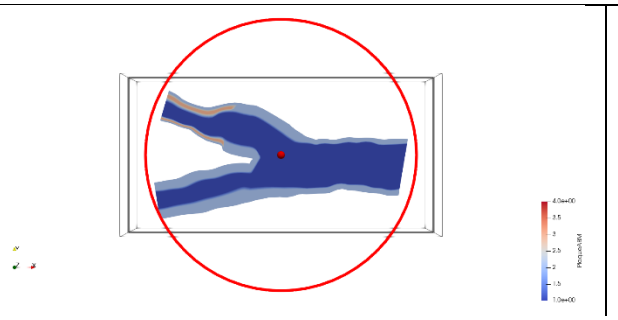	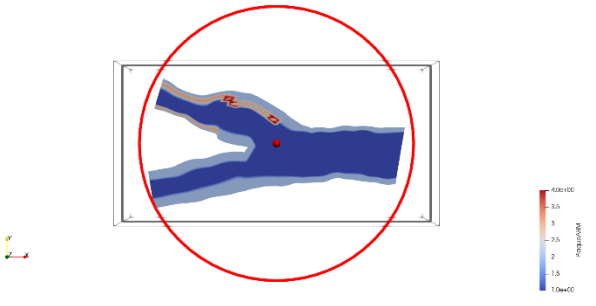
Agent based model (ABM)	

Table 11. ABM results for patient specific geometry 11

Time step 1	Time step 15
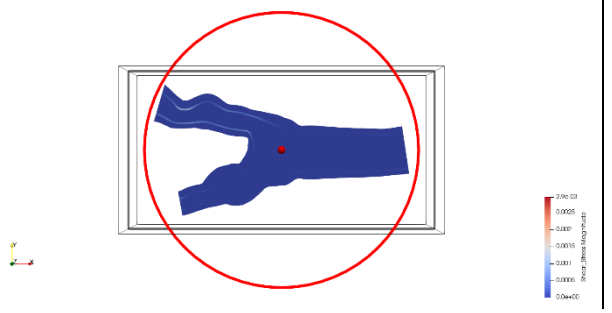	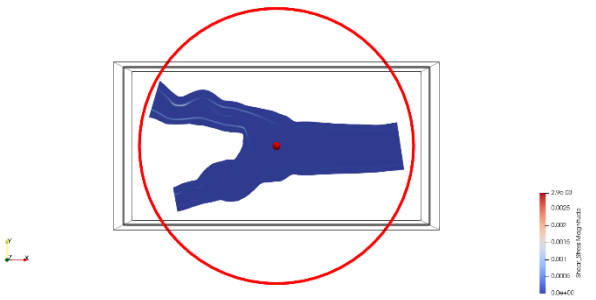
Wall shear stress (WSS)	
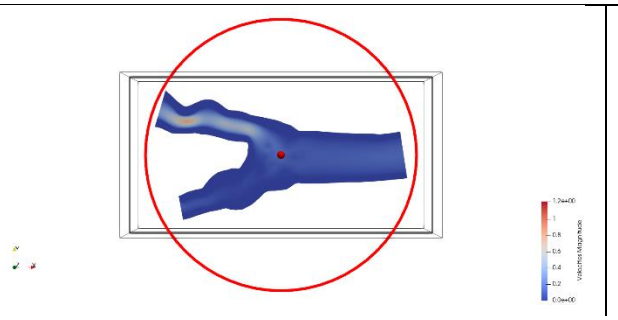	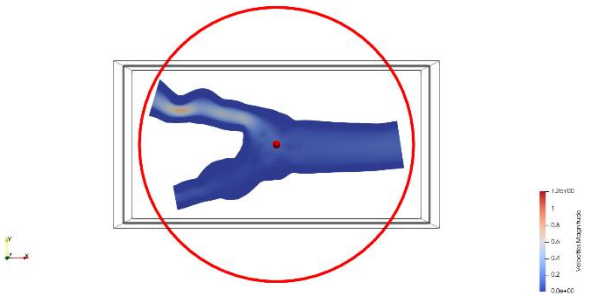
Velocities	
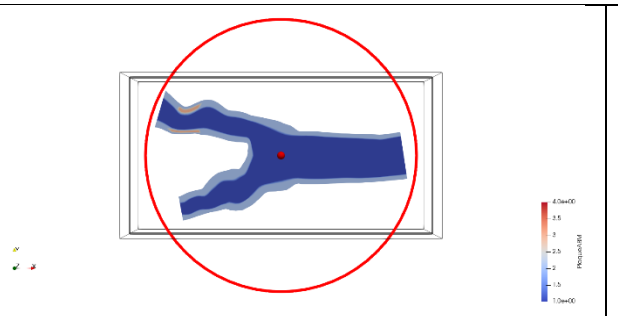	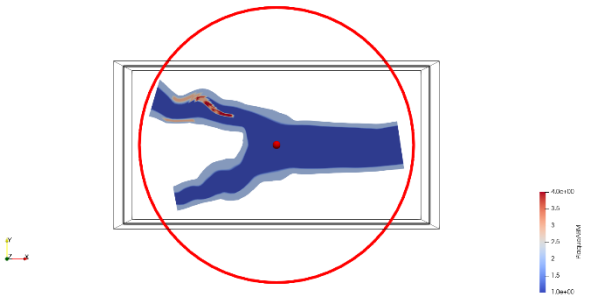
Agent based model (ABM)	

Table 12. ABM results for patient specific geometry 12

Time step 1	Time step 15
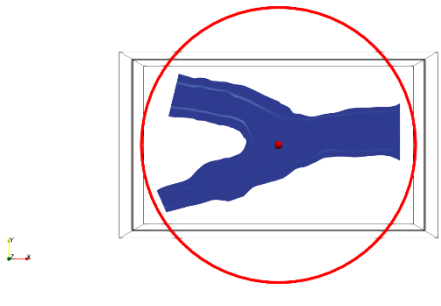	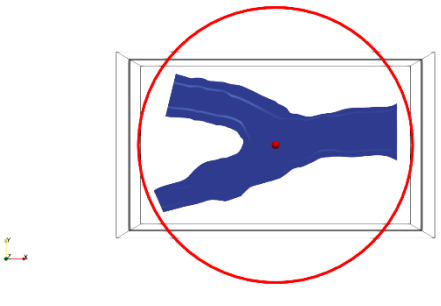
Wall shear stress (WSS)	
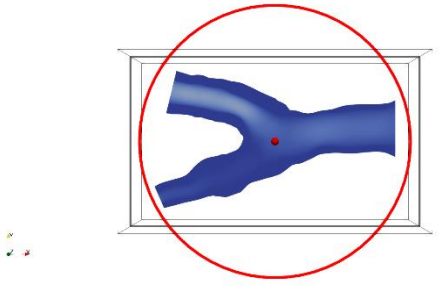	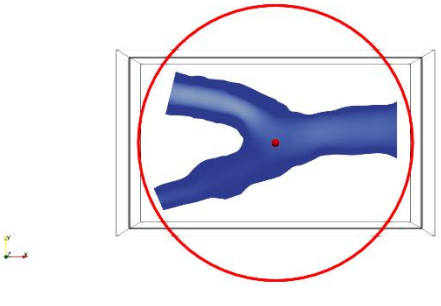
Velocities	
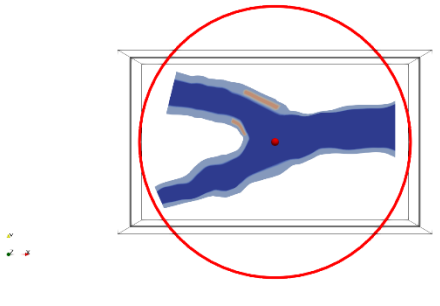	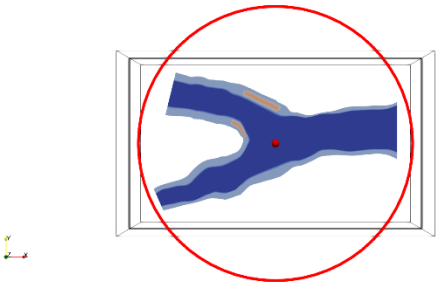
Agent based model (ABM)	

Table 13. ABM results for patient specific geometry 13

Time step 1	Time step 15
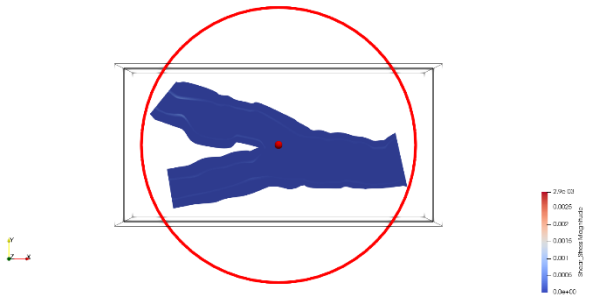	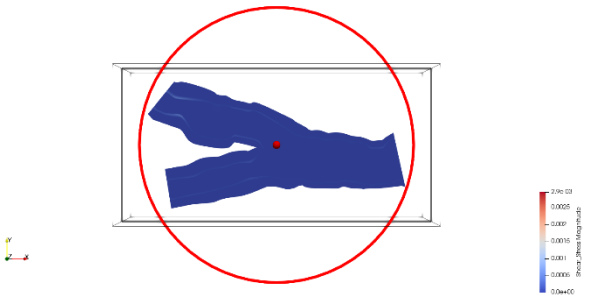
Wall shear stress (WSS)	
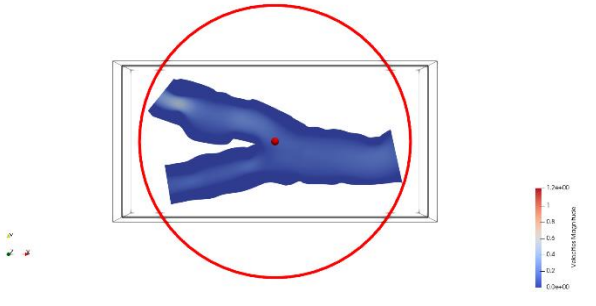	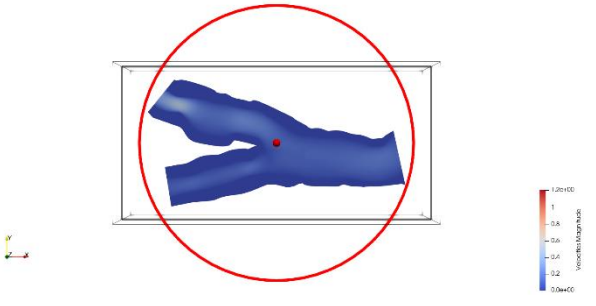
Velocities	
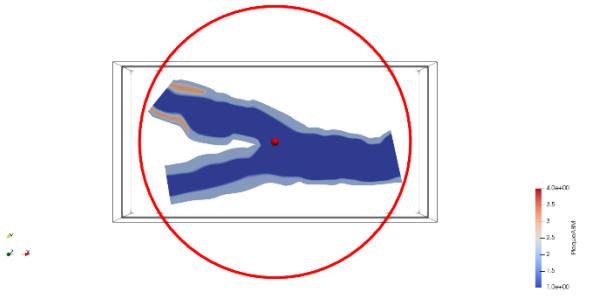	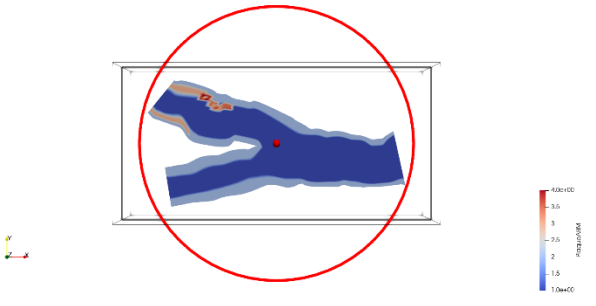
Agent based model (ABM)	

As the initial parameters were homogenous accross all simulations, the changes in plaque progression are only due to initial differences in plaque content and structure accompaniead by vessel geometry. The model was validated with patient follow-up results and indicated fidelity.

4.2. ABM Parameter Sensitivity Analysis

Parameter sensitivity analysis (PSA) is a quantitative method used to determine how the variation in input parameters of a model affects its output. It helps identify which parameters have the most significant impact on the model's predictions, thus providing insights into the model's robustness and reliability. This analysis is crucial in various fields, including engineering, economics, environmental science, and healthcare, where models are used to simulate complex systems and make predictions.
The importance of PSA lies in:

- Model validation: By understanding which parameters significantly influence model outputs, researchers can validate their models more effectively, ensuring that they are accurately representing the underlying processes.

- Uncertainty quantification: PSA helps quantify uncertainties in model predictions resulting from uncertainties in input parameters. This understanding is vital for making informed decisions based on model outputs.
- Optimization: Identifying critical parameters allows for targeted optimization efforts, which can enhance the model's performance while reducing computational costs.
- Decision-making support: In fields like healthcare and environmental management, understanding parameter sensitivities can inform better decision-making by highlighting key factors that influence outcomes.
- Guiding experimental design: Insights gained from sensitivity analysis can help guide experimental design, focusing resources on the most influential parameters.

There are various methods for performing parameter sensitivity analysis, each suited for different types of models and applications. Different types of sensitivity analysis are:

- Local sensitivity analysis
- Global sensitivity analysis
- Screening methods
- Regression-based sensitivity analysis

Local sensitivity analysis which examines how small changes in input parameters affect the output around a nominal point (usually the mean or expected value). It uses the first derivative (gradient) of the output with respect to the input parameters. It typically involves perturbing each parameter slightly while keeping others constant and observing the change in output.

Global sensitivity analysis assesses the influence of input parameters over their entire range of possible values. It considers the joint variability of all parameters and their interactions. Methods of global sensitivity analysis include:

- Variance-based methods, such as Sobol' indices, which decompose the variance of the output into contributions from individual parameters and their interactions.
- Fourier Amplitude Sensitivity Test (FAST) that transforms the parameter space into a Fourier series to quantify sensitivities.
- Monte Carlo Simulations randomly sample input parameters from their probability distributions to observe the resulting output variability.

Screening methods are used as PSA when the number of parameters is large, and the goal is to identify the most influential parameters quickly. These methods can filter out insignificant parameters before conducting a more detailed analysis. Methods of screening can be:

- One-at-a-Time (OAT) Testing that systematically varies one parameter at a time while holding others constant.
- FAST and Morris methods that efficient techniques to identify sensitive parameters in a reduced number of model runs.

Regression-based sensitivity analysis involves fitting a regression model to the output data, with input parameters as predictors. The coefficients of the regression model indicate the sensitivity of the output to changes in each parameter.

A comparison of advantages and limitations of different sensitivity analysis methods is given in Table 14.

Table 14. Comparison of different sensitivity analysis methods

	Advantage	Limitation

Local sensitivity analysis	Simple and computationally efficient for linear models	It assumes linearity and may not capture nonlinear effects or interactions between parameters.
Global sensitivity analysis	Provides a comprehensive view of parameter effects and captures nonlinearities and interactions.	More computationally intensive and requires a larger number of model evaluations.
Screening methods	Efficient and can significantly reduce computational effort.	May miss interactions between parameters.
Regression-based sensitivity analysis	Useful for linear models and provides a straightforward interpretation of sensitivities.	Limited to linear relationships and may not capture complexities in more intricate models.

Latin Hypercube Sampling (LHS) is a powerful statistical technique widely used in PSA and Monte Carlo simulations. It serves as a robust method for efficiently exploring the input parameter space of a model, generating a set of samples that accurately represent potential outcomes. Understanding LHS involves diving into its unique approach, advantages, and applications in sensitivity analysis. At its core, LHS is a stratified sampling method that ensures each parameter is uniformly sampled across its entire range. Unlike traditional random sampling, where each parameter is treated independently, LHS divides the range of each parameter into equally probable intervals, also known as strata. The design of LHS is systematic and intuitive. To start, each input parameter is broken down into N equal intervals, with N representing the total number of desired samples. For every parameter, one value is randomly selected from each of these intervals, and these selected values are then combined to create a complete set of input parameters for the model. This approach guarantees that all combinations of parameter values are covered, resulting in a more efficient exploration of the parameter space.

The advantages of using LHS in PSA are firstly that it enhances efficiency by providing a more accurate representation of the input space with fewer samples compared to simple random sampling. This characteristic is particularly valuable when working with complex models that demand significant computational resources for evaluation. By ensuring that each parameter's range is uniformly sampled, LHS avoids clustering in specific regions, allowing for better coverage of the overall parameter space. Moreover, LHS contributes to reducing the variance of output estimates, as it effectively captures the entire range of each parameter. Implementing LHS is also straightforward, making it accessible for researchers across various fields.

LHS finds its applications in numerous areas of sensitivity analysis. In exploratory studies, for example, it plays a crucial role in identifying which parameters exert the most significant influence on model outputs. In fields such as environmental modeling, finance, and engineering, LHS helps quantify uncertainties by sampling input parameters and assessing their impact on variability in the results. It also supports model calibration and validation by efficiently exploring the parameter space to identify optimal values and validate predictions.

Implementing LHS in parameter sensitivity analysis follows a clear sequence of steps. Initially, the parameters to be analyzed are determined and their corresponding ranges

or probability distributions determined. Next, the number of samples to be generated for the analysis is determined. Each parameter's range is then stratified into equal intervals based on the sample size. Once this is done, one value is randomly selected from each interval for each parameter, ensuring all intervals are represented. The samples are combined to create a comprehensive set of input parameter combinations, which are subsequently used to run the model. Finally, the output data is analyzed to identify influential parameters and their effects. The methodology of LHS-based sensitivity analysis conducted in this research is show in Figure 11.

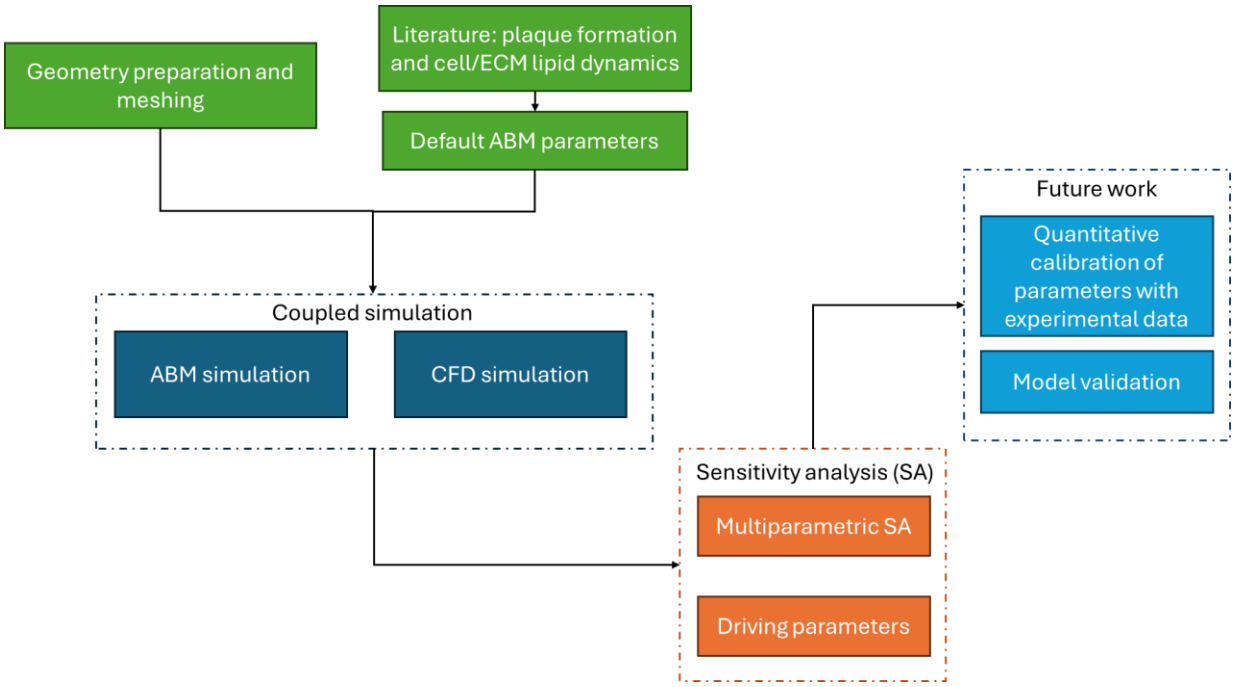

Figure 11. Workflow of LHS PSA

The intrinsic ABM parameters driving the simulation were initially defined by Garbey et al.,(Garbey et al., 2017) and the constant parameters that drive cellular events are:

- Probability of mitosis and apoptosis
- Smooth muscle cell (SMC) division in the intimal layer
- Extracellular matrix (ECM) deposition in intimal layer
- ECM deposition in medial layer
- SMC division in medial layer
- Outward remodeling driven by shear forces
- Outward remodeling driven by tensile forces

All of the aforementioned parameters have been defined in literature and their respective physiological ranges determined (Table 15).

Table 15. ABM parameters and ranges

Parameter name	Parameter description	Parameter type	Range	Default value
α_1	Probability of mitosis and apoptosis	constant	0.05	0.05

α_2	Probability of SMC proliferation in tunica media	variable	2-17	1.5
α_3	Probability of SMC proliferation in intima	variable	0-0.5	0.1
α_4	Probability of ECM degradation	constant	0.008	0.008
α_5	Probability of lipid infiltration	variable	0-0.106	0.005
α_6	Outward remodeling driven by shear forces	Variable	0-24.46	10.0
α_7	Outward remodeling driven by tensile forces	Variable	1.84-100	6.0

Parameter sensitivity analysis results

Multi-parametric sensitivity analysis was conducted using LHS to randomly sample the triangular probability density function of each parameter and define the parameter set for the ABM simulations. This method allowed for the exploratory testing of the entire range of each parameter and is proven to achieve good accuracy with a limited number of simulations. The probability density functions of all parameters were divided into 100 equal probability intervals and an LHS matrix was generated identifying 100 ABM parameter combinations. To account for the influence of these parameters on different initial patient-specific geometries, 100 simulations with different patient-specific geometries were conducted for 13 distinct cases.

The results of PSA were first analyzed graphically in the domain of ABM simulation results. Results of example simulations are presented in Figures 12-18 and parameter comparisons are given in tables 16-22.

Instance 1

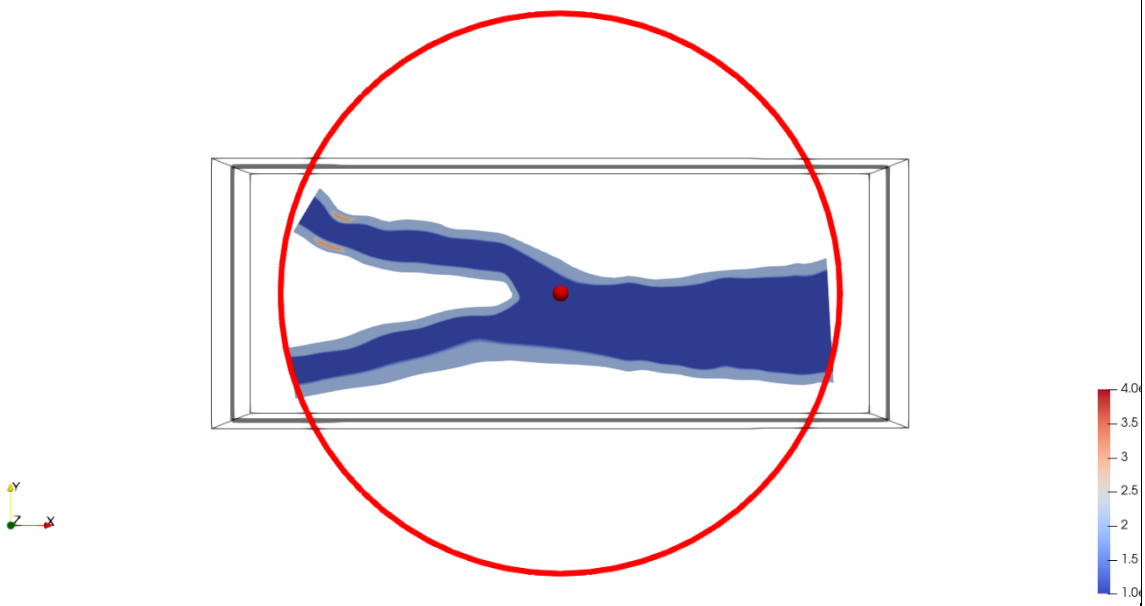

Figure 12.a ABM results with default parameters

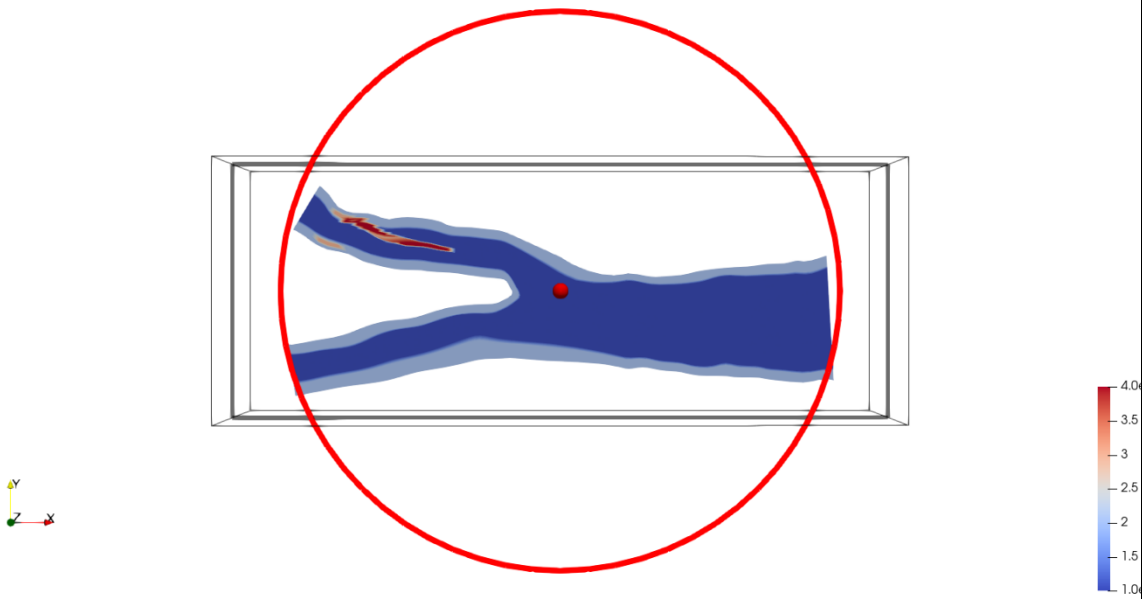

Figure 12.b ABM results with LHS generated parameters (Table 16.)

Figure 12. Graphical result difference for LHS on sample geometry 3

As it can be seen from Figure 12, even a slight increase in α5 causes significant progression of atherosclerosis. The progression of atherosclerosis in this case seems irregular as the process is directed towards the arterial lumen, indicating that the ABM could be oversensitive to changes made to α_5.

Table 16. Parameter comparison LHS (geometry 2)

Parameter	Default simulation parameters	LHS generated simulation parameters	Parameter status
α_1	0.05	0.05	Const
α_2	1.5	1.5	Const
α_3	0.1	0.1	Const
α_4	0.008	0.008	Const.
α_5	0.005	0.009	>
α_6	10.0	10.0	Const
α_7	6.0	6.0	Const

Instance 2

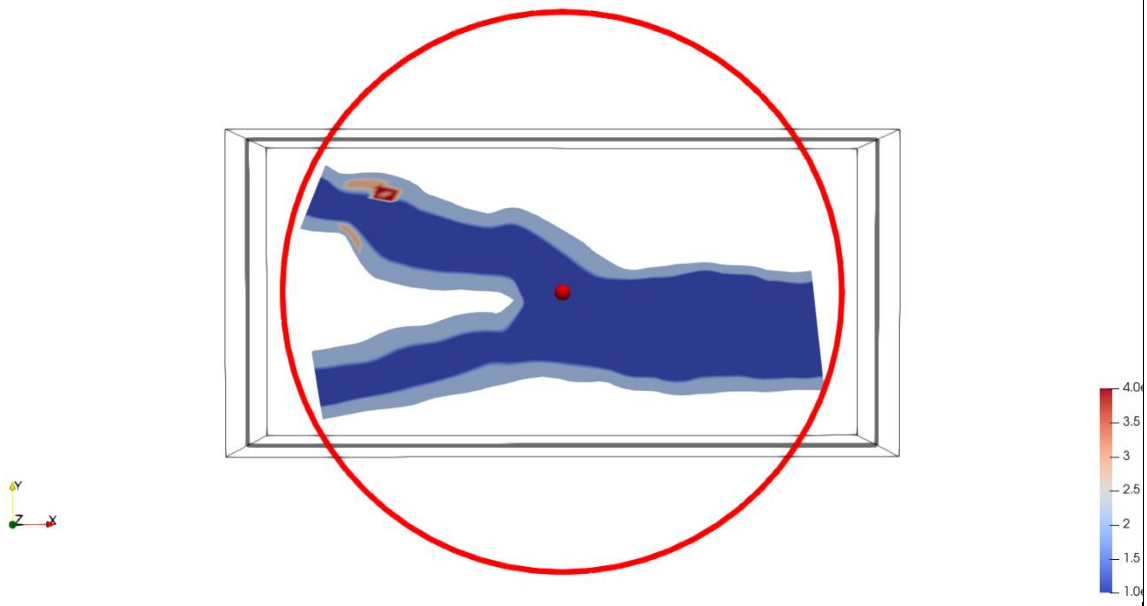

Figure 13.a ABM results with default parameters

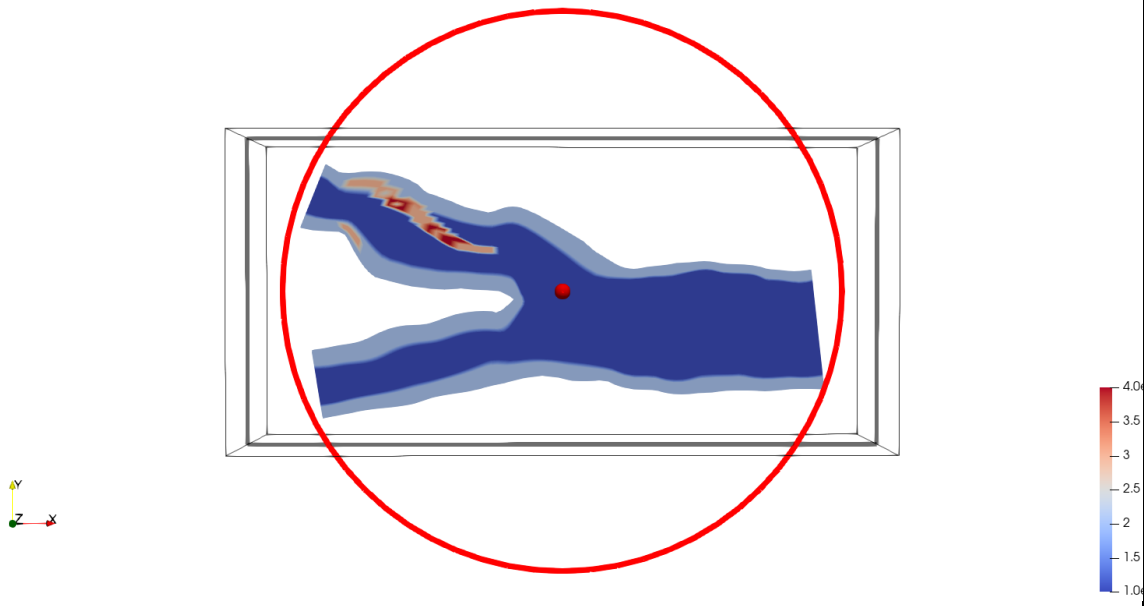

Figure 13.b ABM results with LHS generated parameters (Table 17)

Figure 13. Graphical result difference for LHS on sample geometry 3

In this instance, the LHS parameters intorduced an increase in α_2, α_3, α_5 and α_7 along with a decrease in α_6. Even though the parameter driving the arterial wall remodelling was decreased the contribution of the increase in other parameters resulted in a significantly increased plaque progression. Additionally, the plaque progression in this case is irregular as it is modeled as a migration of the atherosclerotic plaque towards the arterial lumen. Even though this can be interpreted as the breakage of the plaque and thrombus formation, a significant increase in the parameter driving outward remodelling by tensile forces could be a potential disruptor of the simulation.

Table 17. Parameter comparison LHS (geometry 3)

Parameter	Default simulation parameters	LHS generated simulation parameters	Parameter status
α_1	0.05	0.05	Const
α_2	1.5	15.3	>
α_3	0.1	0.35	>
α_4	0.008	0.008	Const.
α_5	0.005	0.062	>
α_6	10.0	3.9	<
α_7	6.0	77.0	>

Instance 3

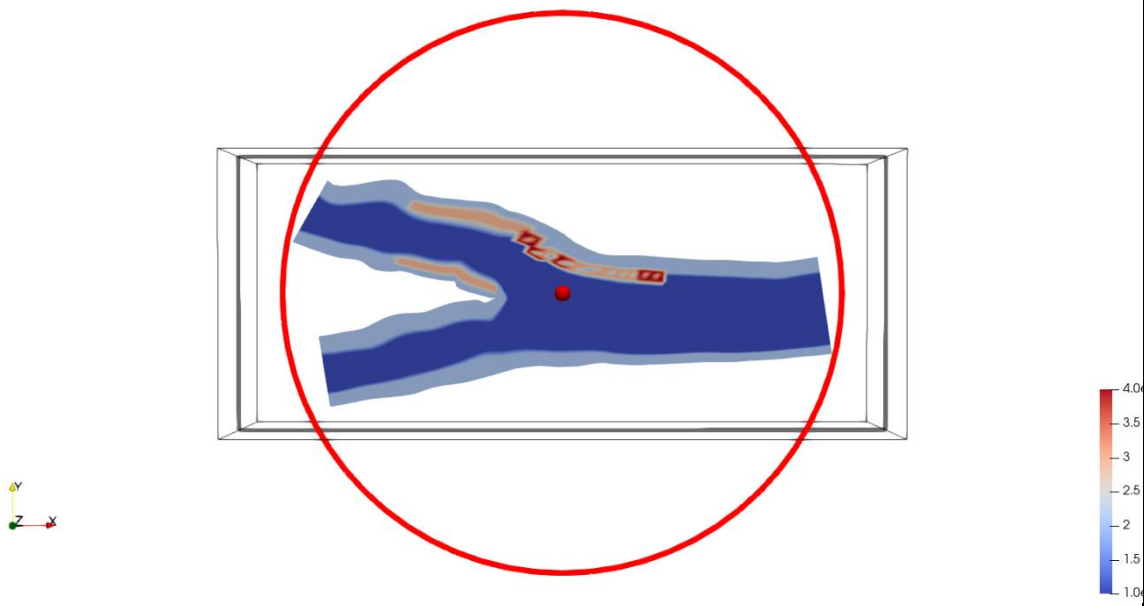

Figure 14.a ABM results with default parameters

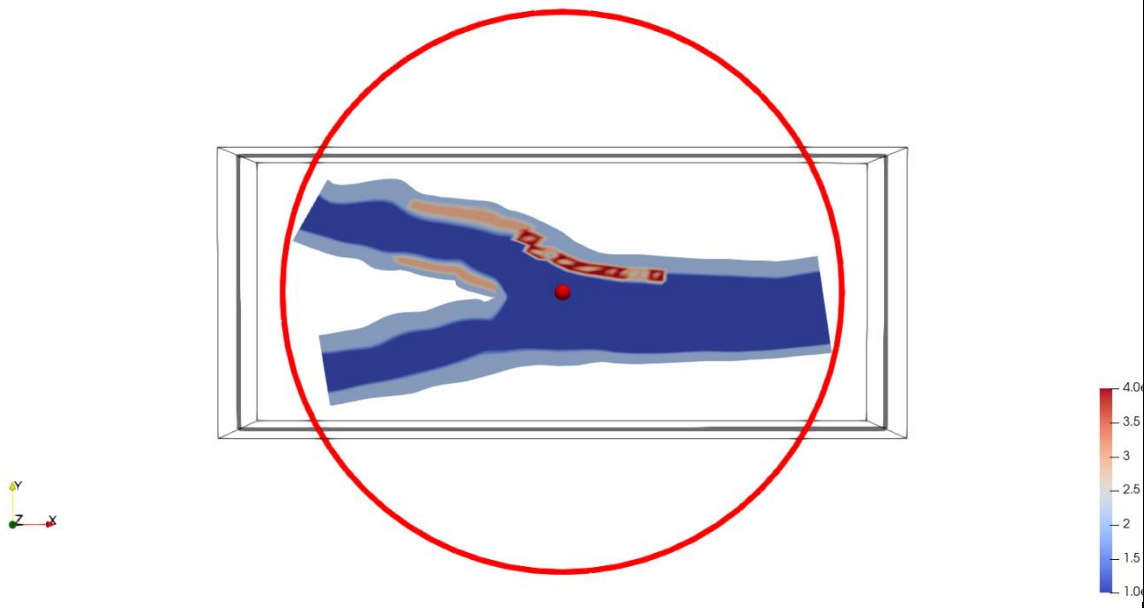

Figure 14.b ABM results with LHS generated parameters (Table 18.)

Figure 14. Graphical result difference for LHS on sample geometry 4

Taking into account the fact that all variable simulation parameters were significantly increased, an the only change to the atherosclerotic plaque progression was in the field of transitioning from fibrous to calcified plaque, it can be said that the ABM deals well with pertrubations in simulation parameters. Contrary to the results from patient-specific geometries 2 and 3 where even slight changes in the parameters caused a significan pertrubation in the simulation, the fidelity of results was kept constant in this case. This leads to a deduction that the simulation results are much more sensitive to the geometry itself than to the parameter pertrubations. If the regularity of the arterial wall and lumen

is compared betwee these three instances, it is clearly visible that geometries 2 and 3 are much more irregular in terms of kinks and narrowings of the vessel than geometry 4.

Table 18. Parameter comparison LHS (geometry 4)

Parameter	Default simulation parameters	LHS generated simulation parameters	Parameter status
α_1	0.05	0.05	Const
α_2	1.5	4.002	>
α_3	0.1	0.243	>
α_4	0.008	0.008	Const.
α_5	0.005	0.017	>
α_6	10.0	21.296	>
α_7	6.0	76.77	>

Instance 4
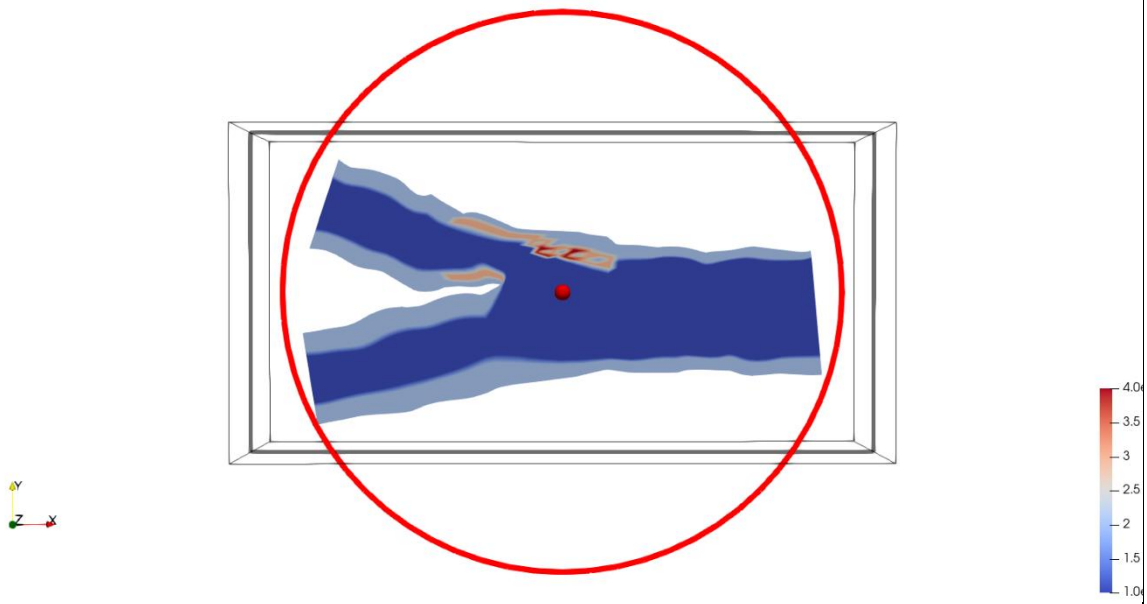
Figure 15. Graphical result difference for LHS on sample geometry 5.a ABM results with default parameters
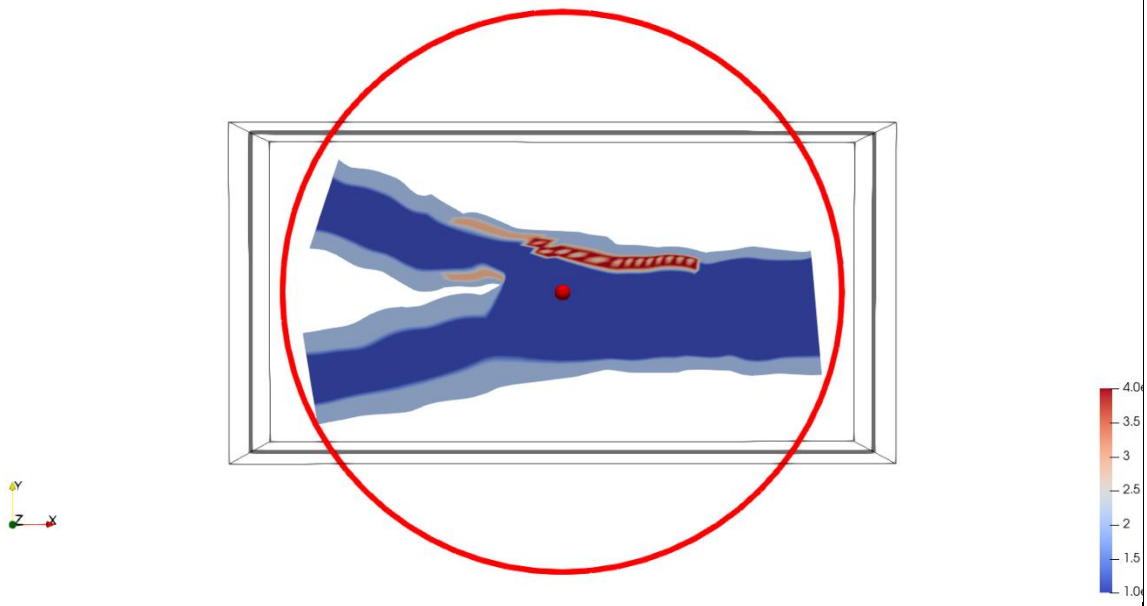
Figure 15.b ABM results with LHS generated parameters (Table 20.)

Figure 15. Graphical result difference for LHS on sample geometry 5

In the context of geometry 5, a significant increase in plaque burden is observed with both transition of the initial fibrous plaque to calcified and progression along the vessel wall. This was caused by an increase in all parameters driving atherosclerotic progression except for α_3. The fidelity of the simulation results was once again preserved regardless of significant changes made to the simulation parameters.

Table 19. Parameter comparison LHS (geometry 5)

Parameter	Default simulation parameters	LHS generated simulation parameters	Parameter status
α_1	0.05	0.05	Const
α_2	1.5	6.1	>
α_3	0.1	0.05	<
α_4	0.008	0.008	Const.
α_5	0.005	0.075	>
α_6	10.0	12.0	>
α_7	6.0	74.0	>

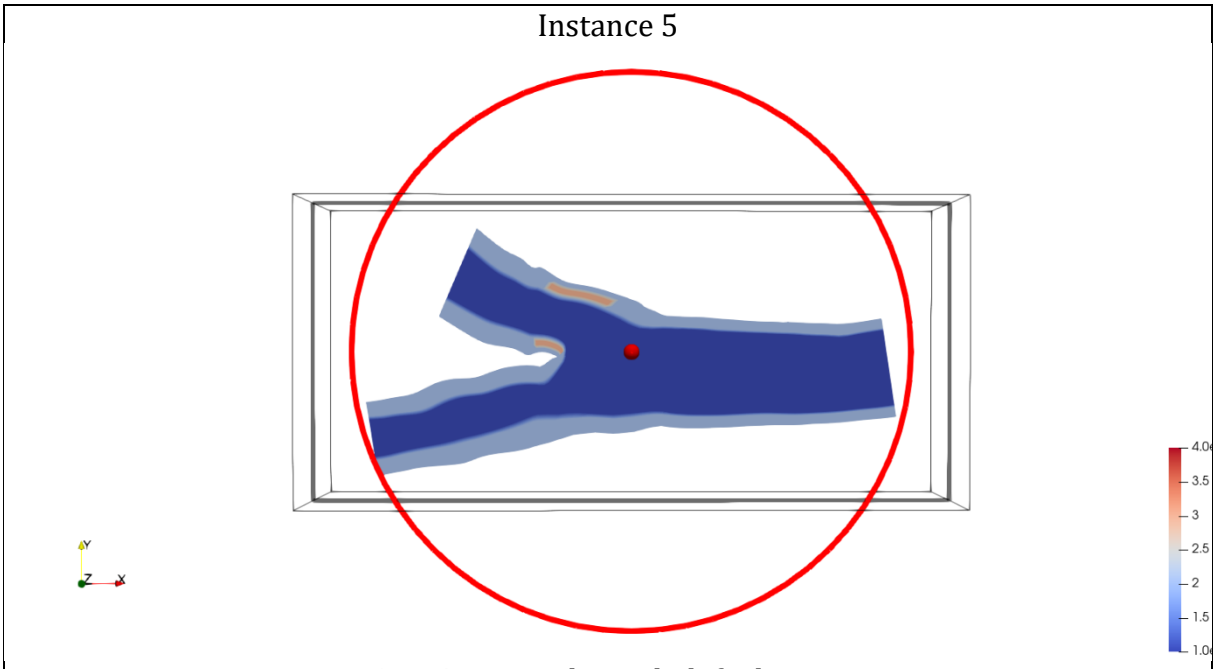

Figure 16.a ABM results with default parameters

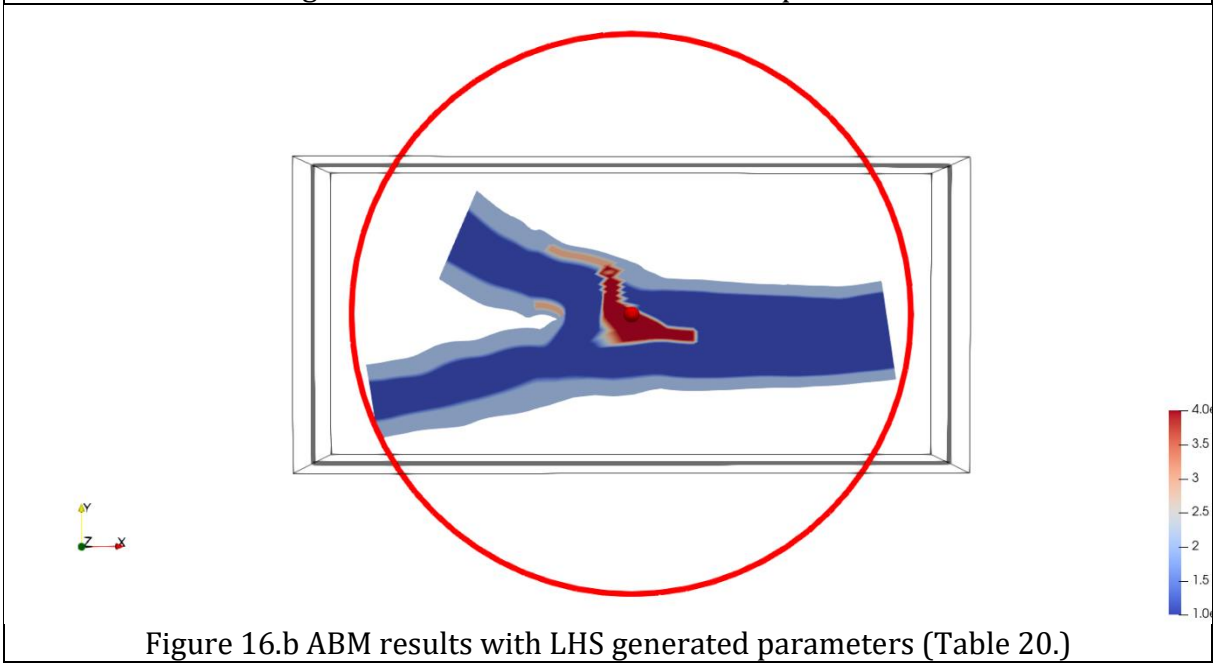

Figure 16.b ABM results with LHS generated parameters (Table 20.)

Figure 16. Graphical result difference for LHS on sample geometry 5

The simulation fidelity was significantly distorted in the case of sample geometry 5 where the simulation results suggest „leakage“ of the plaque content into the bloodstream, an occasion that does not happen in physiological scenarios. Taking into account the changes made to the parameters and the fact that α_7 was increased more than 10-fold it can be concluded that the simulation results are highly sensitive to the changes made to the parameter affecting outward remodeling by tensile forces. Even though the change made to α_7 was within the defined parameter range it still disrupted the simulation. Considering the fact that changes to the same parameter in a similar extent do not disrupt the simulation, geometry was reobserved. What can be quickly noted is that the upper branch

of the artery is significantly shorter. It is known from literature that arteries with bifurcation are prone to plaque development and quick progression in this region. Taking into account the „leakage“ happened at the bifurcation point, the abrupt results of the simulation could be due to the combination of geometric peculiarities combined with significant parameter pertrubations.

Table 20. Parameter comparison LHS (geometry 5)

Parameter	Default simulation parameters	LHS generated simulation parameters	Parameter status
α_1	0.05	0.05	Const
α_2	1.5	4.9	>
α_3	0.1	0.4	>
α_4	0.008	0.008	Const.
α_5	0.005	0.094	>
α_6	10.0	9.3	<
α_7	6.0	99.1	>

Instance 6

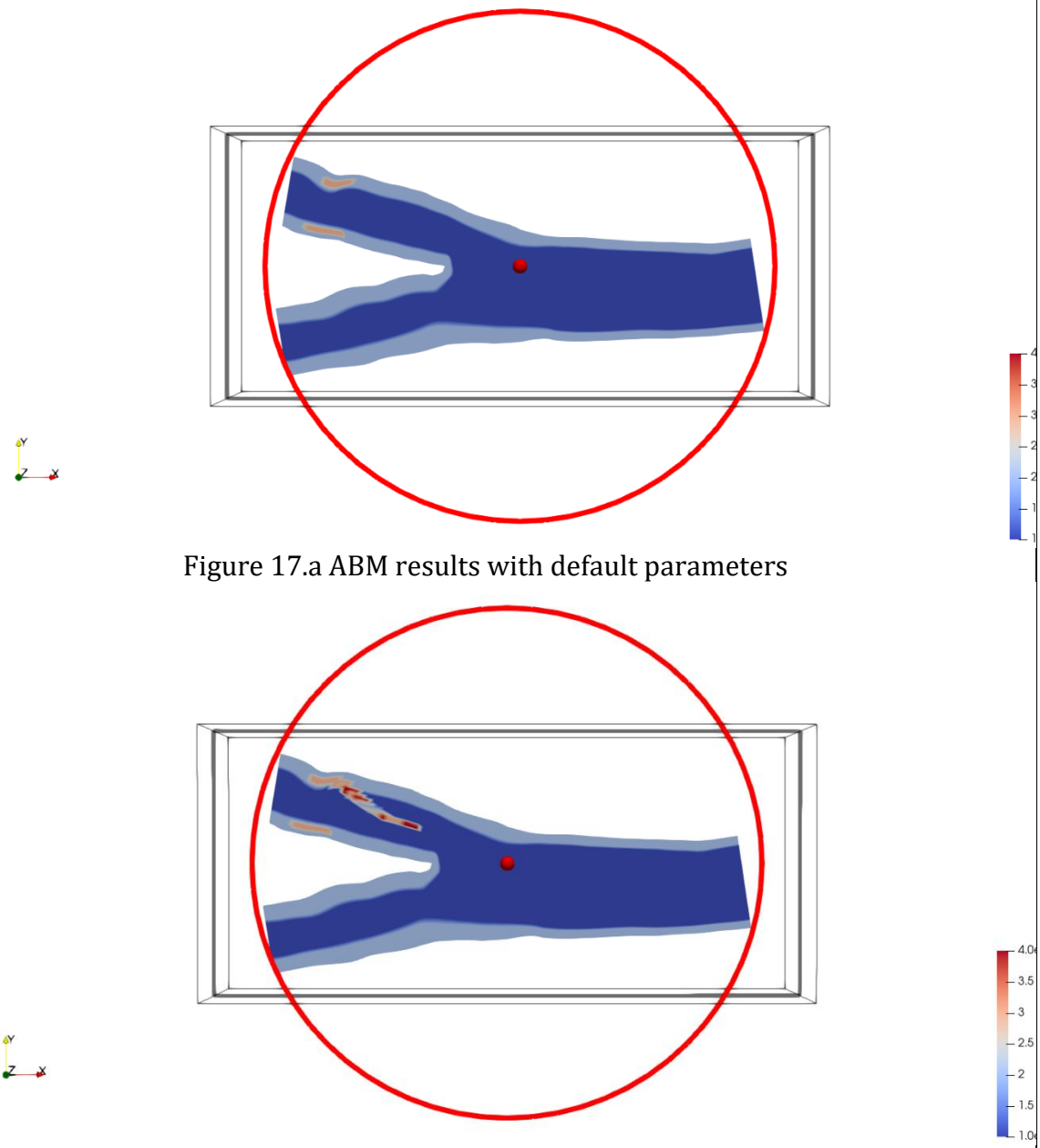

Figure 17.a ABM results with default parameters

Figure 17.b ABM results with LHS generated parameters (Table 21.)

Figure 17. Graphical result difference for LHS on sample geometry 6

In the case of sample geometry 6 there is again a significant pertrubation in the simulation results. Even though the parameter driving the arterial wall remodelling was decreased the contribution of the increase in other parameters resulted in a significantly increased plaque progression. Additionally, the plaque progression in this case is irregular as it is modeled as a migration of the atherosclerotic plaque towards the arterial lumen. Even though this can be interpreted as the breakage of the plaque and thrombus formation, a significant increase in the parameter driving outward remodelling by tensile forces could be a potential disruptor of the simulation.

Table 21. Parameter comparison LHS (geometry 6)

Parameter	Default simulation parameters	LHS generated simulation parameters	Parameter status
α_1	0.05	0.05	Const
α_2	1.5	2.1	>
α_3	0.1	0.4	>
α_4	0.008	0.008	Const.
α_5	0.005	0.026	>
α_6	10.0	6.5	<
α_7	6.0	36.0	>

Instance 7

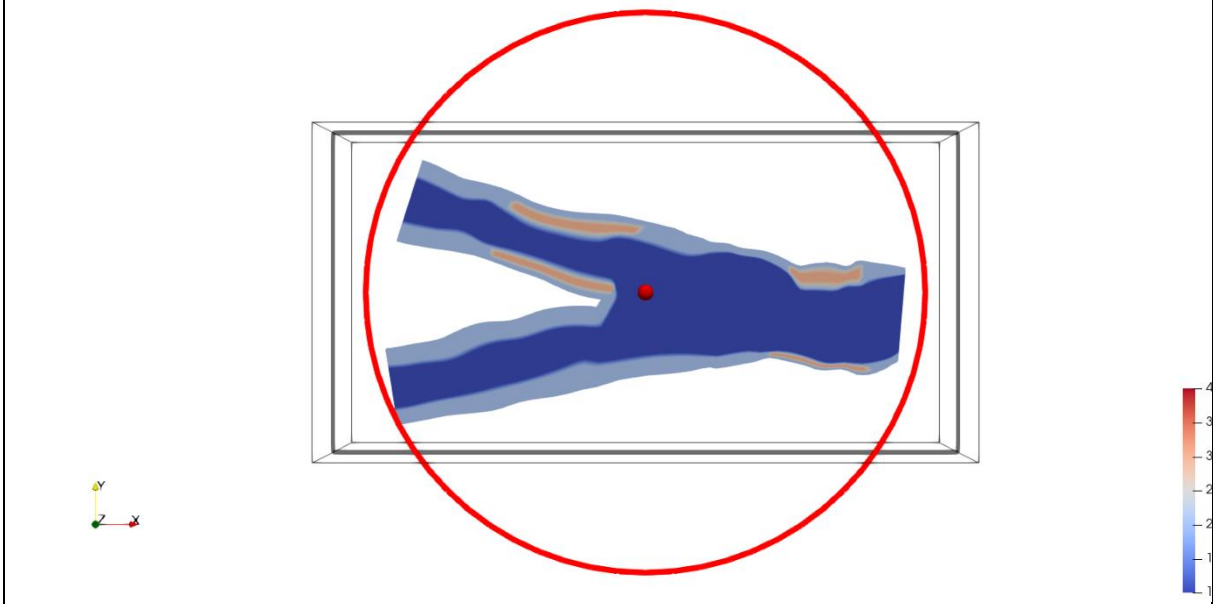

Figure 18.a ABM results with default parameters

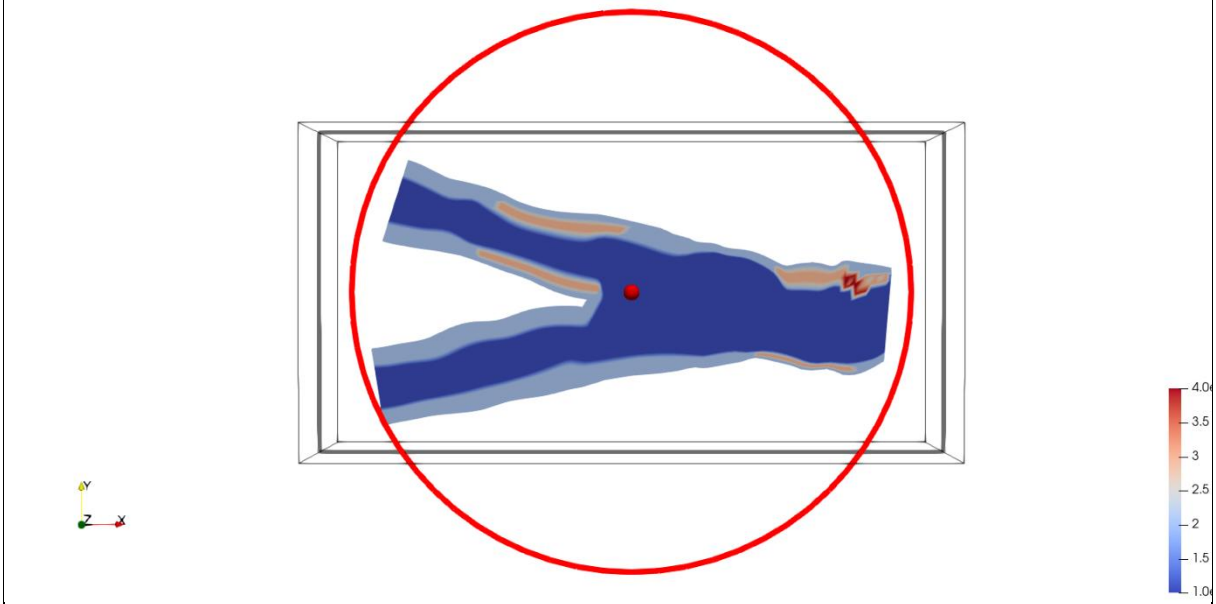

Figure 18.b ABM results with LHS generated parameters (Table 22.)

Figure 18. Graphical result difference for LHS on sample geometry 10

Sample geometry 10 has several peculiarities. Atherosclerotic plaque commonly develops only on a single place along the artery, in close proximity to the bifurcation region. However, in this example, there are paired instances of atherosclerotic plaque in the upper branch of the artery and in the common branch. When it comes to the results of the simulation, once again the ABM exhibits fidelity in results as plaque progression occurs transversally and longitudinally without infiltration into the arterial lumen.

Table 22. Parameter comparison LHS (geometry 10)

Parameter	Default simulation parameters	LHS generated simulation parameters	Parameter status
α_1	0.05	0.05	Const
α_2	1.5	7.4	>
α_3	0.1	0.2	>
α_4	0.008	0.008	Const.
α_5	0.005	0.098	>
α_6	10.0	5.7	<
α_7	6.0	30.0	>

Partial rank correlation coefficient analysis

As the graphical analysis of the results showed several peculiarities, it was necessary to conduct a comprehensive analysis of the results obtained from LHS and to derive conclusions about the parameters most influential on simulation results.

The Partial Rank Correlation Coefficient (PRCC) is a statistical technique commonly used in sensitivity analysis to assess how changes in input parameters influence a model's output, while accounting for the effects of other variables. It is particularly advantageous when dealing with complex systems where input parameters may be interdependent, and the relationships between them and the output are not strictly linear. In many real-world models, variables interact in nonlinear and often non-intuitive ways, making it difficult to identify which inputs have the most significant effect on the results. PRCC addresses this challenge by providing a rank-based correlation measure that can capture monotonic relationships, which are relationships where variables move consistently in one direction, but not necessarily in a linear fashion. PRCC is applied in the sensitivity analysis of systems such as structural models, where various design parameters (material properties, load conditions, geometric configurations) need to be optimized. By identifying which parameters have the most significant impact on the system's behavior, engineers can make informed decisions about resource allocation or design modifications.

At its core, PRCC is built on Spearman's rank correlation coefficient, which measures the strength and direction of the monotonic relationship between two ranked variables. This makes PRCC well-suited for models where traditional linear correlation methods may fall short because the relationships between inputs and outputs are more complex. While Spearman's correlation is useful for bivariate analysis, PRCC extends this to a multivariate context by adjusting for the presence of multiple variables. This adjustment isolates the unique contribution of each input parameter on the output, even when other inputs are correlated with both the parameter and the outcome. This "partial" aspect of PRCC is what makes it so powerful. In traditional sensitivity analysis, correlations might be computed directly between each input and the output, but these raw correlations could be misleading due to the confounding effects of other variables. PRCC, on the other hand, controls for these confounding effects, ensuring that the influence of one parameter is evaluated while holding the others constant.

To compute PRCC, the process involves the following key steps:

- Ranking the data: First, all data (inputs and output) are converted into ranks, which allows PRCC to focus on the relative ordering of data rather than their absolute values. This is particularly useful in scenarios where the inputs and outputs are measured on different scales or where the exact values are not as important as their ordering.

- Regression to adjust for other variables: For each input parameter, a regression analysis is performed with respect to all other input variables. This allows the technique to remove the shared variability between the parameter being analyzed and the other inputs. Essentially, it computes residuals that represent the portion of the parameter that cannot be explained by the other inputs.
- Rank correlation of residuals: Next, a rank correlation (Spearman's) is computed between the residuals of the input parameter and the residuals of the output variable, ensuring that the relationship being evaluated is independent of the effects of other inputs.
- Interpret the PRCC value: The PRCC value ranges from -1 to 1. A PRCC close to 1 indicates that the input has a strong, positive monotonic relationship with the output, meaning that as the input increases, so does the output, even after controlling for the other inputs. A PRCC near -1 indicates a strong, negative monotonic relationship, where increases in the input are associated with decreases in the output. A PRCC around 0 suggests no significant relationship between the input and output when other factors are accounted for.

PRCC offers several advantages, making it a valuable tool for analyzing complex systems:

- Handling nonlinearity: Traditional sensitivity analysis methods like Pearson correlation assume linear relationships between inputs and outputs. PRCC relaxes this assumption by focusing on monotonic relationships, making it more flexible and suitable for systems with nonlinear dynamics.
- Controlling for confounding variables: One of PRCC's primary strengths is its ability to control for the effects of other input parameters. In many models, parameters are interrelated, and simply looking at their raw correlation with the output might lead to incorrect conclusions. PRCC removes the effects of these confounding variables, allowing for a clearer understanding of each input's unique contribution to the output.
- Robustness to outliers and non-normal distributions: Because PRCC is based on rank correlation, it is less sensitive to outliers or the distribution of the data. This makes it particularly useful in real-world applications where input data might not follow a normal distribution, or where occasional extreme values could skew the results of traditional correlation methods.
- Applicable in high-dimensional systems: PRCC is well-suited for analyzing models with many input parameters, as it systematically adjusts for the effects of multiple variables. This makes it useful in fields like environmental science, epidemiology, and engineering, where models often have dozens of inputs and complex, interdependent relationships between variables.
- Interpretable results: The results of a PRCC analysis are straightforward to interpret. Each input is assigned a PRCC value that indicates its relative importance in driving the output, which allows researchers to easily identify the most influential parameters. This information can be crucial for model validation, refinement, and policy decisions in applied fields.

Figures 19-22 show the PRCCs between the variable model inputs (α2, α3, α5, α6 and α7) and target model outputs such as arterial wall, arterial and final content of fibrous plaque type and calcified plaque type respectively.

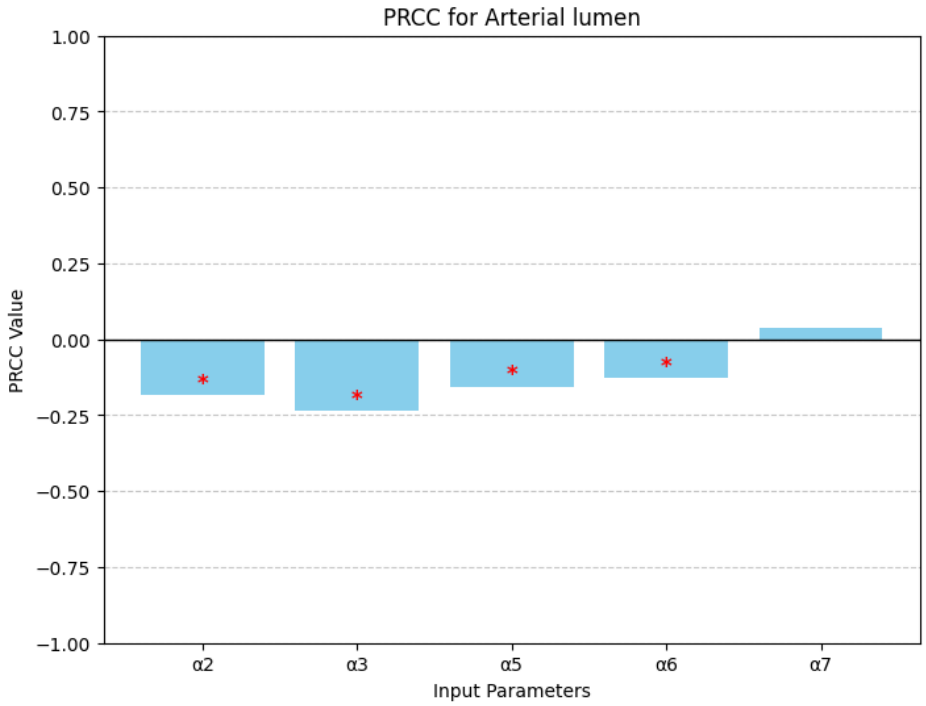

Figure 19. PRCC for arterial lumen

As it can be seen from Figure 19. α2, α3, α5 and α6 exhibit relatively low but statistically significant PRCC. This implies that the input parameters have a meaningful influence on the output, even if the relationship is not extremely strong. This indicates increasing coefficients of SMC proliferation, lipid infiltration and outward remodeling driven by shear forces leads to a slight but consistent reduction in a physiological outcome, which was expected as all of these parameters should stimulate increased plaque growth thus constricting the arterial lumen.

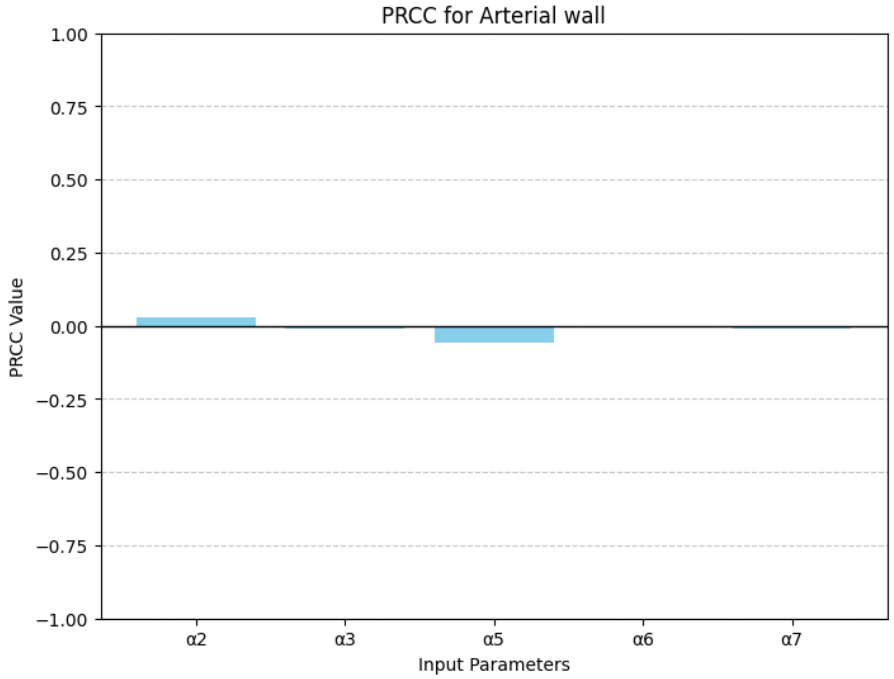

Figure 20. PRCC for arterial wall

There are no statistically significant PRCC scores for the influence of variable simulation parameters on remodeling of the arterial wall. The arterial wall's response might be driven by a combination of factors working together, rather than any single parameter exerting a dominant influence.

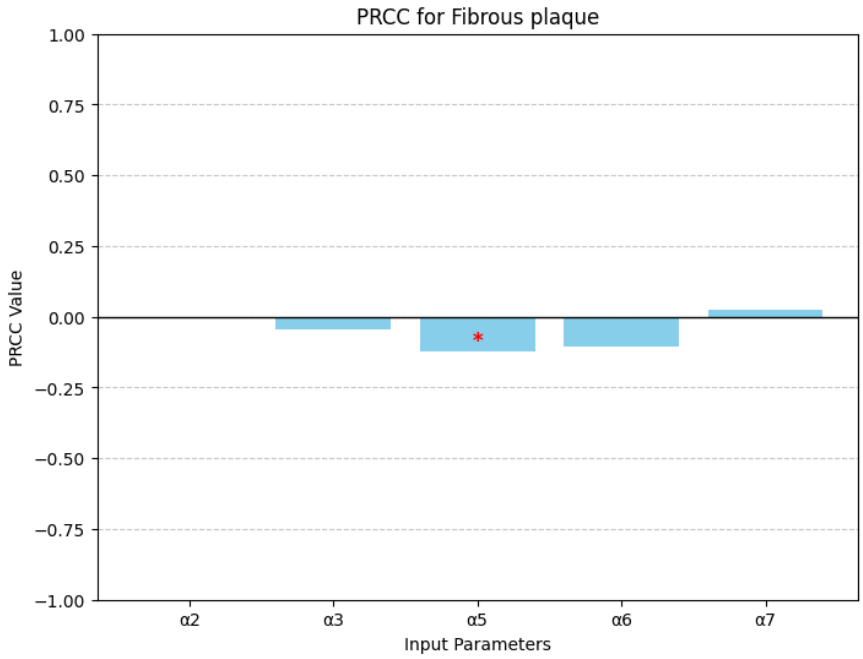

Figure 21. PRCC for fibrous plaque

The only parameter shown to be statistically significant influence on fibrous plaque decrease is the probability of lipid infiltration. From a biological point of view, lipid infiltration leads to plaque progression towards transition to calcified plaque.

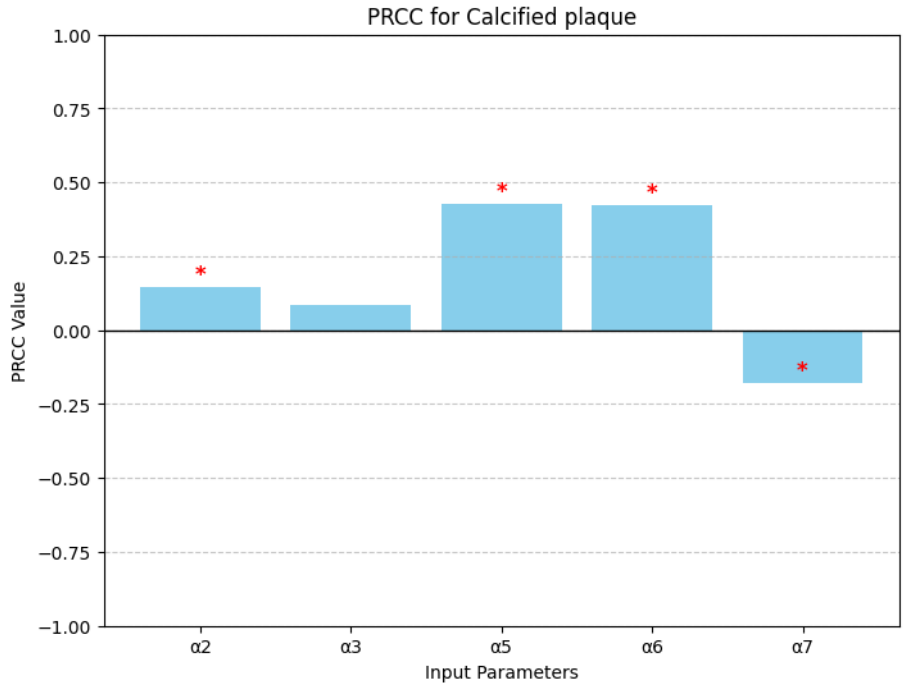

Figure 22. PRCC for calcified plaque

Variable parameters α2, α4, α5, α6 show a statistically significant positive PRCC while α7 shows a relatively low but statistically significant PRCC. A positive PRCC for α2 suggests that increased smooth muscle cell activity contributes to plaque growth, while α4 indicates that weakening of the extracellular matrix exacerbates arterial occlusion. Similarly, α5 plays a crucial role in plaque formation by increasing lipid accumulation within the artery and α6 positively affects the lumen, suggesting that hemodynamic forces help maintain or expand the arterial diameter, while α7 shows a weaker, but still significant, influence on outward remodeling. These findings underscore the complex interplay between cellular proliferation, lipid dynamics, and mechanical forces in the progression of atherosclerosis.

4.3. Surrogate model

Computational modeling framework of coupled ABM and FEM is powerful but it comes at a price of time intensity, lack of flexibility and specific-knowledge required to conduct it. As the aim of biomedical engineering is to simplify processess in healthcare making it more efficient and cost effective, thus enhancing the quality of treatment, an AI-based system for prediction of the extent of plaque progression was developed.
A vast amout of data was generated through LHS and that data was used for the development of the AI algorithm. The workflow is presented in Figure 23.

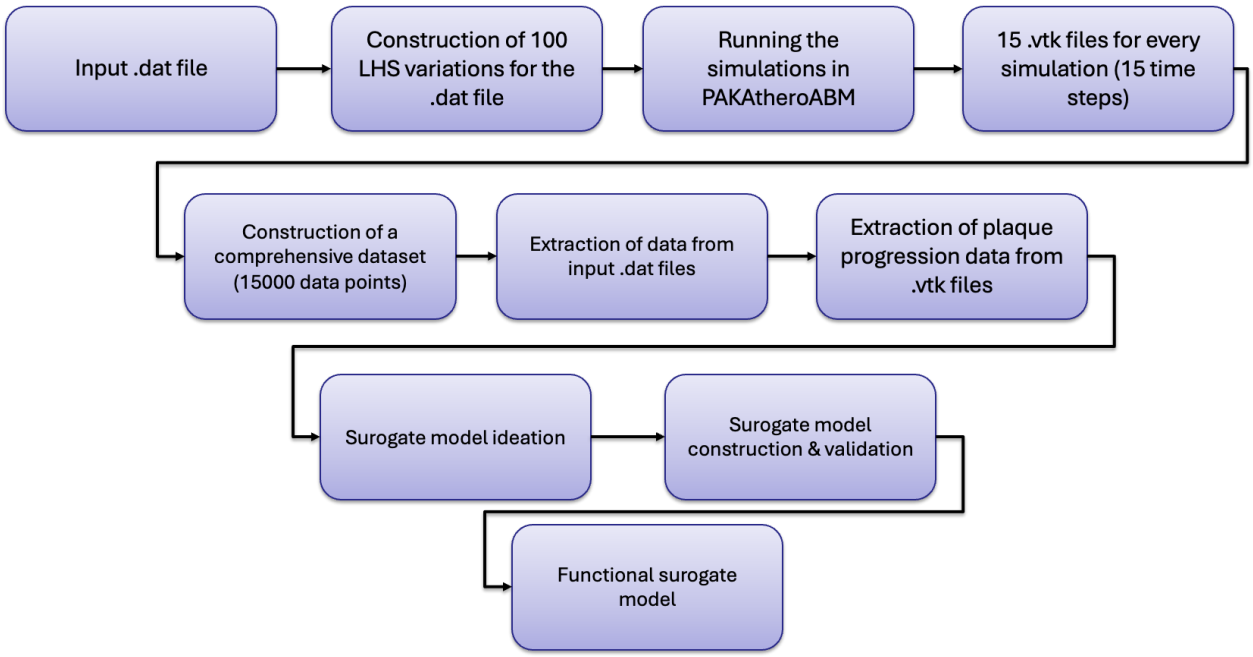

Figure 23. Workflow surrogate model development

The development of a surrogate model for estimating the class of plaque progression based on ABM parameters and initial plaque content involves several critical steps, starting from data preparation to model evaluation. This process aims to replace detailed simulations with a simplified, yet accurate, predictive model, significantly reducing computational time and complexity while maintaining acceptable levels of prediction accuracy.

4.3.1. Dataset curration

The success of a surrogate model relies heavily on the quality and comprehensiveness of the dataset used to train and validate the model. In this work, the dataset was constructed from detailed simulations of plaque development within the arterial wall, using an ABM framework. This approach allowed for the precise modeling of complex biological interactions that occur during plaque formation, providing a rich source of data for building an accurate and efficient surrogate model. The data comprises two fundamental components: initial plaque content and ABM parameters.
The initial plaque content refers to the baseline state of the arterial plaque before any progression or treatment interventions. This data is critical because it establishes the starting point from which plaque growth and progression are simulated. In biological terms, the composition and state of the plaque at this initial stage determine how it evolves over time, driven by cellular and molecular interactions. The initial plaque content serves as the input for ABM simulations, dictating how the plaque behaves under various conditions. The heterogeneity in this starting content provides a wide range of possible plaque development outcomes, which the surrogate model aims to predict.

In addition to the initial plaque content, the dataset includes a series of ABM parameters defined in .. These parameters define the rules and mechanisms governing the behavior of various agents (e.g., cells, molecules) within the ABM. They represent the dynamic processes that drive plaque progression over time.

The key ABM parameters used in this study are:

- Cellular proliferation rates: These rates govern how quickly smooth muscle cells and macrophages divide and accumulate within the plaque. For instance, smooth muscle cells can proliferate in response to inflammatory signals, contributing to the thickening of the plaque's fibrous cap. The rate of macrophage proliferation also impacts inflammation and plaque vulnerability.
- ECM degradation rate: The balance between ECM production and degradation affects plaque stability. Excess ECM degradation, often driven by enzymes secreted by macrophages, can weaken the plaque's structure and increase the risk of rupture. Conversely, excessive ECM production can lead to excessive thickening of the plaque, potentially narrowing the arterial lumen.
- Lipid infiltration and transport dynamics: The rate at which lipids infiltrate the arterial wall and their subsequent transport across different layers of the artery are key drivers of plaque progression. The ABM simulates how lipids accumulate in the plaque and trigger further inflammatory responses, driving the formation of foam cells.
- Parameters driving the arterial wall remodelling on the meso-scale in response to the micro-scale ABM

Each of these parameters influences the evolution of the plaque in a unique way, contributing to the overall complexity of the disease process. For example, higher cellular proliferation rates may lead to a more aggressive form of plaque growth, while increased ECM degradation could result in a more vulnerable plaque prone to rupture.

Given the inherent complexity of the biological processes involved in plaque development, it is critical to ensure that the dataset covers a wide range of possible scenarios. In this study, LHS was used to vary the initial plaque content and ABM parameters across a wide range of plausible values. This approach ensures that all areas of the parameter space are sampled adequately, which is particularly important when modeling complex, non-linear systems like plaque progression. By using LHS, the study was able to generate a diverse set of simulation runs, each representing different combinations of:

- Probability of mitosis and apoptosis
- Smooth muscle cell (SMC) division in the intimal layer
- Extracellular matrix (ECM) deposition in intimal layer
- ECM deposition in medial layer
- SMC division in medial layer
- Outward remodeling driven by shear forces
- Outward remodeling driven by tensile forces

Each simulation run represents a unique instance of plaque development under specific conditions, providing the dataset necessary for training the surrogate model.

The LHS approach was used to generate 1500 simulations, each representing different combinations of initial conditions and ABM parameters. These simulations were run through the agent-based model, which tracks the progression of the plaque over time. The simulation outputs include the final plaque state and the progression class (i.e., no progression, moderate progression, or severe progression), which serves as the target variable for the surrogate model.

The resulting dataset includes a comprehensive range of conditions, making it suitable for training a surrogate model capable of predicting plaque progression based on the initial

plaque content and ABM parameters alone. This dataset forms the basis for all subsequent steps in the surrogate model development process, including feature engineering, model training, and evaluation.

4.3.2. Data retrieval

Once the simulations were completed, the focus shifted to retrieving the critical data for analysis, specifically from large `.vtk` files that contained information about the progression of atherosclerotic plaque within arteries. .vtk files store information about points (vertices), connectivity (how those points form shapes like triangles or polygons), and attributes (e.g., color, scalar values, or vector fields) for visualization and analysis of the agent based simulation. These simulations had been executed across multiple cases, each stored in a dedicated folder. Each folder represented a different simulation scenario with unique input parameters that influenced the progression of plaque. The data extraction process was essential for analyzing how various factors affected plaque buildup and arterial occlusion over time.

Initially, the challenge was to parse through the `.vtk` files. These files, often used for scientific data visualization, contained massive amounts of data across hundreds of thousands of lines. The relevant data regarding plaque progression was stored between specific lines and columns. It was essential to focus on just this subset to reduce unnecessary processing overhead. In this particular case, the lines of interest ranged from 487883 to 532702. Additionally, the desired data was located within certain columns of these lines (columns 5 to 7), meaning that the script had to be precise in targeting the correct sections of the file.

Given the size of the files, manually opening and reviewing them was impractical. Therefore, an automated approach was necessary. A Python script was developed to systematically go through each folder, open the `.vtk` files, read through the relevant lines, and extract the specific column data. The files `PAKF0001.vtk` and `PAKF0015.vtk` were of particular interest since they contained critical data snapshots at different time points in the simulations. These two files represented the progression of the plaque at different stages, and the goal was to compare the data between these stages to understand how the plaque evolved under different conditions.

The script was designed to iterate over all the folders named according to a specific pattern, such as "abm0", "abm1", and so on. It ensured that only folders containing simulation data were processed, thus avoiding any irrelevant files. For each folder, the script accessed the `.vtk` files and read through the required line ranges, collecting the data from the necessary columns. This data was then stored in a Pandas DataFrame, a flexible and powerful data structure used for handling tabular data in Python.

Once the data from the two `.vtk` files was extracted and stored in the DataFrame, the next step was to save this data into an Excel file. The script created a new Excel file for each simulation folder, with the data from both `PAKF0001` and `PAKF0015` represented as separate columns in the spreadsheet. `PAKF0001` and `PAKF0015` contain the simulation results for 2 distinct datapoints in a simulation cycle. This allowed the results of each simulation to be easily accessed and analyzed in Microsoft Excel or any other software that could handle `.xlsx` files.

The initial process involved saving each Excel file in a corresponding subfolder within the output directory. However, as the requirements evolved, it became clear that a more efficient approach was needed to centralize all the Excel files into a single directory, making them easier to access and manage. The code was adjusted accordingly to bypass subfolder structures and place all Excel files directly into one folder.

After the initial data extraction and storage, the focus shifted toward analyzing the transitions between the stages of plaque progression represented by the data in `PAKF0001` and `PAKF0015`. This required calculating the changes in plaque categories between the two stages, essentially identifying how frequently the arterial tissue behaved and how transitions from 1 (vessel lumen) and 2 (vessel wall) to 3 (fibrous plaque) and 4 (calcified plaque) occured and to which extent. The transitions were critical for understanding the dynamics of plaque development and how different simulation parameters affected these dynamics.

To handle this, the data was compared between the two columns of the Excel files corresponding to `PAKF0001` and `PAKF0015`. The transitions were categorized into different scenarios, such as plaque moving from category 1 to category 2, or from category 2 to category 4. A variety of transition types were considered to capture all possible changes, including combinations such as moving from category 1 to either category 3 or 4. The goal was to generate a detailed profile of how the plaque progressed in each simulation.

For each transition type, the total number of occurrences was calculated, and then these occurrences were converted into percentages to give a clearer picture of the distribution of transitions. These percentages reflected the proportion of transitions relative to the total number of data points, allowing for easy comparison between different simulations. Finally, the percentage transitions were arbitrarily classified into three classes to capture the heterogeneity of the plaque progression cases :

- 0 - „insignificant plaque progression“(<0.05%)
- 1 – „significant plaque progression“ (0.05%-0.15%)
- 2 – „severe plaque progression“ (>0.15%)

After the transition analysis for all simulations was completed, the results were compiled into a single Excel workbook. Each sheet in the workbook corresponded to one simulation case and contained the detailed transition analysis for that case. The final output provided a comprehensive overview of how plaque progressed across all the simulations, with easy access to both the raw extracted data and the calculated transition percentages.

4.3.3. Data analysis

Once the data from the simulations had been successfully retrieved and organized into Excel files, the next step was conducting a detailed statistical analysis. This analysis aimed to uncover patterns, correlations, and key insights from the large dataset of plaque progression parameters across various simulations. The process began with basic descriptive statistics to provide an overview of the data and then moved into more advanced techniques such as Principal Component Analysis (PCA) for dimensionality reduction.

The first step in the statistical analysis involved calculating descriptive statistics for each feature extracted from the simulation data. These statistics included measures such as the mean, median, standard deviation, and interquartile range for each variable. Given that

the simulations involved multiple parameters—each influencing the progression of atherosclerotic plaque—it was critical to understand the distribution of these parameters individually before delving into more complex relationships (Figure 24).

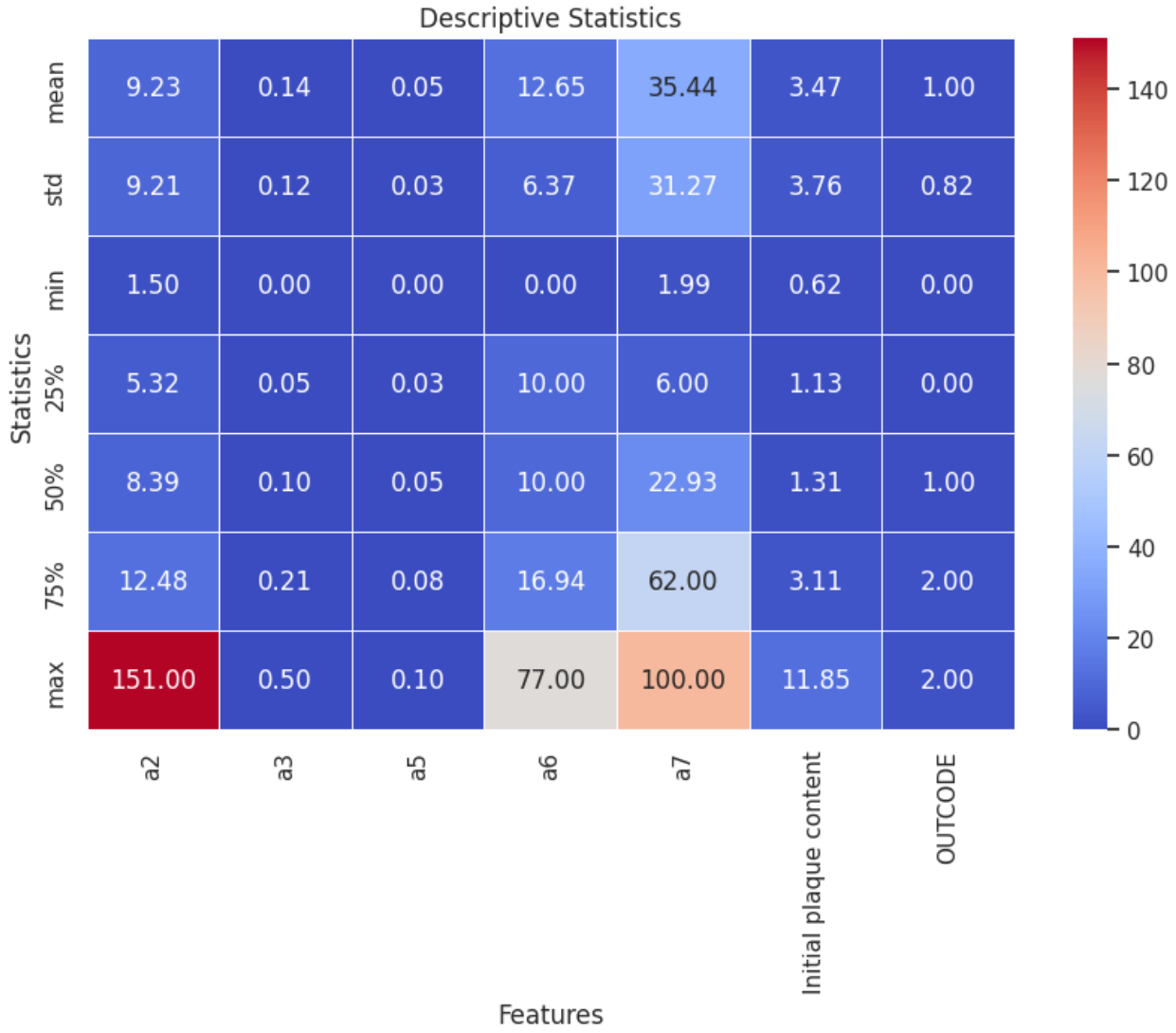

Figure 24. Descriptive statistics of the dataset showing min, max, mean, STD, 25%, 50% and 75% characteristics of the data

The descriptive statistics provided a foundational understanding of how each parameter behaved across different simulations. As the aim of conducting a substantial number of simulations to cover as much as possible variability and different simulation cases it was necessary to observe the statistical behavior of individual parameters. Obserbving the standard deviations revealed the approximate discrepancies amongst different simulation scenarios, important to grasp weather the dataset covers enough variability while analysis of min and max for each parameter enabled understanding weather extremes are covered for parameters. For example, examining the range and variability in plaque thickness or changes in material composition helped to identify any outliers or extreme values that might affect the overall analysis and contribute to extreme cases to cover peculiar pathologies. Skewness and kurtosis were also calculated to assess the symmetry and peakedness of the data distributions, giving further insights into the nature of the dataset.

In this stage, histograms were used to visualize the spread of each variable. These visualizations helped to identify any non-normal distributions or skewed data, both of which would need to be addressed before proceeding to more advanced analyses. For instance, if a parameter exhibited a highly skewed distribution, transformations such as log or square-root transformations were considered to normalize the data, ensuring it was suitable for subsequent steps.

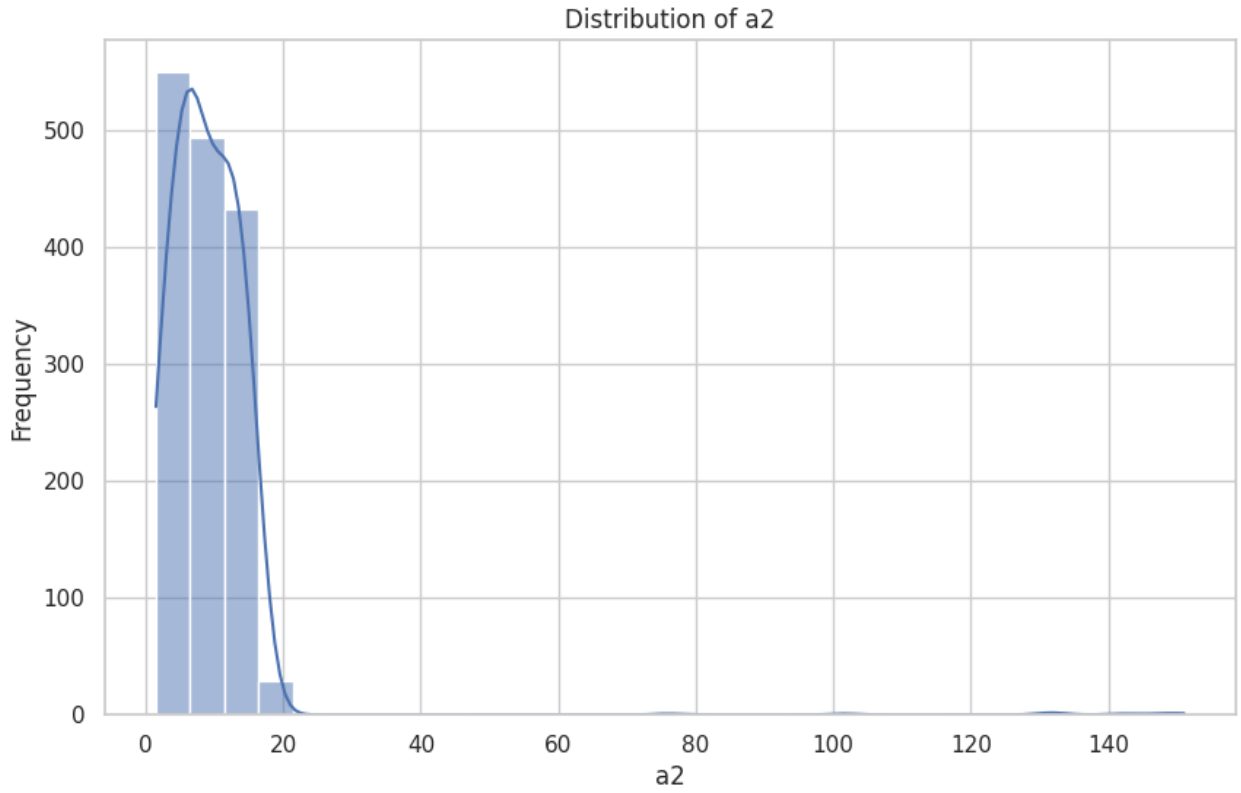

Figure 25. Distribution of parameter α_2.

Parameter α_2 exhibits a highly skewed distribution to the left. When a distribution is characterized by a left skew, or negative skewness, it indicates that the majority of the data points are concentrated on the right side of the distribution, with the tail extending to the left. This scenario often suggests that while most of the values are relatively high, there are a few significantly lower values that are pulling the average down. The distribution of the parameter which represents the probability of smooth muscle cell (SMC) proliferation in the tunica media, exhibits a prominent peak on the left side of the distribution curve. This indicates that the majority of the sampled data points cluster around relatively low probabilities of SMC proliferation, suggesting that under most physiological conditions, SMC proliferation is limited. This leftward concentration is typical of a distribution where most observations reflect normal physiological states, where SMC activity is kept in check to maintain vascular homeostasis. However, the pronounced peak indicates that, while the baseline probability of SMC proliferation is low for most conditions, it is crucial to recognize the context in which these low values exist. The peak signifies that under typical scenarios—where there are no significant pathological stimuli—the probability of SMC proliferation remains minimal. Such conditions might involve a stable vascular environment with balanced biochemical signals, low levels of inflammation, and normal mechanical stresses.

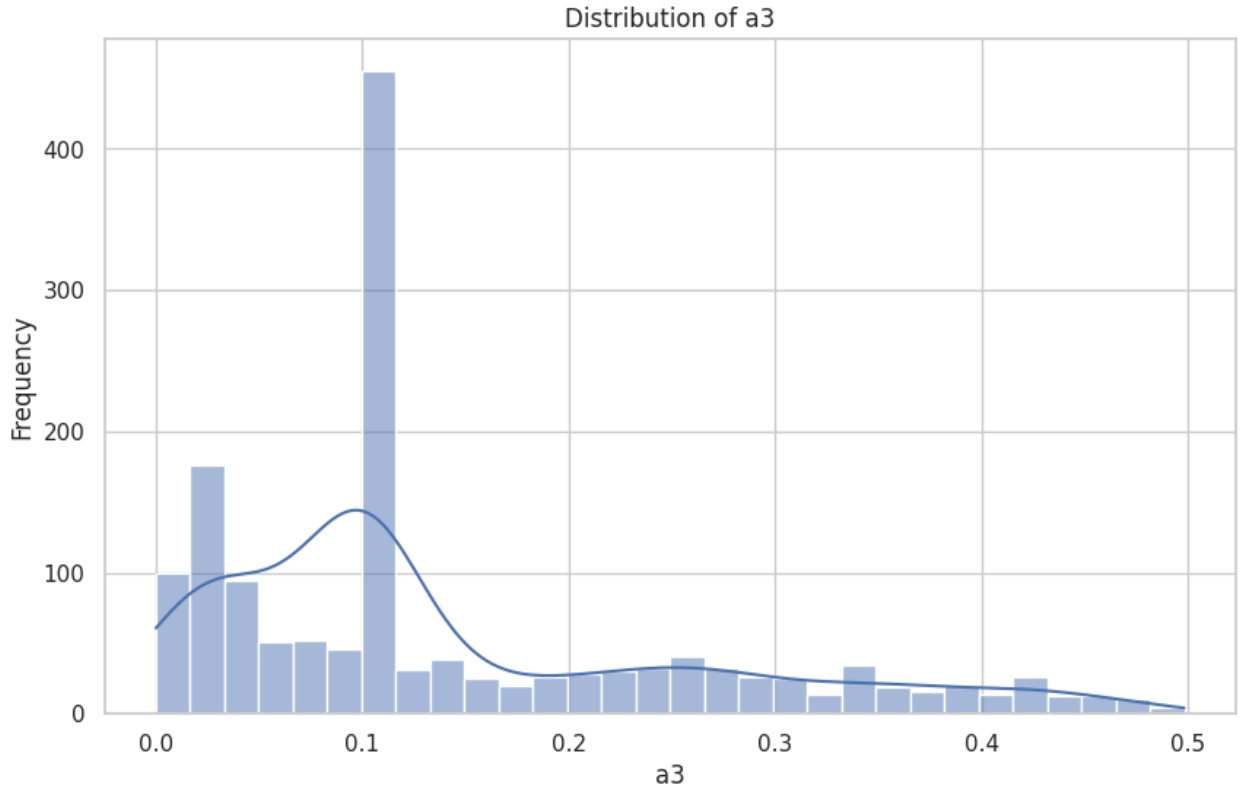

Figure 26. Distribution of parameter α_3

The long right tail of the skewed α_3,or positive skewness, indicates that most of the data points are concentrated on the left side of the distribution, while a few high values extend the tail to the right. This type of distribution is often seen in situations where the majority of observations are relatively low, but there are a small number of exceptionally high values that significantly influence the mean. It suggests that while most of the sampled conditions represent lower probabilities of SMC proliferation—indicating a typical response under most physiological conditions—there are specific cases where the probability spikes to much higher levels. These high-probability cases are likely tied to scenarios where multiple influential factors align favorably, such as elevated concentrations of growth factors, the presence of certain inflammatory signals, or particular biomechanical stresses within the vessel wall. The presence of these outlier conditions is crucial to understand because they can lead to significant pathological outcomes, such as excessive intimal hyperplasia or plaque formation. The LHS approach ensures that these extreme values are not merely a product of random chance but are systematically included in the analysis. Consequently, the long right tail in the resulting distribution reflects a genuine risk of heightened SMC proliferation under specific, albeit less frequent, conditions.

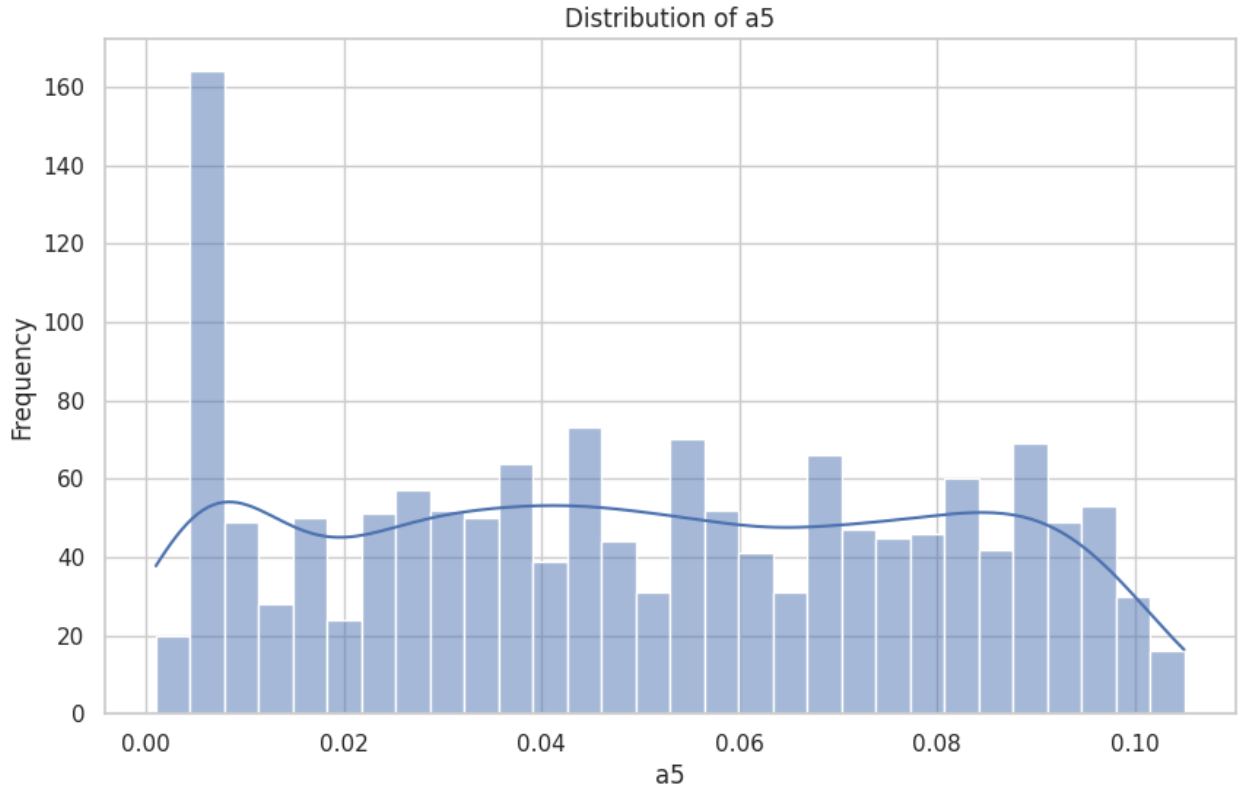

Figure 27. Distribution of parameter α_5

The parameter α_5, representing the probability of lipid infiltration, displays a nearly flat distribution across the range of sampled values. This characteristic indicates a relatively uniform likelihood of lipid infiltration occurring within the studied context, suggesting that the conditions influencing this process do not lead to significant peaks or troughs in probability. In a scenario where the probability distribution is flat, it implies that lipid infiltration can happen across a wide range of circumstances without being significantly influenced by any specific factor. Essentially, the chances of lipid accumulation remain consistent, irrespective of variations in other parameters or environmental conditions. This could be indicative of a physiological state where lipid infiltration is a common process occurring under various influences, rather than a response that is tightly linked to specific triggers or conditions. The flatness of the distribution suggests that lipid infiltration is a somewhat ubiquitous process within the arterial wall, potentially reflecting a baseline state where lipids are consistently present and integrated into the vessel environment. Factors contributing to this uniformity might include steady-state levels of circulating lipoproteins, consistent dietary influences, or a relatively constant state of endothelial function, which does not fluctuate dramatically across the sampled conditions. A flat distribution may also indicate that there is a lack of strong pathological stimuli that would otherwise concentrate the probability of lipid infiltration in particular scenarios. In other words, while lipid infiltration can occur, it does not appear to be heavily influenced by extreme conditions or changes in parameters, thus leading to a more even representation across the entire range.

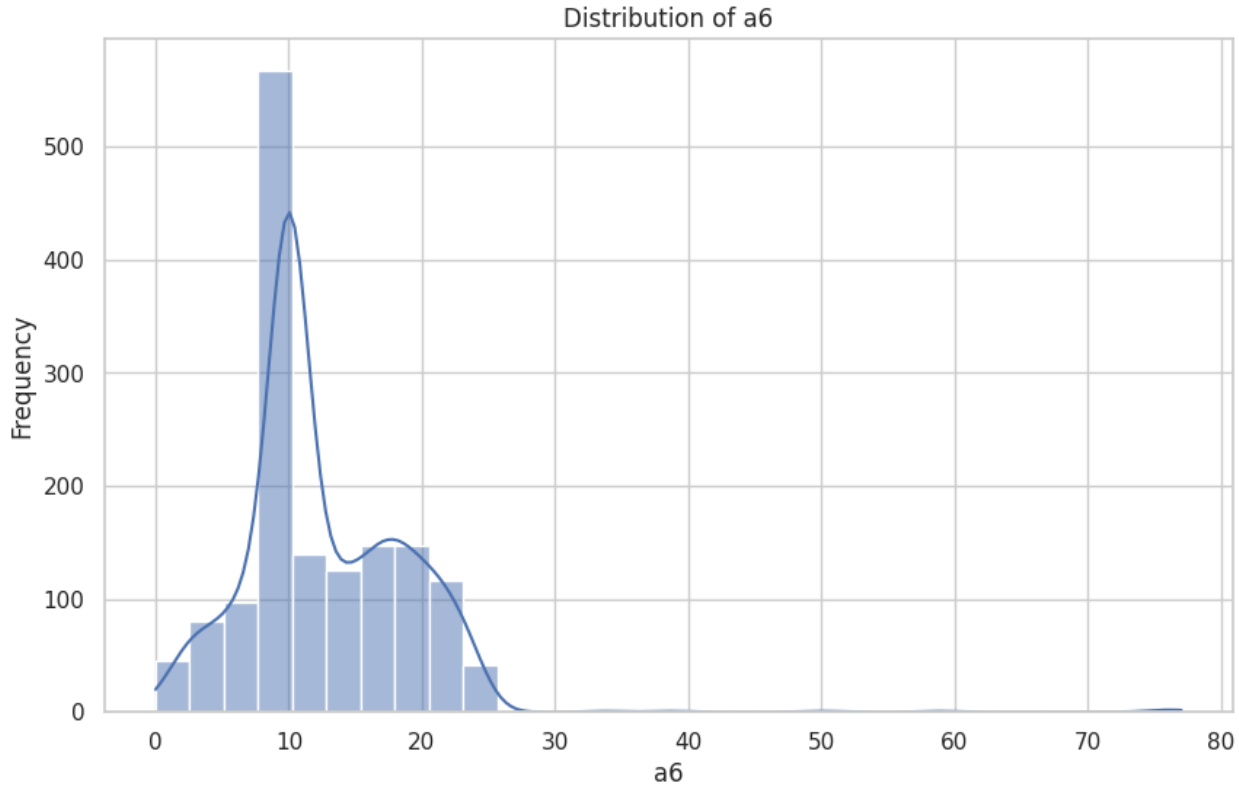

Figure 28. Distribution of parameter α_6

The parameter α_6 , which represents arterial remodeling driven by shear forces, exhibits a distribution characterized by a pronounced peak on the left side and a sharp drop-off towards the right. This shape suggests that most of the observations cluster around lower values, indicating that arterial remodeling due to shear forces typically occurs at minimal levels. The large peak signifies that the majority of cases involve mild to moderate remodeling in response to normal physiological conditions. This clustering of values at the lower end implies that under typical circumstances—such as healthy blood flow patterns—the remodeling processes in the arterial wall are subtle. These adaptations can include slight adjustments in smooth muscle cell behavior, minor changes in extracellular matrix composition, or other physiological mechanisms that support vascular function without leading to significant alterations in arterial structure. The rapid drop-off to the right indicates that as we move toward higher levels of α_6, there are far fewer instances of pronounced arterial remodeling. This steep decline suggests that significant remodeling events driven by shear forces are relatively rare. When they do occur, they may be associated with specific pathological conditions, such as abnormal blood flow patterns, increased turbulence, or heightened hemodynamic stress. Such conditions can lead to substantial changes in arterial architecture, potentially contributing to vascular diseases or conditions like atherosclerosis. The presence of this distribution highlights the importance of understanding the normal range of arterial remodeling driven by shear forces. Most scenarios involve modest remodeling that is essential for maintaining vascular health. However, the few high values that fall off sharply to the right indicate potential risk factors or pathological states that warrant attention. Recognizing these rare but significant remodeling events is crucial for developing strategies to address and mitigate adverse cardiovascular outcomes.

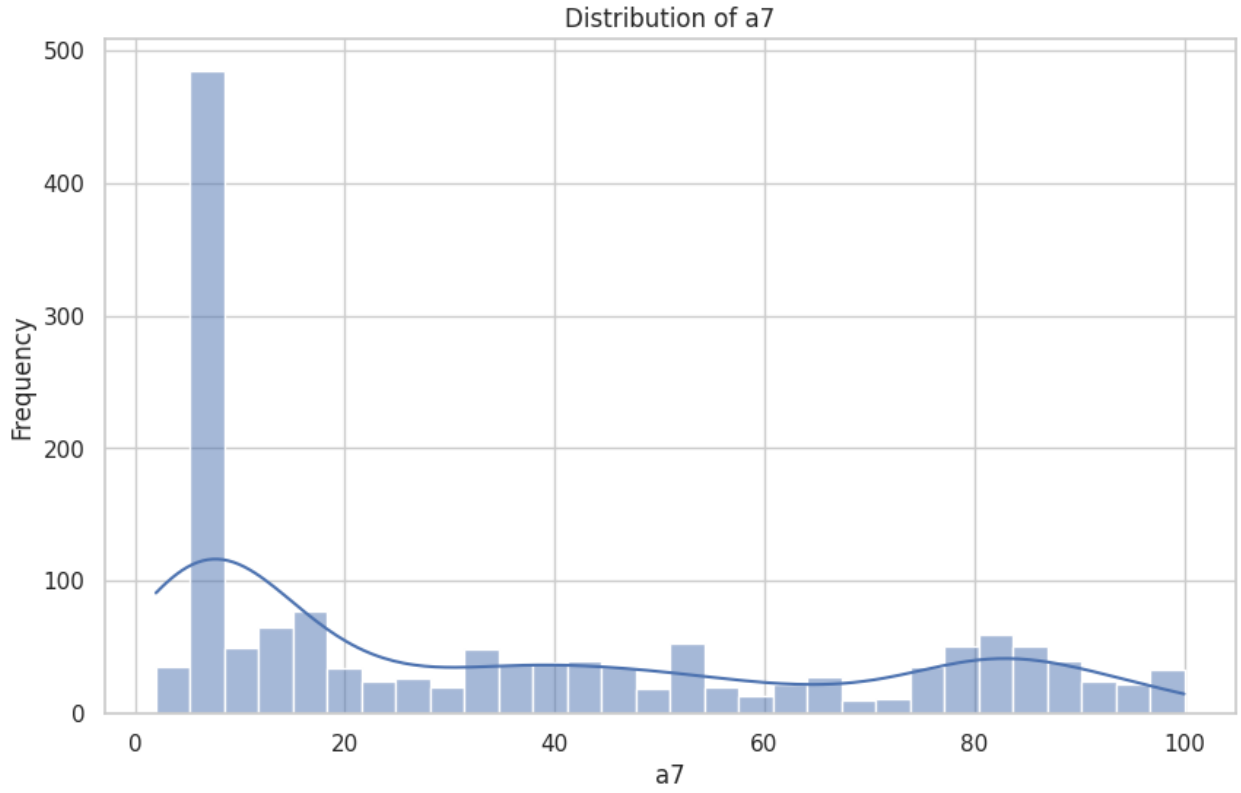

Figure 29. Distribution of parameter α_7

The parameter α_7, which represents remodeling driven by tensile forces, displays a distribution that is largely flat with a distinct peak on the left side. This shape indicates that most of the values are concentrated around lower levels of remodeling, suggesting that tensile forces typically exert a moderate influence on arterial structure. The presence of a prominent peak on the left signifies that the majority of cases involve minimal to moderate remodeling in response to normal tensile stresses experienced by the arterial walls during regular physiological conditions. These low-level adaptations are essential for maintaining the structural integrity and functionality of the artery under the forces exerted by blood flow. They may involve subtle changes, such as slight alterations in the composition or organization of the extracellular matrix or modest adjustments in smooth muscle cell activity. The flat nature of the distribution indicates that there is a broad range of values around this peak, suggesting that while most cases involve lower levels of remodeling, there is a significant variability in how arterial walls respond to tensile forces. This variability could be influenced by factors such as individual differences in vascular biology, local hemodynamic conditions, and the mechanical properties of the arterial wall itself. However, the lack of significant values extending towards the right side of the distribution implies that high levels of remodeling driven by tensile forces are relatively rare. When they do occur, they may be associated with specific conditions, such as pathological hypertension or significant vascular stress, which can lead to excessive remodeling that compromises arterial function.

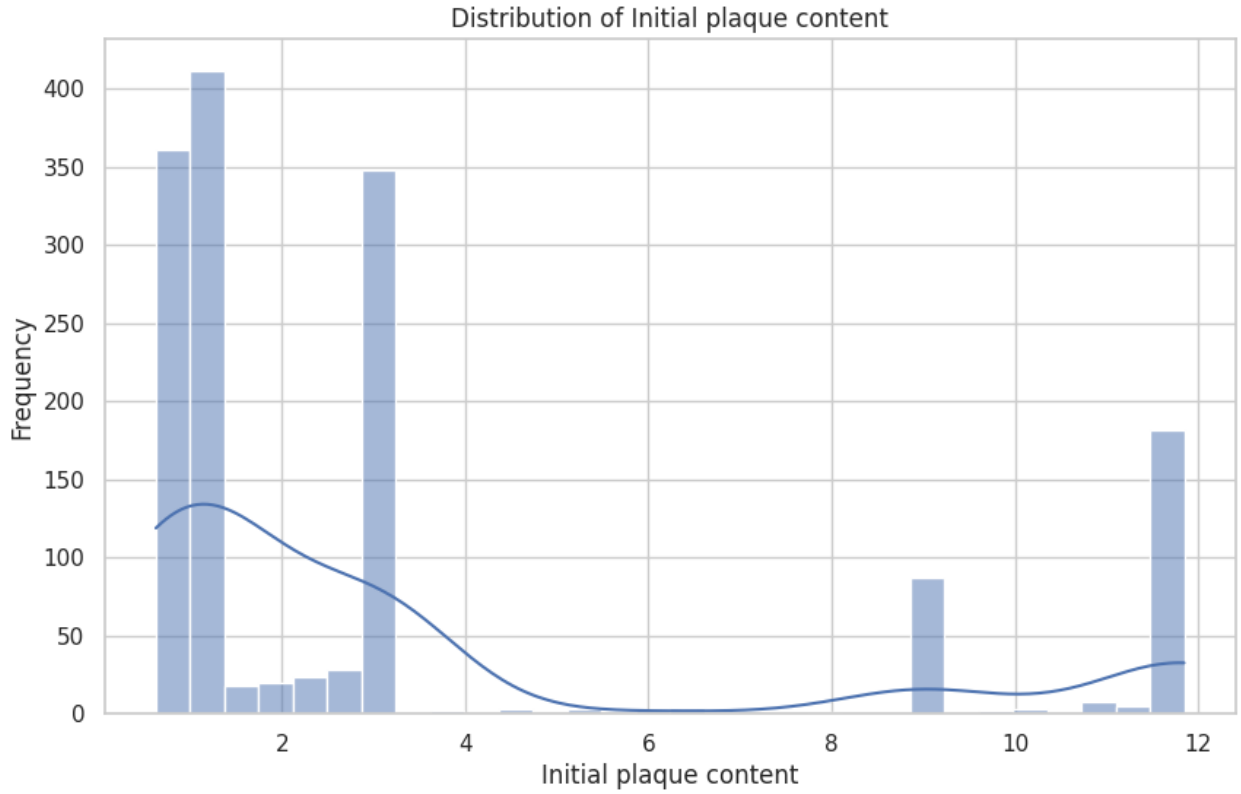

Figure 30. Distribution of "initial plaque content" variable

The initial distribution of plaque content exhibits a unique pattern characterized by several peaks on the left, followed by a gap, and then additional peaks on the right. This multimodal distribution suggests a complex relationship between various factors influencing plaque development within the arterial walls. The presence of multiple peaks on the left side of the distribution indicates that there are several common states of low plaque content, where the majority of cases fall. These peaks likely represent typical physiological conditions where minimal plaque accumulation occurs, reflecting healthy arterial function and effective regulatory mechanisms that prevent excessive lipid deposition and inflammation. Such states may be influenced by factors such as optimal shear stress, the presence of protective endothelial functions, and effective clearance of lipids and inflammatory cells from the arterial wall. The gap between the left and right peaks signifies a notable absence of cases with moderate plaque content, suggesting that this range may represent a transitional phase where arterial health is particularly vulnerable. This void could indicate that under normal physiological conditions, arteries tend to either remain relatively clear of plaque or progress to significant plaque accumulation due to a combination of risk factors such as elevated lipid levels, inflammation, and mechanical stress. The peaks on the right side of the distribution represent scenarios of higher plaque content, indicating that while most conditions tend to favor lower plaque levels, there are specific pathological states where significant plaque accumulation occurs. These peaks might reflect conditions of advanced atherosclerosis, where a combination of risk factors, such as chronic inflammation, prolonged exposure to high lipid levels, and mechanical stress, converge to drive substantial plaque formation.

Once the descriptive statistics were reviewed, the next step involved calculating correlation matrices to assess the relationships between the different variables. This

allowed for an exploration of how different simulation parameters influenced each other. Pearson correlation coefficients were used to quantify the strength and direction of linear relationships between variables, while Spearman's rank correlation was used for non-linear relationships.

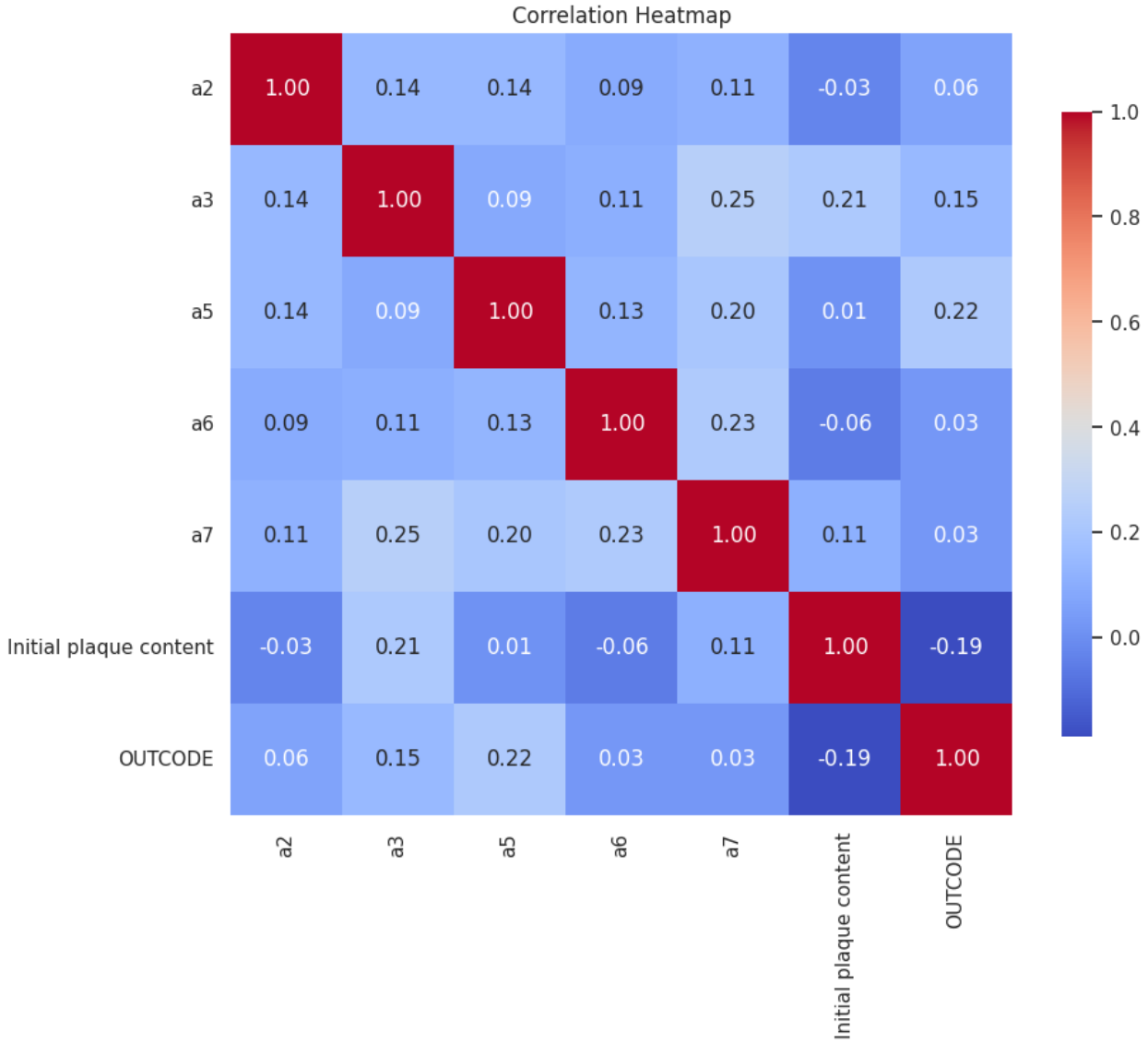

Figure 31. Correlation heatmap for input and output variables

By examining the correlation matrix (Figure 31), it became clear that none of the parameters exhibit strong correlation neither with one another nor with the output. As atherosclerosis is a process dependent on parameters that do not behave in congruency with one another, the correlation matrix of this kind was expected and it confirmed that the simulation instances generated by LHS mimic real-world conditions and that the creation of a realistic virtual population was successful. Understanding these relationships was important to note that complex machine learning algorithms will be necessary in order to draw inference and recognize patterns in this data.

Recognizing and addressing this issue early was key to ensuring that the next phases of analysis, such as PCA, were robust and reliable. Given the high dimensionality of the dataset, multiple parameters for each simulation case, PCA was applied to reduce the dimensionality and simplify the complexity of the data while retaining as much variance

as possible. The main goal of PCA was to transform the data into a new set of uncorrelated variables called principal components. These components represented the directions in which the data varied the most, allowing for a more efficient exploration of the key factors influencing plaque progression.

The PCA process began by standardizing the data, ensuring that each variable had a mean of zero and a standard deviation of one. This step was crucial because PCA is sensitive to the relative scales of the variables; without standardization, variables with larger scales could dominate the first principal components, skewing the results. Once the data was standardized, the PCA algorithm was applied. The first principal component (PC1) explained the maximum amount of variance in the data, followed by the second component (PC2), and so on.

A pairplot of features per class was used to visualize the percentage of variance explained by each principal component, helping to determine how many components should be retained for further analysis. In this case, the first few components typically explained a significant proportion of the variance, allowing the dataset to be reduced to a handful of principal components without sacrificing much information.

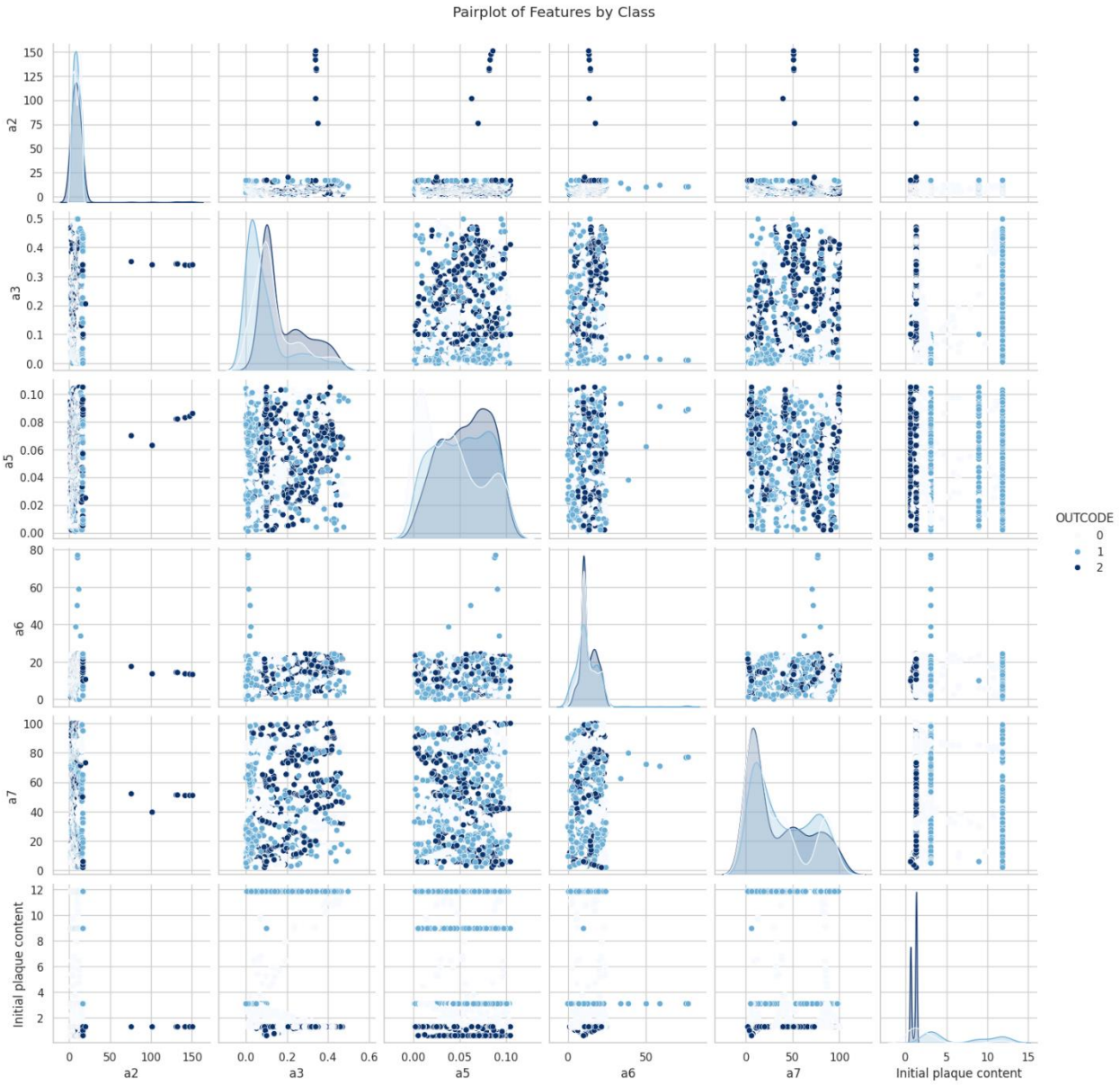

Figure 32. Pairplots of features per class

The pairplot of features per class (Figure 32) provides the same conclusion as the correlation matrix and that is the fact that the features exhibit very low interclass variability and very high intraclass variability making them overlap in all cases except when plaque content (response variable) is considered.

After application on individual variables, PCA was applied to the entire dataset in order to determine weather additional feature engineering will be necessary and to gain insights into the underlying structure of the data. Each principal component was a linear combination of the original variables, and the loadings of these variables indicated their contribution to the component. By examining the loadings, it was possible to understand which variables were the most important in driving plaque progression. For instance, PC1 might heavily load on variables related to arterial stiffness and plaque thickness, indicating that these factors were the primary drivers of variance in the data. Additionally, scatter plots of the first two or three principal components were created to visualize how the simulation cases clustered in the reduced-dimensional space. These plots helped

identify any natural groupings or clusters of simulations, which could indicate different progression patterns. Outliers could also be easily spotted in these plots, offering a way to flag simulations with unusual behavior that warranted further investigation.

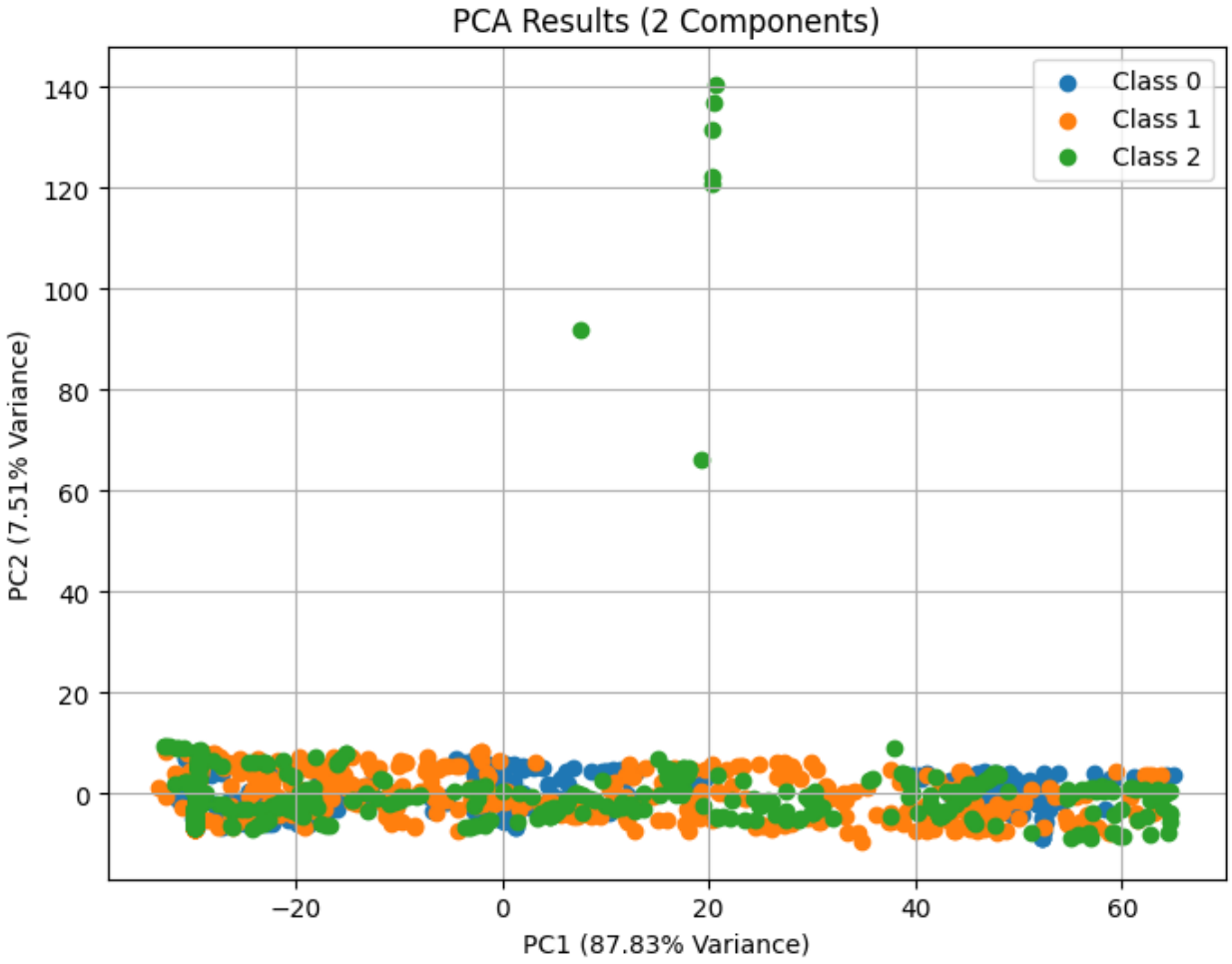

Figure 33. PCA results

After examining the PCA graph (Figure 33), which illustrates the distribution of the dataset in its original feature space, it is essential to consider the implications of reducing the dimensionality of the data. By transforming the data into a lower-dimensional space, we can effectively capture the most significant variance while minimizing the noise associated with irrelevant features. This process not only simplifies the complexity of the data but also enhances visualization, allowing for more straightforward interpretation of the underlying structure. The subsequent analysis was intended to focus on how this reduction facilitates better classification performance and provides clearer insights into the relationships among the data points.

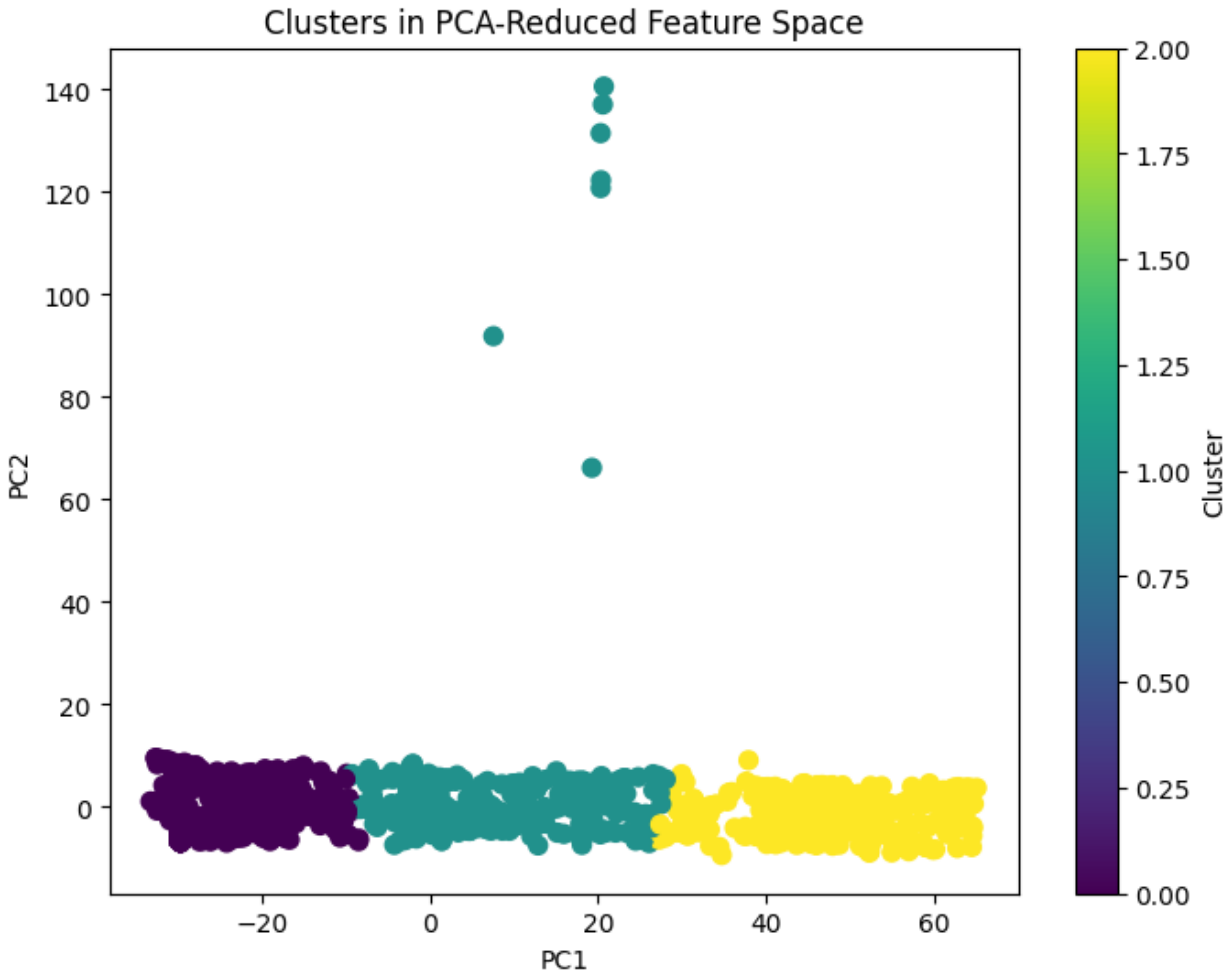

Figure 34. Clusters in PCA-reduced feature space

Due to the complexity of the problem and aforementioned high intraclass variability combined with low interclass variability, dimensionality reduction did not contribute to enhancing the PCA results. This has lead to a conclusion that significant data preprocessing will be necessary prior to the development of the machine learning algorithm.

4.3.4. Dataset preprocessing

Entire statistical analysis was done with the purpose of understanding the dataset better and being able to optimize the preparation of thereof for implementation of the AI algorithm. The analysis began by preparing the environment with the necessary tools for handling imbalanced data and Excel files. The dataset, which contained both input features and an output variable, was then uploaded from an Excel file. The relevant input features were selected for analysis, and the output variable, representing the target for classification, was extracted. This step ensured that the data was correctly formatted and ready for splitting into training and testing subsets.

To develop and validate a predictive model, the dataset was divided into two parts: 80% was allocated for model training, and the remaining 20% was reserved for testing. A fixed

random seed was used to ensure consistency across different runs of the analysis, allowing for reproducibility in the results.

Given that the dataset exhibited class imbalance, an advanced oversampling technique, Adaptive Synthetic Sampling (ADASYN), was applied. This method generates synthetic samples for underrepresented classes by creating data points that are similar to the minority class but slightly varied, ensuring a more balanced distribution. The goal was to equalize the representation of all target classes, which would otherwise lead to biased model training. The synthetic data generation process was tailored to create an equal number of samples for each class, ensuring that all classes were sufficiently represented.

Following the resampling process, the newly balanced dataset was organized and saved for further analysis. The synthetic samples and the target labels were combined and exported to an Excel file, preserving the resampled data for future model development.

To verify the effectiveness of the resampling technique, the distribution of the classes in the new dataset was assessed. The analysis confirmed that each class was now represented equally, validating the success of the synthetic sampling approach. By addressing the issue of class imbalance, the dataset was better prepared for model training, ensuring that the subsequent predictive models would not be biased toward the overrepresented classes and could produce more reliable and generalized predictions.

4.4. ANN model

The development of the classification model was introduced with challenges primarily arising from significant intraclass variability, which adversely affected predictive performance. To address these challenges, a systematic approach was adopted, incorporating both class and parameter weights alongside regularization techniques and optimized activation functions. This comprehensive strategy was essential in achieving a robust and reliable model capable of accurately predicting plaque progression in atherosclerosis.

The issue was characterized by a disproportionate distribution of samples or intraclass variability across classes. Even though the sample size was consistent accross classess, an issue arises with overexpressed interclass similarity and lack of overall intraclass variability, leading to biased predictions, where the model favors outcomes more represented in a certain class. To counter this, class weights were assigned to each class, strategically focusing on enhancing the model's sensitivity to the most sensitive class, that being „insignificant atherosclerotic progression“

Class weights were calculated based on the inverse frequency of each class, reflecting the necessity for the model to prioritize learning from underrepresented samples. For instance, class 0 was assigned a weight of 3.0, while classes 1 and 2 received weights of 1.5 and 2.5, respectively. By implementing these weights, the model was empowered to treat the loss function as a more balanced representation of the underlying class distribution, thereby compensating for the imbalance.

In conjunction with class weights, parameter weights were integrated into the training process to further refine the model's learning dynamics. Parameter weights were assigned based on the importance of each feature, which enabled the model to prioritize more influential variables during training. This adjustment facilitated enhanced learning

from critical features, allowing the model to effectively distinguish between classes. The dual implementation of class and parameter weights resulted in substantial improvements in performance metrics, such as accuracy, recall, and F1 scores, particularly for the minority classes. The model's ability to correctly classify instances from these underrepresented groups improved significantly, thereby leading to a more equitable performance across all classes.

To further mitigate the risk of overfitting—a common issue in machine learning where the model learns the noise in the training data rather than the underlying patterns—regularization techniques were employed. L2 regularization (also known as weight decay) was incorporated into the loss function, which penalizes large weights and discourages the model from fitting noise in the training data. This technique is particularly beneficial in high-dimensional spaces, where overfitting is prevalent due to the abundance of features relative to the number of training samples. By applying L2 regularization, the model was encouraged to learn a simpler representation of the data, which improved generalization to unseen data. Regularization not only enhanced the model's robustness but also led to improved interpretability of the learned parameters. The model was able to focus on the most relevant features while minimizing the impact of irrelevant or redundant features, thereby streamlining the decision-making process. This strategic modification was pivotal in enhancing the model's overall reliability and predictive capability.

The choice of activation functions significantly influenced the model's performance and learning efficiency. The Rectified Linear Unit (ReLU) activation function was utilized in the hidden layers, promoting faster convergence and allowing the model to capture complex relationships within the data effectively. ReLU addresses the vanishing gradient problem, which is common in traditional activation functions like sigmoid or tanh, by maintaining non-zero gradients for positive input values. This characteristic enables deeper networks to learn more efficiently, as the gradients do not diminish as they are backpropagated through the network layers. The softmax activation function was employed in the output layer, generating a probability distribution across the target classes. This approach allowed for interpretable output, where the class with the highest probability score was selected as the model's prediction. The softmax function effectively normalized the output scores, making it easier to assess the relative confidence of the model in its predictions. The combination of ReLU and softmax functions ensured that the model was not only capable of learning complex patterns but also provided a probabilistic framework for decision-making.

Two architectures were intensively tested to determine the impact of hyperparameter adjustment and architecture remodeling on the prediction results.

Table 23. Comparison of key ANN parameters between the two developed architectures

Parameter	Definition	Purpose	Impact on Training	Mechanism	Architecture 1 VS 2
Regularization Strength	Controls penalty on weights for	Prevent overfitting	Affects model complexity; high = underfit, low = overfit	Adds penalty to the loss function	L2 (0.01) VS L2 (0.0001)

	complexity				
Training Duration (Epochs)	Number of complete passes over the dataset	Determine learning time	Low = underfit, high = overfit	Each epoch involves forward and backward pass	100 epochs VS 400 epochs
Batch Size	Number of samples processed before weight updates	Controls update frequency	Small = noisy but better generalization, large = smoother but potential overfit	Subset of data used for gradient computation	Batch size 16 VS Batch size 8

Regularization strength is a critical hyperparameter that plays a vital role in managing model complexity. Its main purpose is to prevent overfitting, which occurs when a model learns not only the underlying patterns in the training data but also the noise. Regularization achieves this by adding a penalty to the loss function, which discourages the model from assigning excessive importance to any particular weight. When regularization strength is high, the model is forced to simplify, which can lead to underfitting; in other words, it may not learn enough from the data. Conversely, when the regularization strength is low, the model can become too complex, capturing not just the essential features of the data but also the random fluctuations, resulting in overfitting. Different types of regularization, such as L1 and L2, have unique characteristics, with L1 potentially leading to sparse solutions (many weights becoming zero) and L2 shrinking all weights but retaining more features. Overall, the choice of regularization strength is crucial as it directly impacts the model's generalization ability. The choice of a lower L2 regularization strength (0.001 VS 0.1) may significantly affect the model's ability to generalize beyond the training data. Regularization is intended to prevent overfitting by penalizing overly complex models. A lower L2 regularization strength means that the model is less constrained, allowing it to assign larger weights to features. While this can help the model capture more nuances in the training data, it may also result in a higher risk of overfitting. Consequently, the model might perform well on the training dataset but struggle with unseen data due to its excessive reliance on specific patterns that do not hold in a broader context. Therefore, while a lower regularization strength can lead to improved performance during training, it can ultimately compromise the model's generalization ability.

Training duration, measured in epochs, refers to how many times the model is exposed to the entire training dataset. The main goal of determining the right number of epochs is to ensure that the model learns effectively from the data. If the number of epochs is too low, the model may not have enough opportunities to learn, resulting in underfitting. This means the model fails to capture essential patterns within the data. On the other hand, too many epochs can lead to overfitting, where the model becomes excessively tailored to the training data and performs poorly on unseen data. To strike the right balance, validation loss during training is monitored and strategies like early stopping employed, which halts training when performance on a validation set begins to degrade. Thus, training duration

is about finding the sweet spot where the model learns adequately without memorizing the training data. By opting for a longer training duration, the model has more opportunities to learn from the training data. This extended exposure can be beneficial, particularly if the training set is complex or large. However, it also increases the risk of overfitting, especially if the model is not regularized adequately. Monitoring validation performance is crucial during this phase to ensure that the model is improving its ability to generalize rather than merely memorizing the training examples.

Batch size is the number of training samples processed before the model's weights are updated. It directly influences how the model learns during training. Choosing a small batch size results in more frequent updates to the model's weights, which can lead to noisier gradient estimates. This noise can sometimes help the model generalize better, as it introduces variability in the training process. However, smaller batches can also slow down training since more iterations are needed to complete an epoch. In contrast, a larger batch size means fewer updates per epoch, leading to smoother gradient estimates. While this can accelerate training and make better use of computational resources (like GPUs), it may also lead to poorer generalization, as the model could get stuck in sharp minima that don't perform well on unseen data. Therefore, the choice of batch size should consider the trade-offs between computational efficiency and model performance. Choosing a smaller batch size means the model updates its weights more frequently. While this can introduce beneficial noise into the gradient estimates—potentially aiding in convergence—it also means that each update might be less stable. The noise can help escape local minima but can also slow down the convergence process as the model may take longer to find the optimal solution. Additionally, because smaller batches require more iterations to complete an epoch, this can significantly extend the total training time.

The decisions made in the second architecture reflect a careful balance between improving model performance and managing the risks associated with overfitting. A lower L2 regularization strength, while potentially enhancing training performance, could hinder the model's generalization ability. Meanwhile, the combination of a longer training duration and a smaller batch size facilitates a more nuanced learning process but at the cost of increased training time. Together, these choices highlight the importance of tuning hyperparameters thoughtfully to achieve a well-balanced model that performs well on both training and unseen data.

4.4.1. ANN performance evaluation

In this section, the performance of the developed artificial neural network (ANN) is evaluated by examining the impact of incorporating class and feature weights during training. The objective is to assess how these adjustments affect the model's performance in terms of loss and accuracy, particularly in the context of an imbalanced dataset. A comparative analysis was conducted involving two distinct training configurations for our ANN: the standard model without any weighting and the enhanced model that utilized class and feature weights. The standard model served as a baseline, while the enhanced model aimed to address the inherent challenges posed by class imbalance and to amplify the influence of critical features identified during the initial analysis.

Class weights were computed based on the frequency of each class in the dataset. This approach ensures that the model pays more attention to underrepresented classes, effectively countering the bias that can occur when training on imbalanced data. By assigning higher weights to these classes, the model is encouraged to learn more from the less frequent examples, thus improving its overall performance. Feature weights were employed to prioritize the most influential input parameters during the training process. This strategy enhances the model's ability to focus on features that significantly contribute to class differentiation, potentially leading to a more nuanced understanding of the underlying patterns within the data.

In analyzing the loss curves, the standard ANN configuration displayed significant fluctuations throughout the training epochs. This instability suggested that the model struggled to find a reliable convergence point, which is often indicative of overfitting—where the model performs well on training data but poorly on validation data. Conversely, the implementation of class and feature weights resulted in a markedly smoother decline in both training and validation loss. The reduced variability in the loss curves reflects the model's improved stability, suggesting that the weights helped to regularize the training process and enabled the ANN to generalize better to unseen data.

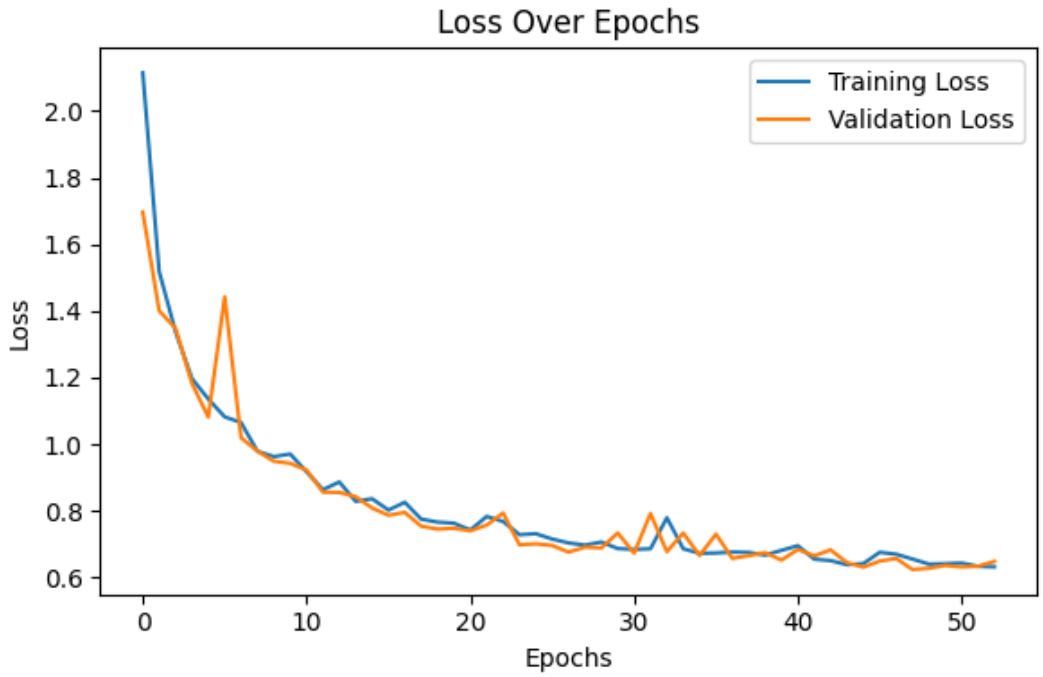

Figure 35. Loss over epochs graph for architecture 1

The first achitecture employed an early stopping method and the training was halted at epoch 50 as convergence of training and validation loss was achieved. However, the training and validation curves converget at loss of ≈0.6 which is considered high.

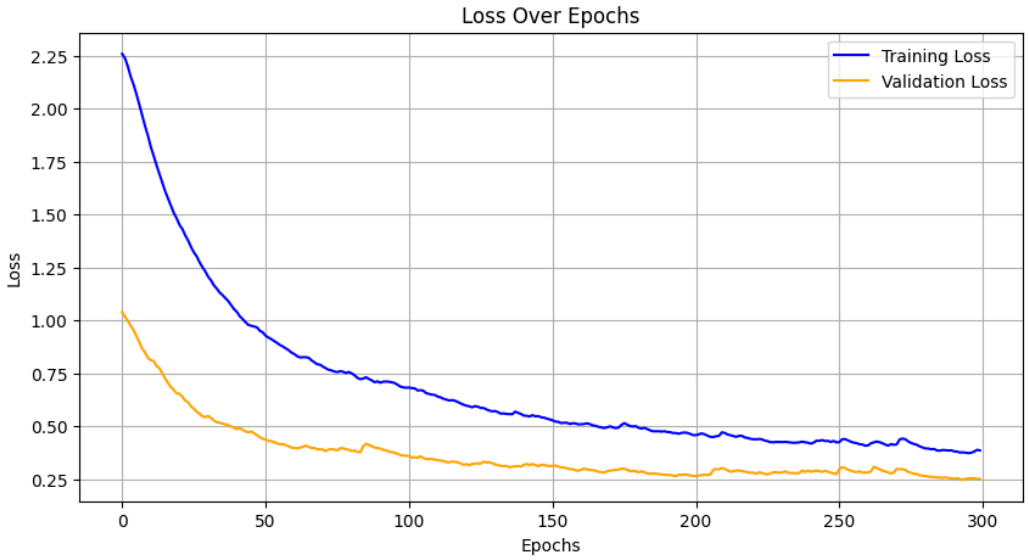

Figure 36. Loss over epochs graph for architecture 2

The second architecture did not include the early stoping criterion and the training was conducted up to 300 epochs. Even though the loss curves did not converge as in the first case, the local minima was achieved at ≈0.4 for the training dataset and ≈0.25 for the validation dataset. Hence, the predictive and generalization capabilities of the second model were shown to improve.

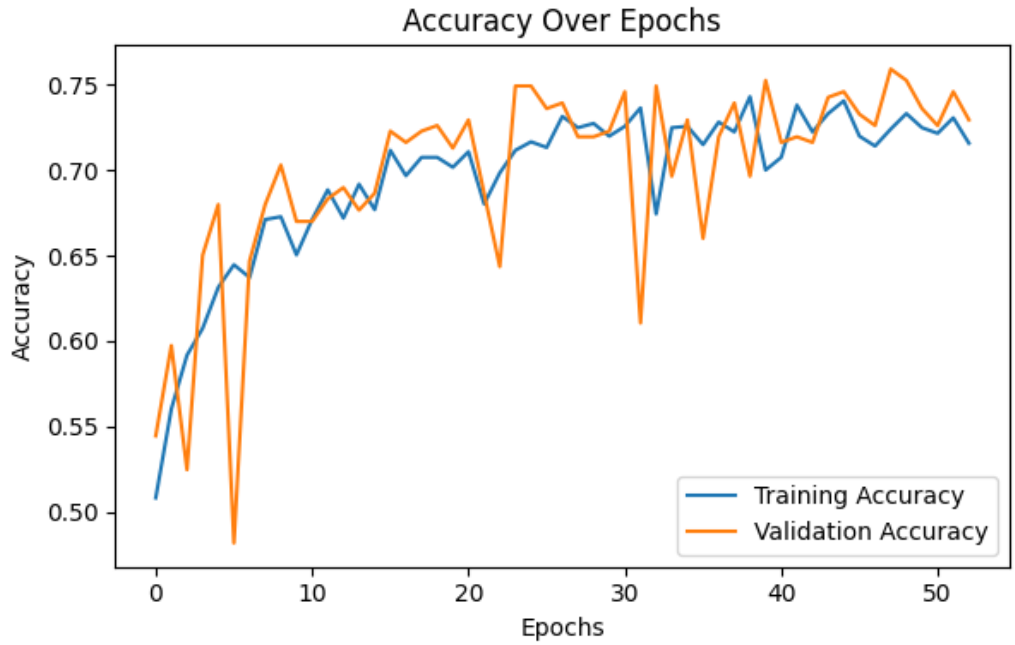

Figure 37. Accuracy plot for architecture 1

The accuracy over epochs plot for the first scenario is characteristic for significant overfitting. The abrupt peaks in the curve indicate that the accuracy is unstable over epochs and even though the model converges in terms of loss, its predictive accuracy is very low (≈0.7).

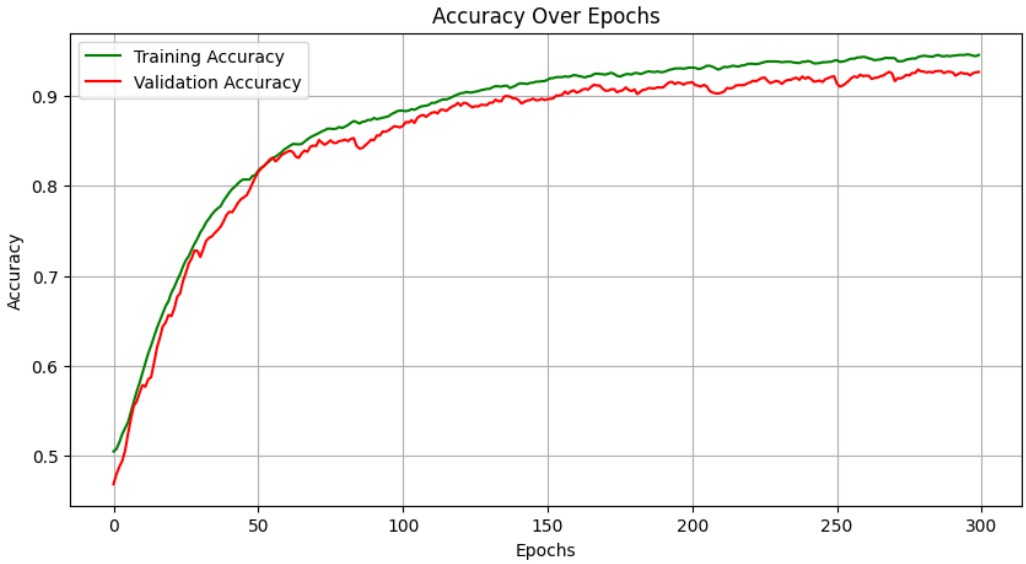

Figure 38. Accuracy plot for architecture 2

.

Compared to the accuracy plot of the first instance, the accuracy plot for the adjusted architecture is much smoother and training and validation accuracy converge at above 0.9 indicating very high and trustworth predictive capability of the model.

The most compelling evidence of the performance improvement emerged from the accuracy analysis. The standard model achieved a peak validation accuracy of only 0.68, indicating that a significant portion of predictions were incorrect, particularly for the less frequent classes. However, when class and feature weights were introduced, the validation accuracy soared to 0.9. This dramatic increase of 27 percentage points not only signifies a substantial enhancement in predictive performance but also illustrates the model's newfound capability to accurately classify instances across all classes, including those that were previously misclassified.

Table 24. Performance metrics comparison

Performance metric	**Score architecture 1**			**Score architecture 2**		
Accuracy	0.681			0.909		
Recall	0.679			0.905		
F1 score	0.684			0.903		
MCC	0.523			0.871		
Sensitivity	0.571	1.0	0.714	1.0	0.714	0.750
Specificity	0.733	0.933	1.0	0.923	0.933	0.857

The improvement in accuracy (Table 24) underscores the effectiveness of utilizing weights, as it highlights the model's enhanced ability to discern between similar classes, which is particularly vital in medical applications where accurate classifications can have critical implications.

In order to evaluate the performance of the ANN in more detail, ROC curves, AUC scores (Figure 39.) and precision-recall curves (.) were analzed for all 3 classes durring training.

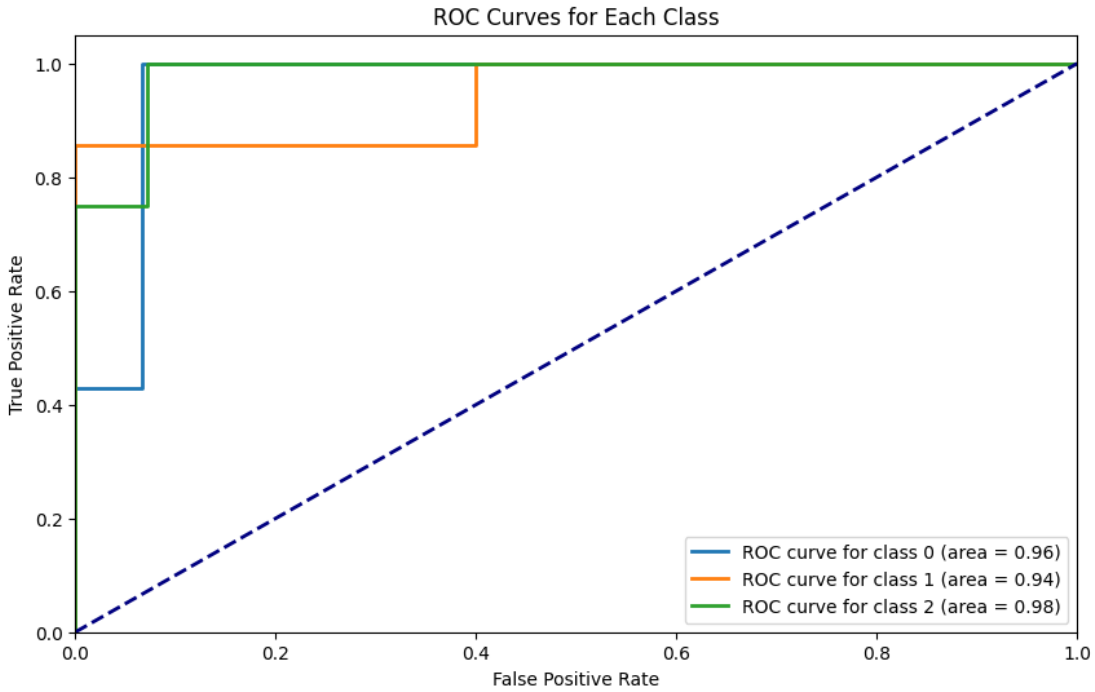

Figure 39. ROC curves for each class

An AUC of 0.94, 0.96, and 0.98 for the three classes of plaque progression prediction indicates the model's excellent discriminatory performance across all stages of progression. The AUC of 0.94 suggests that the model is highly effective in distinguishing the first class of plaque progression, capturing the critical risk factors associated with it. The AUC of 0.96 for the second class indicates an even stronger capability to identify patients at risk, implying improved sensitivity and specificity in detecting subtle changes in plaque characteristics. Lastly, the AUC of 0.98 for the third class highlights an exceptional classification ability, demonstrating the model's capacity to accurately identify patients at the highest risk of plaque progression. These high AUC values signify that the model not only excels in classifying plaque progression stages but also underscores its potential application in clinical settings for personalized risk assessment and management. The impressive performance across all classes suggests that the model can effectively assist healthcare professionals in making informed decisions regarding patient care and interventions, ultimately contributing to improved outcomes in cardiovascular health.

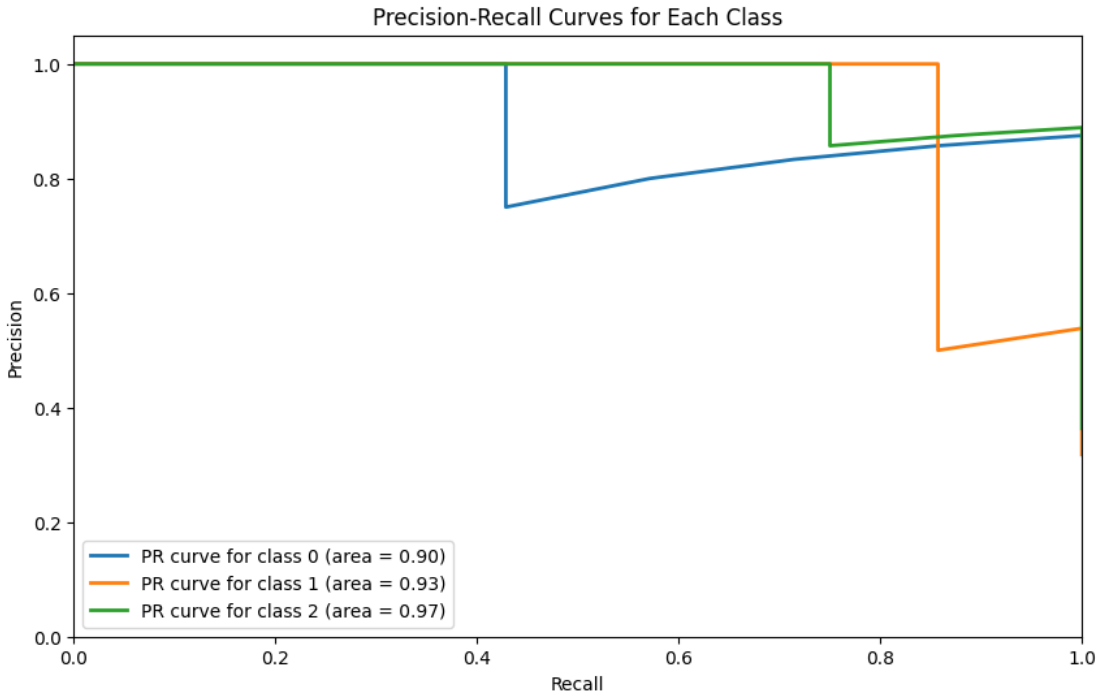

Figure 40. Precision-recall curves for each class

The average precision scores of 0.90, 0.93, and 0.97 for the precision-recall curves indicate a compelling trend in the model's performance across the three classes of plaque progression prediction. These scores reflect the model's capacity to effectively distinguish between true positive instances and false positives, showcasing an increase in precision as the severity of plaque progression escalates. In clinical terms, high precision is critical, as it suggests that when the model predicts a positive outcome, it is highly likely to be correct. A precision of 0.90 indicates that 90% of the identified positive cases in the first class are true positives, while 0.97 in the most advanced class suggests an excellent ability to identify those at greatest risk with minimal misclassification. This improvement highlights the model's potential utility in risk stratification, enabling healthcare providers to focus interventions on those who are more likely to benefit from them. Moreover, the increasing precision suggests that the model not only identifies patients effectively but also provides confidence in its predictions. This characteristic is essential in a clinical setting, where false positives can lead to unnecessary stress and interventions for patients. As the model approaches a precision score of 1.0, it indicates an exemplary performance, which could significantly enhance decision-making processes in managing plaque progression and related cardiovascular risks. Ultimately, these precision-recall scores underscore the potential of the predictive model in a healthcare context, advocating for its application in clinical practices for improved outcomes in patients at risk of significant cardiovascular events associated with plaque progression.

4.4.2. Comparison to state of the art

Han et al. (2020) (Han et al., 2020) integrated coronary computed tomography angiography-determined qualitative and quantitative plaque features within a machine learning (ML) framework to determine its performance for predicting rapid coronary plaque progression (RPP). They have used CTA data from 1083 patients and tested several machine learning algorithms to achieve an AUC of 0.618 for the model where only

clinical and laboratory variables were used and 0.833 when clinical and laboratory variables were combined with qualitative and quantitative CT variables. A significant aspect of their methodology was the proactive approach to address feature importance within their dataset. Predictive classifiers for prediction of RPP were developed using an ensemble classification approach ("boosting") where a set of weak base classifiers can be combined to create a single strong classifier by iteratively adjusting their appropriate weighting according to misclassifications.

Rosandeel et al. (2018) (van Rosendael et al., 2018) aimed to investigate whether a ML score, incorporating only the 16 segment coronary tree information derived from coronary computed tomography angiography (CCTA), provides enhanced risk stratification compared with current CCTA based risk scores. In a study that involved 8844 patients with no known history of CAD and employed a methodology where a total 35 CCTA variables (stenosis severity and plaque composition considering the 16 coronary segments, 2 variables for posterolateral branch when dominance was unknown and coronary artery dominance) were incorporated in the machine learning score. A machine learning algorithm based on XGBoost achieved an AUC of 0.84.

In a previous study (Spahić et al., 2023) we have conducted using data mining and artificial neural networks to predict coronary plaque progression the aim was to determine the risk and pace of progression of CATS, based on lipid-species, anti-thrombotic drugs, clinical data, risk factors and general biomarkers. The methodology relied on feature selection using ReliefF, MRMR & wrapper techniques followed by a simple architecture of ANN. The overall achieved accuracy of 0.81 was satisfactory, however the classification power of the developed system was significantly hindered by low specificity indicating that the ANN does not generalize well for the insignificant plaque progression samples. This problem persisted across all iterations of the ANN considering significant class imbalance of the dataset where only 22% of the data corresponded to the minority class.

Corti et al., (2023) have developed a surrogate model to be coupled with FEM as a substitute for the previously employed agent based model to reduce the computational cost by preserving the modeling accuracy. The surrogate models were (i) used to explore the relation between the ABM parameters and the global outputs, and (ii) employed in the calibration process, in which the selected ABM parameters were calibrated through genetic algorithm optimization. The developed surrogate model achieved an R^2 in the range from 0.985-0.995 indicating high fidelity and potential to substitute the computationally-intensive ABM.

Table 25. State of the art benchmarking

Aspect	Rosandeel et al. (2018)	Han et al. (2020)	Spahic et al. (2023)	Corti et al. (2023)	Model in this study
Model Structure	XGBoost	Ensemble models	Simple ANN with employed	Surrogate model based on	Advanced ANN with ABM parameters

			regularizatio n	physiological data	
	Moderate complexity, less dynamic	Employing an iterative LogitBoost algorithm	Captures complex feature interactions	Limited in complex feature interactions	Captures complex feature interactions
Feature Engineering	CT images and CCTA scores	clinical and laboratory variables & CT variables	Feature selection using ReliefF, MRMR & wrapper technigues	Physiological and imaging data	Includes simulation-based ABM parameters
	Feature importance score assessment	information-gain attribute ranking	SMOTE algorithm to address class imbalance	Focuses on physiological modeling	ADASYN class imbalance mitigation and feature weighing
Performance Metrics	AUC 0.84	AUC 0.618 – 0.833	Accuracy: 81.81%, Sensitivity: 96%, Specificity: 37.5%	R^2 0.985-0.995	Accuracy: 90.9%, Sensitivity: 82.1%, Specificity: 90.3% .
Computational Efficiency	Moderate resource requirements	Moderate resource requirements	Scalable architecture with lower resource demands	Requires significant resources	Low resource requirement
	Feasible for many settings	Resource-intensive becuase of image processing	Suitable for clinical applications	May limit practical applicability	Feasible for many settings

4.5. Integration into DECODE cloud platform

Through the seamless integration of ABM and AI into the DECODE cloud platform via an API, the system will be able to harness the best of both worlds: the detailed simulation of biological processes and the predictive power of AI. To achieve this integration, a robust API framework will be developed, allowing the DECODE platform to interface with both the ABM and AI systems. The API will serve as a bridge, handling the flow of data between the cloud-based platform, the simulation models, and healthcare providers. By employing adaptable architectures, the system ensures scalability, reliability.

The ABM module simulates the behavior of individual agents (such as cells, proteins, or plaques) within the arterial environment, capturing the dynamic interactions that contribute to disease progression, particularly in conditions like atherosclerosis. The integration of ABM into DECODE will involve deploying the model on the cloud. This allows for the detailed and resource-intensive simulations required for accurate modeling

of biological processes. Once the ABM is integrated, the API will facilitate the following workflow:

- Input of patient-specific data: Clinical data, such as imaging results, biochemical markers, and patient demographics, will be submitted through the API. This data will be pre-processed by the DECODE platform and then sent to the ABM module for simulation.
- Execution of ABM simulations: The API will initiate the simulation of disease progression within the ABM, simulating how individual agents behave and interact in the vascular system. The model will run in parallel, allowing multiple simulations to take place concurrently.
- Return of simulation results: The API will return the results of these simulations to the DECODE platform, where the data can be analyzed, visualized, and compared with patient data to enhance diagnosis or treatment planning. This could include insights into plaque progression, risk of rupture, and treatment outcomes.

The integration of AI models adds an essential layer of predictive power and machine learning to the DECODE platform. By leveraging AI algorithms, the system can process large datasets, identify complex patterns, and generate patient-specific predictions that evolve over time. AI is trained on multimodal datasets, combining clinical data, genetic information, and imaging results to predict plaque progression, intervention success, and disease outcomes. The integration of AI follows a similar workflow facilitated by the API:

- Data input and preprocessing: The DECODE platform will use the API to feed the AI models with the same patient-specific data utilized by the ABM, including any new data collected over time.
- AI-driven predictions: The AI module, powered by advanced machine learning algorithms, will analyze the data to predict atherosclerotic plaque behavior and assess the risk of peripheral artery disease progression. The API ensures that the AI model can continuously update predictions as new patient data becomes available, making the platform adaptive and real-time.
- Feedback to DECODE platform: The API will facilitate the return of AI-driven insights, which can then be displayed to clinicians via the DECODE interface, supporting decision-making with precise, data-driven guidance.

The combined integration of ABM and AI allows for a powerful synergy within the DECODE platform. While ABM provides mechanistic insights into the behavior of biological agents, AI enhances the system by learning from vast amounts of data, offering predictions that can be continuously refined. The API will act as the central conduit, enabling the smooth exchange of data between these two models. For example, the results from ABM simulations can serve as input features for the AI model, further refining predictions and offering a holistic understanding of patient-specific disease progression.

5. Conclusion

In this research, the transformative potential of artificial intelligence and agent-based modeling in understanding and managing cardiovascular diseases, particularly atherosclerosis, was investigated. Agent-based modeling has provided a robust framework for simulating complex biological interactions and understanding the multifaceted nature of cardiovascular disease development. By modeling the behaviors of individual agents, such as cells and tissues, ABM has elucidated critical mechanisms underlying plaque formation and progression, revealing insights that could inform targeted therapeutic strategies. The findings demonstrate that AI, through advanced machine learning and deep learning techniques, significantly enhances the early detection of atherosclerosis and improves risk stratification by analyzing large and diverse datasets from electronic health records, medical imaging, and genetic profiles. The integration of AI has shown the capacity to identify patterns and predict disease progression with a level of accuracy that can surpass traditional methods, thereby offering new avenues for personalized patient care.

However, this research also highlighted the inherent limitations associated with both methodologies. Issues related to data quality, model interpretability, and the complexity of biological systems underscore the need for ongoing refinement and validation of these models. Overcoming these challenges is essential for ensuring the reliability and applicability of ABM and AI in clinical settings.

ABM serves as a powerful tool for simulating the intricate interactions among various biological agents, such as cells and tissues, within the cardiovascular system. By representing each agent with unique behaviors and interactions, ABM can illuminate how individual cellular activities contribute to the development and progression of cardiovascular diseases. As shown in this research, ABM has successfully simulated plaque progression and the utilized methodology was confirmed as congruent with patient data. However, in cases where extreme variations of simulation parameters were introduced, the ABM failed in accurately capturing the plaque progression pattern, and provided results that are unexpected in real-world scenarios. This is due to the fact that the complexity of biological systems poses significant challenges. The intricate interplay of multiple factors, including genetic, environmental, and lifestyle influences, makes it difficult to capture the full spectrum of interactions in a comprehensive model. ABM requires extensive data for parameterization and validation, often necessitating high-quality biological and clinical datasets. These data may not always be readily accessible, and any inconsistencies or biases in the dataset can lead to misleading conclusions. The calibration of ABM is another crucial step, as it requires meticulous attention to detail to ensure that the model accurately reflects biological realities. This process can be time-consuming and resource-intensive, often requiring advanced expertise and computational power. In addition, ABM outcomes can be sensitive to variations in parameters. Small changes in how agents interact can lead to significant differences in model predictions, making it essential for researchers to conduct thorough sensitivity analyses. However, identifying the most impactful parameters can be a complex task, often requiring extensive experimentation and iteration.

On the other hand, AI modeling—especially machine learning and deep learning techniques—has revolutionized the analysis of large datasets in cardiovascular medicine. These algorithms excel at identifying patterns within electronic health records, medical

imaging, and genetic profiles, potentially leading to early detection and improved risk stratification for patients. Yet, the reliance on data quality is a double-edged sword. If the input data is incomplete, noisy, or biased, the AI model's predictions may be flawed, potentially leading to detrimental clinical outcomes. The dynamic nature of cardiovascular diseases adds another layer of complexity. As patients undergo treatment and lifestyle changes, their cardiovascular status evolves. AI models may struggle to keep pace with these changes, leading to outdated or irrelevant predictions that fail to address the patient's current health status. Surrogate modeling opens an avenue for creating AI-based models by using virtual populations generated by running simulations such as ABM. The surrogate model for atherosclerotic plaque progression developed in this research was based on artificial neural networks and deep learning. The model was developed on the basis of a comprehensive dataset created for the purpose of the development of the surrogate model. The dataset captured a landscape of patient-specific variability and provided significant variation for the model to learn. The model performed with 90.9% accuracy and congruency with the ABM indicating its strong potential to be used in practice.

While both ABM and AI modeling present unique opportunities to advance cardiovascular medicine, their limitations must be thoughtfully addressed. By continuing to advance these innovative approaches, we can significantly enhance our understanding of cardiovascular diseases, leading to more precise risk assessments, personalized treatment plans, and improved patient outcomes. Creating interpretable AI and ABM models is vital for fostering trust among healthcare providers and patients. Stakeholders must prioritize transparency in model design, enabling clinicians to understand how predictions are made and empowering them to explain these insights to patients. This interpretability is essential for gaining acceptance in clinical settings, where decisions are often based on a combination of evidence, experience, and patient preferences. Additionally, ethical considerations must be at the forefront of research and implementation, ensuring that AI and ABM applications do not perpetuate biases or inequities in healthcare. To translate research findings into tangible benefits for patients, ongoing validation studies are necessary. These studies should involve diverse patient populations to ensure that models are generalizable and effective across different demographics. Real-world clinical trials can provide valuable feedback on the usability and efficacy of AI and ABM systems, paving the way for their adoption in everyday clinical practice.

References

ABDULLAH, K., BOU DARGHAM, B., STEINBRECHER, M., SUN, B., HUIQIANG, Z., KHALILI, H., BRILAKIS, E. S. & BANERJEE, S. 2018. Drug-eluting stents for treatment of peripheral artery disease. *American Journal of Cardiovascular Drugs,* 18**,** 175-180.

AHMED, W. 2016. The Study and Risk of Coronary Artery Disease. *Research and reviews: journal of medical and health sciences,* 2016.

ALEXANDER, J. H. & SMITH, P. K. 2016. Coronary-artery bypass grafting. *New England Journal of Medicine,* 374**,** 1954-1964.

ALFONSO, F., ELGENDY, I. Y. & CUESTA, J. 2018. Drug-coated balloons versus drug-eluting stents for in-stent restenosis: the saga continues. *Eurointervention: Journal of Europcr in Collaboration with the Working Group on Interventional Cardiology of the European Society of Cardiology,* 14**,** 1069-1072.

ALIĆ, B., GURBETA, L., BADNJEVIĆ, A., BADNJEVIĆ-ČENGIĆ, A., MALENICA, M., DUJIĆ, T., ČAUŠEVIĆ, A. & BEGO, T. Classification of metabolic syndrome patients using implemented expert system. CMBEBIH 2017: Proceedings of the International Conference on Medical and Biological Engineering 2017, 2017. Springer, 601-607.

AMAL, S., SAFARNEJAD, L., OMIYE, J. A., GHANZOURI, I., CABOT, J. H. & ROSS, E. G. 2022. Use of multi-modal data and machine learning to improve cardiovascular disease care. *Frontiers in cardiovascular medicine,* 9**,** 840262.

AMMENWERTH, E. & RIGBY, M. 2016. *Evidence-based health informatics: Promoting safety and efficiency through scientific methods and ethical policy*, IOS press.

ARDILA, D., KIRALY, A. P., BHARADWAJ, S., CHOI, B., REICHER, J. J., PENG, L., TSE, D., ETEMADI, M., YE, W. & CORRADO, G. 2019. End-to-end lung cancer screening with three-dimensional deep learning on low-dose chest computed tomography. *Nature medicine,* 25**,** 954-961.

ARNETT, D. K., BLUMENTHAL, R. S., ALBERT, M. A., BUROKER, A. B., GOLDBERGER, Z. D., HAHN, E. J., HIMMELFARB, C. D., KHERA, A., LLOYD-JONES, D. & MCEVOY, J. W. 2019. 2019 ACC/AHA guideline on the primary prevention of cardiovascular disease: a report of the American College of Cardiology/American Heart Association Task Force on Clinical Practice Guidelines. *Circulation,* 140**,** e596-e646.

ATHANASIOU, L. S., BOURANTAS, C. V., RIGAS, G., SAKELLARIOS, A. I., EXARCHOS, T. P., SIOGKAS, P. K., RICCIARDI, A., NAKA, K. K., PAPAFAKLIS, M. I. & MICHALIS, L. K. 2014. Methodology for fully automated segmentation and plaque characterization in intracoronary optical coherence tomography images. *Journal of biomedical optics,* 19**,** 026009-026009.

BĂDILĂ, E., CÂLMÂC, L., ZAMFIR, D., PENES, D., WEISS, E. & BATAILA, V. 2017. The Cardiovascular System and the Coronary Circulation. 13-59.

BACIGALUPI, E., Pizzicannella, J., Rigatelli, G., Scorpiglione, L., Foglietta, M., Rende, G., Mantini, C., Fiore, F.M., Pelliccia, F. and Zimarino, M., 2024. Biomechanical factors and atherosclerosis localization: insights and clinical applications. Frontiers in Cardiovascular Medicine, 11, p.1392702.

BADNJEVIC, A., CIFREK, M. & KORUGA, D. Classification of Chronic Obstructive Pulmonary Disease (COPD) using integrated software suite. XIII Mediterranean Conference on Medical and Biological Engineering and Computing 2013: MEDICON 2013, 25-28 September 2013, Seville, Spain, 2014. Springer, 911-914.

BADNJEVIĆ, A., GURBETA, L., BOŠKOVIĆ, D. & DŽEMIĆ, Z. Medical devices in legal metrology. 2015 4th Mediterranean Conference on Embedded Computing (MECO), 2015. IEEE, 365-367.

BADNJEVIĆ, A. & POKVIĆ, L. G. 2020. Medical devices maintenance. *Clinical Engineering Handbook.* Elsevier.

BADNJEVIĆ, A., POKVIĆ, L. G., DEUMIĆ, A. & BEĆIROVIĆ, L. S. 2022. Post-market surveillance of medical devices: A review. *Technology and Health Care,* 30**,** 1315-1329.

BADNJEVIĆ, A., POKVIĆ, L. G., SMAJLHODŽIĆ-DELJO, M., SPAHIĆ, L., BEGO, T., MESELDŽIĆ, N., PRNJAVORAC, L., PRNJAVORAC, B. & BEDAK, O. 2024. Application of artificial intelligence for the classification of the clinical outcome and therapy in patients with viral infections: The case of COVID-19. *Technology and Health Care***,** 1-12.

BADNJEVIC, A., SPAHIC, L., JORDAMOVIC, N. B. & POKVIC, L. G. 2023. A novel method for conformity assessment testing of infant incubators for post-market surveillance purposes. *Technology and Health Care,* 31**,** 389-399.

BADNJEVIĆ, A. & VUKOVIĆ, D. 2020. Improving the accuracy and efficiency of medical devices in the legal metrology system of Bosnia and Herzegovina. *Clinical Engineering Handbook.* Elsevier.

BANGALORE, S., TOKLU, B., AMOROSO, N., FUSARO, M., KUMAR, S., HANNAN, E. L., FAXON, D. P. & FEIT, F. 2013. Bare metal stents, durable polymer drug eluting stents, and biodegradable polymer drug eluting stents for coronary artery disease: mixed treatment comparison meta-analysis. *Bmj,* 347.

BARDIN, M., 2022. Lipid mediators of the resolution of inflammation in vascular ageing (Doctoral dissertation, Université de Lorraine).

BATTY, M., BENNETT, M. R. & YU, E. 2022. The role of oxidative stress in atherosclerosis. *Cells,* 11**,** 3843.

BEĆIROVIĆ, L. S., DEUMIĆ, A., POKVIĆ, L. G. & BADNJEVIC, A. Aritificial Inteligence Challenges in COPD management: a review. 2021 IEEE 21st International Conference on Bioinformatics and Bioengineering (BIBE), 2021. IEEE, 1-7.

BEĆIROVIĆ, L. S., POKVIĆ, L. G., DEUMIĆ, A., FEJZIĆ, A. & BADNJEVIĆ, A. Industry 4.0 & medical devices-application of artificial intelligence for surveillance and management.

BENJAMIN, E. J., VIRANI, S. S., CALLAWAY, C. W., CHAMBERLAIN, A. M., CHANG, A. R., CHENG, S., CHIUVE, S. E., CUSHMAN, M., DELLING, F. N. & DEO, R. 2018. Heart disease and stroke statistics—2018 update: a report from the American Heart Association. *Circulation,* 137**,** e67-e492.

BENTZON, J., OTSUKA, F., VIRMANI, R. & FALK, E. 2014. Mechanisms of plaque formation and rupture. *Circulation research,* 114 12**,** 1852-1866.

BERTRAND, M., VLACHOPOULOS, C. & MOURAD, J. 2016. Triple Combination Therapy for Global Cardiovascular Risk: Atorvastatin, Perindopril, and Amlodipine. *American Journal of Cardiovascular Drugs,* 16**,** 241-253.

BHATT, R. 2018. A13469 Total Cholesterol to Good Cholesterol Ratio: Simple but Significant Marker to Predict Atherosclerosis in Diabetic Patients. *Journal of Hypertension,* 36.

BHUI, R. & HAYENGA, H. N. 2017. An agent-based model of leukocyte transendothelial migration during atherogenesis. *PLoS computational biology,* 13**,** e1005523.

BLAGOJEVIC, A., SUSTERSIC, T. & FILIPOVIC, N. 2022. Simulation of Atherosclerotic Plaque Development using Agent-based Modelling.

BOUMA, B., VILLIGER, M., OTSUKA, K. & OH, W. 2017. Intravascular optical coherence tomography [Invited]. *Biomedical optics express,* 8 5**,** 2660-2686.

BUTNARIU, L. I., GORDUZA, E. V., FLOREA, L., ȚARCĂ, E., MOISĂ, Ș. M., TRADAFIR, L. M., COJOCARU, E., LUCA, A.-C., STĂTESCU, L. & BĂDESCU, M. C. 2022. The Genetic Architecture of the Etiology of Lower Extremity Peripheral Artery Disease: Current Knowledge and Future Challenges in the Era of Genomic Medicine. *International Journal of Molecular Sciences,* 23**,** 10481.

BYRNE, R. A., JONER, M., ALFONSO, F. & KASTRATI, A. 2014. Drug-coated balloon therapy in coronary and peripheral artery disease. *Nature Reviews Cardiology,* 11**,** 13-23.

CAMERON, J., MEHTA, O., MICHAIL, M., CHAN, J., NICHOLLS, S., BENNETT, M. & BROWN, A. 2020. Exploring the relationship between biomechanical stresses and coronary atherosclerosis. *Atherosclerosis,* 302**,** 43-51.

CAMPION, E. W., DORSEY, E. & TOPOL, E. 2016. State of telehealth. *N Engl J Med,* 375**,** 154-161.

CARPENTER, H. J., GHOLIPOUR, A., GHAYESH, M. H., ZANDER, A. C. & PSALTIS, P. J. 2020. A review on the biomechanics of coronary arteries. *International Journal of Engineering Science,* 147**,** 103201.

CARRASCO-RIBELLES, L. A., LLANES-JURADO, J., GALLEGO-MOLL, C., CABRERA-BEAN, M., MONTEAGUDO-ZARAGOZA, M., VIOLÁN, C. & ZABALETA-DEL-OLMO, E. 2023. Prediction models using artificial intelligence and longitudinal data from electronic health records: a systematic methodological review. *Journal of the American Medical Informatics Association,* 30**,** 2072-2082.

CASEY, S., LANTING, S., OLDMEADOW, C. & CHUTER, V. 2019. The reliability of the ankle brachial index: a systematic review. *Journal of foot and ankle research,* 12**,** 1-10.

CHATZIZISIS, Y. S., COSKUN, A. U., JONAS, M., EDELMAN, E. R., FELDMAN, C. L. & STONE, P. H. 2007. Role of endothelial shear stress in the natural history of coronary atherosclerosis and vascular remodeling: molecular, cellular, and vascular behavior. *Journal of the American College of Cardiology,* 49**,** 2379-2393.

CHEN, H., ENGKVIST, O., WANG, Y., OLIVECRONA, M. & BLASCHKE, T. 2018. The rise of deep learning in drug discovery. *Drug discovery today,* 23**,** 1241-1250.

CHRISTIANSEN, M. K., NISSEN, L., WINTHER, S., MØLLER, P. L., FROST, L., JOHANSEN, J. K., JENSEN, H. K., GUÐBJARTSSON, D., HOLM, H. & STEFÁNSSON, K. 2020. Genetic risk of coronary artery disease, features of atherosclerosis, and coronary plaque burden. *Journal of the American Heart Association,* 9**,** e014795.

CORNELISSEN, A. & VOGT, F. J. 2019. The effects of stenting on coronary endothelium from a molecular biological view: time for improvement? *Journal of cellular and molecular medicine,* 23**,** 39-46.

CORTI, A., CASARIN, S., CHIASTRA, C., COLOMBO, M., MIGLIAVACCA, F. & GARBEY, M. A multiscale model of atherosclerotic plaque development: toward a coupling between an agent-based model and CFD simulations. Computational Science–ICCS 2019: 19th International Conference, Faro, Portugal, June 12–14, 2019, Proceedings, Part IV 19, 2019. Springer, 410-423.

CORTI, A., CHIASTRA, C., COLOMBO, M., GARBEY, M., MIGLIAVACCA, F. & CASARIN, S. 2020a. A fully coupled computational fluid dynamics--agent-based model of atherosclerotic plaque development: multiscale modeling framework and parameter sensitivity analysis. *Computers in Biology and Medicine,* 118**,** 103623.

CORTI, A., CHIASTRA, C., COLOMBO, M., GARBEY, M., MIGLIAVACCA, F. & CASARIN, S. 2020b. A fully coupled computational fluid dynamics–agent-based model of

atherosclerotic plaque development: multiscale modeling framework and parameter sensitivity analysis. *Computers in biology and medicine,* 118**,** 103623.

CORTI, A., COLOMBO, M., MIGLIAVACCA, F., RODRIGUEZ MATAS, J. F., CASARIN, S. & CHIASTRA, C. 2021. Multiscale computational modeling of vascular adaptation: a systems biology approach using agent-based models. *Frontiers in Bioengineering and Biotechnology,* 9**,** 744560.

CORTI, A., COLOMBO, M., ROZOWSKY, J. M., CASARIN, S., HE, Y., CARBONARO, D., MIGLIAVACCA, F., RODRIGUEZ MATAS, J. F., BERCELI, S. A. & CHIASTRA, C. 2022. A predictive multiscale model of in-stent restenosis in femoral arteries: linking haemodynamics and gene expression with an agent-based model of cellular dynamics. *Journal of the Royal Society Interface,* 19**,** 20210871.

CORTI, A., MIGLIAVACCA, F., BERCELI, S. A. & CHIASTRA, C. 2023. Predicting 1-year in-stent restenosis in superficial femoral arteries through multiscale computational modelling. *Journal of the Royal Society Interface,* 20**,** 20220876.

CRAWFORD, F., WELCH, K., ANDRAS, A. & CHAPPELL, F. M. 2016. Ankle brachial index for the diagnosis of lower limb peripheral arterial disease. *Cochrane Database of Systematic Reviews*.

CURTIN, A. E. & ZHOU, L. 2014. An agent-based model of the response to angioplasty and bare-metal stent deployment in an atherosclerotic blood vessel. *PLoS One,* 9**,** e94411.

DERIC, M., KOJIC-DAMJANOV, S. & EREMIC, N. 2008. Biochemical markers of atherosclerosis. *Journal of Medical Biochemistry,* 27**,** 148.

DESAI, P. M., HARKINS, S., RAHMAN, S., KUMAR, S., HERMANN, A., JOLY, R., ZHANG, Y., PATHAK, J., KIM, J. & D'ANGELO, D. 2024. Visualizing machine learning-based predictions of postpartum depression risk for lay audiences. *Journal of the American Medical Informatics Association,* 31**,** 289-297.

DEVINDER, S. D., SANDESARA, P., SHAPIRO, M. & WONG, N. 2020. The Evolving Understanding and Approach to Residual Cardiovascular Risk Management. *Frontiers in Cardiovascular Medicine,* 7.

DJOROVIC, S., SAVELJIC, I. & FILIPOVIC, N. Advanced Modelling Approach of Carotid Artery Atherosclerosis. Computational Bioengineering and Bioinformatics: Computer Modelling in Bioengineering 8, 2020. Springer, 143-150.

DORAN, A., MELLER, N. & MCNAMARA, C. 2008. Role of smooth muscle cells in the initiation and early progression of atherosclerosis. *Arteriosclerosis, thrombosis, and vascular biology,* 28**,** 812-819.

DŽAFEROVIĆ, S., MELIĆ, D., MIHAJLOVIĆ, M., SMAJOVIĆ, A., BEČIĆ, E., BEĆIROVIĆ, L. S., POKVIĆ, L. G. & BADNJEVIĆ, A. 2022. Diagnosis of Addison's disease Using Artificial Neural Network. *IFAC-PapersOnLine,* 55**,** 68-73.

EIBERG, J. P., RASMUSSEN, J. G., HANSEN, M. A. & SCHROEDER, T. V. 2010. Duplex ultrasound scanning of peripheral arterial disease of the lower limb. *European Journal of Vascular and Endovascular Surgery,* 40**,** 507-512.

ESTEVA, A., ROBICQUET, A., RAMSUNDAR, B., KULESHOV, V., DEPRISTO, M., CHOU, K., CUI, C., CORRADO, G., THRUN, S. & DEAN, J. 2019. A guide to deep learning in healthcare. *Nature medicine,* 25**,** 24-29.

FILIPOVIC, N. 2020. Computational modeling of atherosclerosis. 1-39.

FILIPOVIC, N., FOTIADIS, D., PELOSI, W. & PARODI, O. Experimental and computer model of plaque formation in the artery. 2011 10th International Workshop on Biomedical Engineering, 2011. IEEE, 1-4.

FILIPOVIC, N., ISAILOVIC, V., MILOSEVIC, Z., NIKOLIC, D., SAVELJIC, I., RADOVIC, M., NIKOLIC, M., CIRKOVIC-ANDJELKOVIC, B., THEMIS, E. & FOTIADIS, D. Computational modeling of plaque development in the coronary arteries. CMBEBIH 2017: Proceedings of the International Conference on Medical and Biological Engineering 2017, 2017. Springer, 269-274.

FILIPOVIC, N., RADOVIC, M., ISAILOVIC, V., MILOSEVIC, Z., NIKOLIC, D., SAVELJIC, I., DJUKIC, T., THEMIS, E., FOTIADIS, D. & PARODI, O. 2013. Computer modeling of atherosclerosis. *Computational Medicine in Data Mining and Modeling.* Springer.

FILIPOVIC, N., TOMASEVIC, S., ARSIC, B., ANIC, M., DJUKIC, T. & KONCAR, I. Agent Based with Finite Element Method for Plaque Progression in the Carotid Artery. 2023 24th International Conference on Digital Signal Processing (DSP), 2023. IEEE, 1-5.

FILIPOVIC, N., ZIVIC, M., OBRADOVIC, M., DJUKIC, T., MARKOVIC, Z. & ROSIC, M. 2014. Numerical and experimental LDL transport through arterial wall. *Microfluidics and nanofluidics,* 16**,** 455-464.

FITZGERALD, M. L., MUJAWAR, Z. & TAMEHIRO, N. 2010. ABC transporters, atherosclerosis and inflammation. *Atherosclerosis,* 211**,** 361-370.

FLEISCHMANN, D., HALLETT, R. L. & RUBIN, G. D. 2006. CT angiography of peripheral arterial disease. *Journal of vascular and interventional radiology,* 17**,** 3-26.

FÖLLMER, B., WILLIAMS, M. C., DEY, D., ARBAB-ZADEH, A., MAUROVICH-HORVAT, P., VOLLEBERG, R. H., RUECKERT, D., SCHNABEL, J. A., NEWBY, D. E. & DWECK, M. R. 2024. Roadmap on the use of artificial intelligence for imaging of vulnerable atherosclerotic plaque in coronary arteries. *Nature Reviews Cardiology,* 21**,** 51-64.

GARBEY, M., CASARIN, S. & BERCELI, S. A. 2017. Vascular adaptation: pattern formation and cross validation between an agent based model and a dynamical system. *Journal of theoretical biology,* 429**,** 149-163.

GARBEY, M., CASARIN, S. & BERCELI, S. A. 2019. A versatile hybrid agent-based, particle and partial differential equations method to analyze vascular adaptation. *Biomechanics and Modeling in Mechanobiology,* 18**,** 29-44.

GARBEY, M., RAHMAN, M. & BERCELI, S. 2015. A multiscale computational framework to understand vascular adaptation. *Journal of computational science,* 8**,** 32-47.

GLAGOV, S., WEISENBERG, E., ZARINS, C. K., STANKUNAVICIUS, R. & KOLETTIS, G. J. 1987. Compensatory enlargement of human atherosclerotic coronary arteries. *New England Journal of Medicine,* 316**,** 1371-1375.

GOLPE, R., BLANCO-CID, N., DACAL-RIVAS, D., MARTÍN-ROBLES, I., VEIGA, I., GUZMÁN-PERALTA, I., CASTRO-AÑÓN, O. & PÉREZ-DE-LLANO, L. A. 2022. Incidence and profile of severe exacerbations of chronic obstructive pulmonary disease due to biomass smoke or tobacco. *Annals of Thoracic Medicine,* 17**,** 193-198.

GRÜNTZIG, A., KUHLMANN, U., VETTER, W., LÜTOLF, U., MEIER, B. & SIEGENTHALER, W. 1978. Treatment of renovascular hypertension with percutaneous transluminal dilatation of a renal-artery stenosis. *Lancet (London, England),* 1**,** 801-802.

GUPTA, T., WEINREICH, M., GREENBERG, M., COLOMBO, A. & LATIB, A. 2019. Rotational atherectomy: a contemporary appraisal. *Interventional Cardiology Review,* 14**,** 182.

GURBETA, L., ALIC, B., DZEMIC, Z. & BADNJEVIC, A. Testing of dialysis machines in healthcare institutions in Bosnia and Herzegovina. EMBEC & NBC 2017: Joint Conference of the European Medical and Biological Engineering Conference (EMBEC) and the Nordic-Baltic Conference on Biomedical Engineering and Medical Physics (NBC), Tampere, Finland, June 2017, 2018a. Springer, 470-473.

GURBETA, L. & BADNJEVIĆ, A. 2017. Inspection process of medical devices in healthcare institutions: software solution. *Health and Technology,* 7**,** 109-117.

GURBETA, L., BADNJEVIC, A., DZEMIC, Z., JIMENEZ, E. R. & JAKUPOVIC, A. Testing of therapeutic ultrasound in healthcare institutions in Bosnia and Herzegovina. 2nd EAI international conference on future access enablers of ubiquitous and intelligent infrastructures, 2016a. 24-25.

GURBETA, L., BADNJEVIĆ, A., ŽUNIĆ, E., PINJO, N. & LJUMIĆ, F. Software package for tracking status of inspection dates and reports of medical devices in healthcare institutions of Bosnia and Herzegovina. 2015 XXV International Conference on Information, Communication and Automation Technologies (ICAT), 2015. IEEE, 1-5.

GURBETA, L., DZEMIC, Z., BEGO, T., SEJDIC, E. & BADNJEVIC, A. 2017. Testing of anesthesia machines and defibrillators in healthcare institutions. *Journal of medical systems,* 41**,** 1-10.

GURBETA, L., IZETBEGOVIĆ, S. & BADNJEVIĆ-ČENGIĆ, A. 2018b. Inspection and Testing of Pediatric and Neonate Incubators. *Inspection of Medical Devices: For Regulatory Purposes***,** 221-249.

GURBETA, L., SEJDINOVIĆ, D., ALIĆ, B., ABD EL-ILAH, L., BADNJEVIĆ, A. & ŽUNIĆ, E. Software solution for tracking inspection processes of medical devices from legal metrology system. XIV Mediterranean Conference on Medical and Biological Engineering and Computing 2016: MEDICON 2016, March 31st-April 2nd 2016, Paphos, Cyprus, 2016b. Springer, 957-961.

HADŽIĆ, L., FAZLIĆ, A., HASANIĆ, O., KUDIĆ, N. & SPAHIĆ, L. Expert system for performance prediction of anesthesia machines. CMBEBIH 2019: Proceedings of the International Conference on Medical and Biological Engineering, 16– 18 May 2019, Banja Luka, Bosnia and Herzegovina, 2020. Springer, 671-679.

HAFIZOVIĆ, L., ČAUŠEVIĆ, A., DEUMIĆ, A., BEĆIROVIĆ, L. S., POKVIĆ, L. G. & BADNJEVIĆ, A. The use of artificial intelligence in diagnostic medical imaging: systematic literature review. 2021 IEEE 21st International Conference on Bioinformatics and Bioengineering (BIBE), 2021. IEEE, 1-6.

HALL, J. E. & HALL, M. E. 2020. *Guyton and Hall Textbook of Medical Physiology E-Book: Guyton and Hall Textbook of Medical Physiology E-Book*, Elsevier Health Sciences.

HAN, D., KOLLI, K. K., AL'AREF, S. J., BASKARAN, L., VAN ROSENDAEL, A. R., GRANSAR, H., ANDREINI, D., BUDOFF, M. J., CADEMARTIRI, F. & CHINNAIYAN, K. 2020. Machine learning framework to identify individuals at risk of rapid progression of coronary atherosclerosis: from the PARADIGM registry. *Journal of the American Heart Association,* 9**,** e013958.

HART, C. S. 2024. Nurturing the Capabilities to Aspire, Voice and Realise Aspirations: A Theoretical Analysis of the Transformative Potential of the National Health Service in England. *Journal of Human Development and Capabilities***,** 1-22.

HAYENGA, H. N. 2011. *Mechanics of atherosclerosis, hypertension induced growth, and arterial remodeling*, Texas A&M University.

HAYENGA, H. N., THORNE, B. C., PEIRCE, S. M. & HUMPHREY, J. D. 2011. Ensuring congruency in multiscale modeling: towards linking agent based and continuum biomechanical models of arterial adaptation. *Annals of biomedical engineering,* 39**,** 2669-2682.

HELD, C., WHITE, H. D., STEWART, R. A., BUDAJ, A., CANNON, C. P., HOCHMAN, J. S., KOENIG, W., SIEGBAHN, A., STEG, P. G. & SOFFER, J. 2017. Inflammatory biomarkers interleukin-6 and C-reactive protein and outcomes in stable coronary heart disease: experiences from the STABILITY (stabilization of atherosclerotic

plaque by initiation of darapladib therapy) trial. *Journal of the American Heart Association,* 6**,** e005077.
HIGASHI, Y. 2022. Roles of Oxidative Stress and Inflammation in Vascular Endothelial Dysfunction-Related Disease. *Antioxidants,* 11.
HIRAHATAKE, K.M., Dicklin, M.R. and Maki, K.C., 2021. Epidemiology of atherosclerotic cardiovascular disease. Therapeutic Lipidology, pp.91-105.
HRVAT, F., SPAHIĆ, L., POKVIĆ, L. G. & BADNJEVIĆ, A. Artificial Neural Networks for prediction of medical device performance based on conformity assessment data: Infusion and perfusor pumps case study. 2020 9th Mediterranean conference on embedded computing (MECO), 2020. IEEE, 1-4.
HWANG, M., GARBEY, M., BERCELI, S. A. & TRAN-SON-TAY, R. 2009. Rule-based simulation of multi-cellular biological systems—a review of modeling techniques. *Cellular and molecular bioengineering,* 2**,** 285-294.
INIESTA, R., STAHL, D. & MCGUFFIN, P. 2016. Machine learning, statistical learning and the future of biological research in psychiatry. *Psychological medicine,* 46**,** 2455-2465.
ISAILOVIC, V., MILOSEVIC, Z., NIKOLIC, D., SAVELJIC, I., NIKOLIC, M., GACIC, M., CIRKOVIC-ANDJELKOVIC, B., THEMIS, E., FOTIADIS, D. & PELOSI, G. Coupled computer modeling of atherosclerosis development in the coronary arteries. 2017 IEEE 17th International Conference on Bioinformatics and Bioengineering (BIBE), 2017. IEEE, 415-418.
JACKSON, J. E. & MEANEY, J. F. 2015. Angiography: Principles, Techniques. *Grainger & Allison's Diagnostic Radiology: Interventional Imaging***,** 2.
JIANG, F., JIANG, Y., ZHI, H., DONG, Y., LI, H., MA, S., WANG, Y., DONG, Q., SHEN, H. & WANG, Y. 2017. Artificial intelligence in healthcare: past, present and future. *Stroke and vascular neurology,* 2.
JOHNSON, K. W., TORRES SOTO, J., GLICKSBERG, B. S., SHAMEER, K., MIOTTO, R., ALI, M., ASHLEY, E. & DUDLEY, J. T. 2018. Artificial intelligence in cardiology. *Journal of the American College of Cardiology,* 71**,** 2668-2679.
JOUDA, H., LARREA MURILLO, L. & WANG, T. 2022. Current progress in vascular engineering and its clinical applications. *Cells,* 11**,** 493.
KATSANOS, K., SPILIOPOULOS, S., KITROU, P., KROKIDIS, M. & KARNABATIDIS, D. 2018. Risk of death following application of paclitaxel-coated balloons and stents in the femoropopliteal artery of the leg: a systematic review and meta-analysis of randomized controlled trials. *Journal of the American Heart Association,* 7**,** e011245.
KHERA, A. & HEGELE, R. 2020. What Is Familial Hypercholesterolemia, and Why Does It Matter? *Circulation*.
KOLLURU, C. 2018. *Deep neural networks for A-line based plaque classification in intravascular optical coherence tomography images.* Case Western Reserve University.
KOLOSSVÁRY, M., KARÁDY, J., SZILVESZTER, B., KITSLAAR, P., HOFFMANN, U., MERKELY, B. & MAUROVICH-HORVAT, P. 2017. Radiomic features are superior to conventional quantitative computed tomographic metrics to identify coronary plaques with napkin-ring sign. *Circulation: Cardiovascular Imaging,* 10**,** e006843.
KRISHNAN GANAPATHY, M. N. 2021. Artificial intelligence and healthcare regulatory and legal concerns. *Telehealth and Medicine Today,* 6.

KRITTANAWONG, C., JOHNSON, K. W., CHOI, E., KAPLIN, S., VENNER, E., MURUGAN, M., WANG, Z., GLICKSBERG, B. S., AMOS, C. I. & SCHATZ, M. C. 2022. Artificial intelligence and cardiovascular genetics. *Life,* 12**,** 279.

KUNCHUR, N. N. & MOSTAÇO-GUIDOLIN, L. B. 2022. Development of an image classification pipeline for atherosclerotic plaques assessment using supervised machine learning. *BMC bioinformatics,* 23**,** 542.

LAAN, S. W. V. D., SIEMELINK, M., HAITJEMA, S., HASSAN FOROUGHI, A., PERISIC, L., MOKRY, M., SETTEN, J. V., MALIK, R., DICHGANS, M., WORRALL, B., SAMANI, N., SCHUNKERT, H., ERDMANN, J., HEDIN, U., PAULSSON-BERNE, G., JOHAN, L. M. B., BORST, G. D. D., ASSELBERGS, F., FOLKERT, W. D. R., BAKKER, P. D. D. & PASTERKAMP, G. 2018. Genetic Susceptibility Loci for Cardiovascular Disease and Their Impact on Atherosclerotic Plaques. *Circulation. Cardiovascular Genetics,* 11.

LECHNER, K., SCHACKY, C. V., MCKENZIE, A., WORM, N., NIXDORFF, U., LECHNER, B., KRÄNKEL, N., HALLE, M., KRAUSS, R. & SCHERR, J. 2019. Lifestyle factors and high-risk atherosclerosis: Pathways and mechanisms beyond traditional risk factors. *European Journal of Preventive Cardiology,* 27**,** 394-406.

LEE, S.-E., CHANG, H.-J., RIZVI, A., HADAMITZKY, M., KIM, Y.-J., CONTE, E., ANDREINI, D., PONTONE, G., VOLPATO, V. & BUDOFF, M. J. 2016. Rationale and design of the Progression of AtheRosclerotic PlAque DetermIned by Computed TomoGraphic Angiography IMaging (PARADIGM) registry: a comprehensive exploration of plaque progression and its impact on clinical outcomes from a multicenter serial coronary computed tomographic angiography study. *American heart journal,* 182**,** 72-79.

LEE, S.-E., CHANG, H.-J., SUNG, J. M., PARK, H.-B., HEO, R., RIZVI, A., LIN, F. Y., KUMAR, A., HADAMITZKY, M. & KIM, Y. J. 2018. Effects of statins on coronary atherosclerotic plaques: the PARADIGM study. *JACC: Cardiovascular Imaging,* 11**,** 1475-1484.

LIBBY, P., RIDKER, P. M. & HANSSON, G. K. 2011. Progress and challenges in translating the biology of atherosclerosis. *Nature,* 473**,** 317-325.

LINDQUIST, J. & SCHRAMM, K. Drug-eluting balloons and drug-eluting stents in the treatment of peripheral vascular disease. Seminars in interventional radiology, 2018. Thieme Medical Publishers, 443-452.

LOPES, U. & VALIATI, J. F. 2017. Pre-trained convolutional neural networks as feature extractors for tuberculosis detection. *Computers in biology and medicine,* 89**,** 135-143.

MARAGNA, R., GIACARI, C. M., GUGLIELMO, M., BAGGIANO, A., FUSINI, L., GUARICCI, A. I., ROSSI, A., RABBAT, M. & PONTONE, G. 2021. Artificial intelligence based multimodality imaging: a new frontier in coronary artery disease management. *Frontiers in Cardiovascular Medicine,* 8**,** 736223.

MEDINA-LEYTE, D. J., ZEPEDA-GARCÍA, O., DOMÍNGUEZ-PÉREZ, M., GONZÁLEZ-GARRIDO, A., VILLARREAL-MOLINA, T. & JACOBO-ALBAVERA, L. 2021. Endothelial dysfunction, inflammation and coronary artery disease: potential biomarkers and promising therapeutical approaches. *International journal of molecular sciences,* 22**,** 3850.

MESHKOV, A., ERSHOVA, A., KISELEVA, A., ZOTOVA, E., SOTNIKOVA, E., PETUKHOVA, A., ZHARIKOVA, A., MALYSHEV, P., ROZHKOVA, T., BLOKHINA, A., LIMONOVA, A., RAMENSKY, V., DIVASHUK, M., KHASANOVA, Z., BUKAEVA, A., KURILOVA, O., SKIRKO, O., POKROVSKAYA, M., MIKOVA, V., SNIGIR, E., AKINSHINA, A., MITROFANOV, S., KASHTANOVA, D., MAKAROV, V., KUKHARCHUK, V., BOYTSOV,

S., YUDIN, S. & DRAPKINA, O. 2021. The LDLR, APOB, and PCSK9 Variants of Index Patients with Familial Hypercholesterolemia in Russia. *Genes,* 12.

MOSES, J. W., LEON, M. B., POPMA, J. J., FITZGERALD, P. J., HOLMES, D. R., O'SHAUGHNESSY, C., CAPUTO, R. P., KEREIAKES, D. J., WILLIAMS, D. O. & TEIRSTEIN, P. S. 2003. Sirolimus-eluting stents versus standard stents in patients with stenosis in a native coronary artery. *New England Journal of Medicine,* 349**,** 1315-1323.

MUJKIĆ, A., BARALIĆ, E., OMBAŠIĆ, A., BEĆIROVIĆ, L. S., POKVIĆ, L. G. & BADNJEVIĆ, A. Machine intelligence in biomedical data modeling, processing, and analysis. 2022 11th Mediterranean Conference on Embedded Computing (MECO), 2022. IEEE, 1-10.

MUSHENKOVA, N. V., SUMMERHILL, V. I., ZHANG, D., ROMANENKO, E. B., GRECHKO, A. V. & OREKHOV, A. N. 2020. Current advances in the diagnostic imaging of atherosclerosis: insights into the pathophysiology of vulnerable plaque. *International journal of molecular sciences,* 21**,** 2992.

NELEMANS, P. J., LEINER, T., DE VET, H. C. & VAN ENGELSHOVEN, J. M. 2000. Peripheral arterial disease: meta-analysis of the diagnostic performance of MR angiography. *Radiology,* 217**,** 105-114.

NISSEN, S. E., TUZCU, E. M., LIBBY, P., THOMPSON, P. D., GHALI, M., GARZA, D., BERMAN, L., SHI, H., BUEBENDORF, E. & TOPOL, E. J. 2004. Effect of antihypertensive agents on cardiovascular events in patients with coronary disease and normal blood pressure: the CAMELOT study: a randomized controlled trial. *Jama,* 292**,** 2217-2225.

NOVELLI, C., CASOLARI, F., ROTOLO, A., TADDEO, M. & FLORIDI, L. 2023. Taking AI risks seriously: a new assessment model for the AI Act. *AI & SOCIETY***,** 1-5.

NUHIĆ, J., SPAHIĆ, L., ĆORDIĆ, S. & KEVRIĆ, J. Comparative study on different classification techniques for ovarian cancer detection. CMBEBIH 2019: Proceedings of the International Conference on Medical and Biological Engineering, 16–18 May 2019, Banja Luka, Bosnia and Herzegovina, 2020. Springer, 511-518.

OKSER, S., PAHIKKALA, T., AIROLA, A., SALAKOSKI, T., RIPATTI, S. & AITTOKALLIO, T. 2014. Regularized machine learning in the genetic prediction of complex traits. *PLoS genetics,* 10**,** e1004754.

OLIVARES, A. L., GONZÁLEZ BALLESTER, M. A. & NOAILLY, J. 2017. Virtual exploration of early stage atherosclerosis. *Bioinformatics,* 33**,** 309-309.

OTSUKA, F., NAKANO, M., SAKAKURA, K., LADICH, E., KOLODGIE, F. & VIRMANI, R. 2013. Unique demands of the femoral anatomy and pathology and the need for unique interventions. *The Journal of Cardiovascular Surgery,* 54**,** 91-210.

PAPPALARDO, F., MUSUMECI, S. & MOTTA, S. 2008. Modeling immune system control of atherogenesis. *Bioinformatics,* 24**,** 1715-1721.

PARKER, W. A. & STOREY, R. F. 2021. Antithrombotic therapy for patients with chronic coronary syndromes. *Heart,* 107**,** 925-933.

PATRONO, C., MORAIS, J., BAIGENT, C., COLLET, J.-P., FITZGERALD, D., HALVORSEN, S., ROCCA, B., SIEGBAHN, A., STOREY, R. F. & VILAHUR, G. 2017. Antiplatelet agents for the treatment and prevention of coronary atherothrombosis. *Journal of the American College of Cardiology,* 70**,** 1760-1776.

PAYNTER, N., RIDKER, P. & CHASMAN, D. 2016. Are Genetic Tests for Atherosclerosis Ready for Routine Clinical Use? *Circulation research,* 118 4**,** 607-619.

PEACH, G., GRIFFIN, M., JONES, K., THOMPSON, M. & HINCHLIFFE, R. 2012. Diagnosis and management of peripheral arterial disease. *Bmj,* 345.

PIEL, F. B., PARKES, B. L., DABY, H., HANSELL, A. L. & ELLIOTT, P. 2018. The challenge of opt-outs from NHS data: a small-area perspective. *Journal of Public Health,* 40**,** e594-e600.

PIZZOLATO, R., HIRSCH, J. A. & ROMERO, J. M. 2014. Imaging challenges of carotid artery in-stent restenosis. *Journal of neurointerventional surgery,* 6**,** 32-41.

POBIRUCHIN, M., SULEDER, J., ZOWALLA, R. & WIESNER, M. 2017. Accuracy and adoption of wearable technology used by active citizens: a marathon event field study. *JMIR mHealth and uHealth,* 5**,** e6395.

POKVIC, L. G., SPAHIC, L. & BADNJEVIC, A. 2020. Implementation of Industry 4.0 in Transformation of Medical Device Maintenance Systems. *Handbook of Research on Integrating Industry 4.0 in Business and Manufacturing.* IGI Global.

POLAK, J. F. 2001. Carotid ultrasound. *Radiologic Clinics of North America,* 39**,** 569-589.

PRAKASH, S., BALAJI, J. N., JOSHI, A. & SURAPANENI, K. M. 2022. Ethical Conundrums in the application of artificial intelligence (AI) in healthcare—a scoping review of reviews. *Journal of Personalized Medicine,* 12**,** 1914.

PRATI, F., REGAR, E., MINTZ, G., ARBUSTINI, E., MARIO, C. D., JANG, I., AKASAKA, T., MARCO, C., GUAGLIUMI, G., GRUBE, E., OZAKI, Y., PINTO, F. & SERRUYS, P. 2010. Expert review document on methodology, terminology, and clinical applications of optical coherence tomography: physical principles, methodology of image acquisition, and clinical application for assessment of coronary arteries and atherosclerosis. *European heart journal,* 31 4**,** 401-415.

RAFIEIAN-KOPAEI, M., SETORKI, M., DOUDI, M., BARADARAN, A. & NASRI, H. 2014. Atherosclerosis: process, indicators, risk factors and new hopes. *International journal of preventive medicine,* 5**,** 927.

ROBERT, H., SCHLATTMANN, P., PASCAL, G., ANDREINI, D., PONTONE, G., ALKADHI, H., JÖRG, H., MARIO, J. G., SEBASTIAN, L., MEIJBOOM, W. B., ELKE, Z., BERNHARD, G., SCHOEPF, U., SHABESTARI, A., NØRGAARD, B., MEIJS, M., AKIRA, S., OVREHUS, K., DIEDERICHSEN, A., JENKINS, S. M., KNUUTI, J., ASHRAF, H., HALVORSEN, B. A., VLADIMIR, M.-R., ROCHITTE, C., RIXE, J., YUNG-LIANG, W., CHRISTOPH, L., NUNO, B., EUGENIO, M., SAID, G., BUECHEL, R., KONSTANTIN, N., MICKLEY, H., LIN, Y., ZHAQOI, Z., MARCUS, Y. C., HALON, D., RIEF, M., KAI, S., BEATRICE, H.-M., NIINUMA, H., MARCUS, R., SIMONE, M., JAKAMY, R., CHOW, B. J. W., KAUFMANN, P., TARDIF, J., NOMURA, C., KOFOED, K., LAISSY, J., ARBAB-ZADEH, A., KITAGAWA, K., LAHAM, R., MASAHIRO, J., HOE, J., FRANK, R., SCHOLTE, A., NARINDER, P., SWEE YAW, T., YOSHIOKA, K., RÖHLE, R., SCHUETZ, G. M., SCHUELER, S., MARIA, H. C., VIKTORIA, W., ACHENBACH, S., BUDOFF, M., LAULE, M., DAVID, E. N. & MARC, D. 2019. Diagnosis of obstructive coronary artery disease using computed tomography angiography in patients with stable chest pain depending on clinical probability and in clinically important subgroups: meta-analysis of individual patient data. *The BMJ,* 365.

ROGERS, M. A. & AIKAWA, E. 2019. Cardiovascular calcification: artificial intelligence and big data accelerate mechanistic discovery. *Nature Reviews Cardiology,* 16**,** 261-274.

SAMADY, H., ESHTEHARDI, P., MCDANIEL, M., SUO, J., DHAWAN, S., MAYNARD, C., TIMMINS, L., QUYYUMI, A. & GIDDENS, D. P. 2011. Coronary artery wall shear stress is associated with progression and transformation of atherosclerotic plaque and arterial remodeling in patients with coronary artery disease. *Circulation,* 124**,** 779-788.

SANCHEZ-MARTINEZ, S., CAMARA, O., PIELLA, G., CIKES, M., GONZÁLEZ-BALLESTER, M. Á., MIRON, M., VELLIDO, A., GÓMEZ, E., FRASER, A. G. & BIJNENS, B. 2022. Machine

learning for clinical decision-making: challenges and opportunities in cardiovascular imaging. *Frontiers in cardiovascular medicine,* 8**,** 765693.

SAVELJIC, I., NIKOLIC, D., MILOSEVIC, Z. & FILIPOVIC, N. Atherosclerotic plaque formation in the coronary arteries. CMBEBIH 2019: Proceedings of the International Conference on Medical and Biological Engineering, 16–18 May 2019, Banja Luka, Bosnia and Herzegovina, 2020. Springer, 315-319.

SCHIEFFER, B., SELLE, T., HILFIKER, A., HILFIKER-KLEINER, D., GROTE, K., TIETGE, U. J., TRAUTWEIN, C., LUCHTEFELD, M., SCHMITTKAMP, C. & HEENEMAN, S. 2004. Impact of interleukin-6 on plaque development and morphology in experimental atherosclerosis. *Circulation,* 110**,** 3493-3500.

SHAO, C., WANG, J., TIAN, J. & TANG, Y.-D. 2020. Coronary artery disease: from mechanism to clinical practice. *Coronary Artery Disease: Therapeutics and Drug Discovery***,** 1-36.

SHEARER, E., CHO, M. & MAGNUS, D. 2021. Regulatory, social, ethical, and legal issues of artificial intelligence in medicine. *Artificial Intelligence in Medicine.* Elsevier.

SHIBUTANI, H., FUJII, K., UEDA, D., KAWAKAMI, R., IMANAKA, T., KAWAI, K., MATSUMURA, K., HASHIMOTO, K., YAMAMOTO, A. & HAO, H. 2021. Automated classification of coronary atherosclerotic plaque in optical frequency domain imaging based on deep learning. *Atherosclerosis,* 328**,** 100-105.

SIGNORELLI, S. S., MARINO, E., SCUTO, S. & DI RAIMONDO, D. 2020. Pathophysiology of Peripheral Arterial Disease (PAD): a review on oxidative disorders. *International Journal of Molecular Sciences,* 21**,** 4393.

SILVERTHORN, D. U. 2020. Principles of Epithelial Transport. *Basic Epithelial Ion Transport Principles and Function: Ion Channels and Transporters of Epithelia in Health and Disease-Vol. 1***,** 53-82.

SLOVUT, D. P., DEAN, S. M., JAFF, M. R. & SCHNEIDER, P. A. 2012. Comprehensive review in vascular and endovascular medicine.

SONKA, M., STOLPEN, A., LIANG, W. & STEFANCIK, R. M. 2000. Vascular imaging and analysis. *Handbook of Medical Imaging: Medical Image Processing and Analysis,* 2**,** 809-914.

SPAHIĆ, L., BENOLIĆ, L., QAMAR, S. U. R., SIMIC, V., MILIČEVIĆ, B., MILOŠEVIĆ, M., GEROSKI, T. & FILIPOVIĆ, N. Prediction of Coronary Plaque Progression Using Data Mining and Artificial Neural Networks. Conference on Information Technology and its Applications, 2023. Springer, 3-13.

SPAHIĆ, L. & ĆORDIĆ, S. Prostate tissue classification based on prostate-specific antigen levels and mitochondrial DNA copy number using artificial neural network. CMBEBIH 2019: Proceedings of the International Conference on Medical and Biological Engineering, 16– 18 May 2019, Banja Luka, Bosnia and Herzegovina, 2020. Springer, 649-654.

SPAHIĆ, L., KURTA, E., ĆORDIĆ, S., BEĆIROVIĆ, M., GURBETA, L., KOVACEVIC, Z., IZETBEGOVIC, S. & BADNJEVIC, A. Machine learning techniques for performance prediction of medical devices: infant incubators. CMBEBIH 2019: Proceedings of the International Conference on Medical and Biological Engineering, 16–18 May 2019, Banja Luka, Bosnia and Herzegovina, 2020. Springer, 483-490.

STOKES, K., CASTALDO, R., FRANZESE, M., SALVATORE, M., FICO, G., POKVIC, L. G., BADNJEVIC, A. & PECCHIA, L. 2021. A machine learning model for supporting symptom-based referral and diagnosis of bronchitis and pneumonia in limited resource settings. *Biocybernetics and biomedical engineering,* 41**,** 1288-1302.

SU, C., LU, Y., WANG, Z., GUO, J., HOU, Y., WANG, X., QIN, Z., GAO, J., SUN, Z. & DAI, Y. 2023. Atherosclerosis: the involvement of immunity, cytokines and cells in pathogenesis, and potential novel therapeutics. *Aging and Disease,* 14**,** 1214.

TEPE, G., LAIRD, J., SCHNEIDER, P., BRODMANN, M., KRISHNAN, P., MICARI, A., METZGER, C., SCHEINERT, D., ZELLER, T. & COHEN, D. J. 2015. Drug-coated balloon versus standard percutaneous transluminal angioplasty for the treatment of superficial femoral and popliteal peripheral artery disease: 12-month results from the IN. PACT SFA randomized trial. *Circulation,* 131**,** 495-502.

TOMASEVIC, S., DJUKIC, T., ANIC, M., ARSIC, B., SAVELJIC, I., GAKOVIC, B., KONCAR, I. & FILIPOVIC, N. Simulation of Atherosclerosis Progression Within Patient-Specific Carotid Artery. Conference on Information Technology and its Applications, 2024. Springer, 176-184.

TOMEY, M. I., KINI, A. S. & SHARMA, S. K. 2014. Current status of rotational atherectomy. *JACC: Cardiovascular Interventions,* 7**,** 345-353.

TOTH, P. 2005. Cardiology patient page. The "good cholesterol": high-density lipoprotein. *Circulation,* 111 5.

TSOMPOU, P. I., POTSIKA, V. T., PETROVIC, N., PEZOULAS, V. C., SIOGKAS, P. K., TSAKANIKAS, V. D., PLEOURAS, D. S., PAPAFAKLIS, M., NIKOPOULOS, S. & SAKELLARIOS, A. I. Computational modeling of atherosclerotic plaque progression through an efficient 3D agent-based modeling approach. 2022 IEEE-EMBS International Conference on Biomedical and Health Informatics (BHI), 2022. IEEE, 01-04.

TSUTSUI, R. S., SAMMOUR, Y., KALRA, A., REED, G., KRISHNASWAMY, A., ELLIS, S., NAIR, R., KHATRI, J., KAPADIA, S. & PURI, R. 2021. Excimer laser atherectomy in percutaneous coronary intervention: a contemporary review. *Cardiovascular Revascularization Medicine,* 25**,** 75-85.

UGURLU, N., GERCEKER, S., YÜLEK, F., UGURLU, B., SARI, C., BARAN, P. & ÇAGIL, N. 2013. The levels of the circulating cellular adhesion molecules ICAM-1, VCAM-1 and endothelin-1 and the flow-mediated vasodilatation values in patients with type 1 diabetes mellitus with early-stage diabetic retinopathy. *Internal Medicine,* 52**,** 2173-2178.

UNVERDORBEN, M., VALLBRACHT, C., CREMERS, B., HEUER, H., HENGSTENBERG, C., MAIKOWSKI, C., WERNER, G. S., ANTONI, D., KLEBER, F. X. & BOCKSCH, W. 2009. Paclitaxel-coated balloon catheter versus paclitaxel-coated stent for the treatment of coronary in-stent restenosis. *Circulation,* 119**,** 2986-2994.

USOVA, E. I., ALIEVA, A. S., YAKOVLEV, A. N., ALIEVA, M. S., PROKHORIKHIN, A. A., KONRADI, A. O., SHLYAKHTO, E. V., MAGNI, P., CATAPANO, A. L. & BARAGETTI, A. 2021. Integrative analysis of multi-omics and genetic approaches—a new level in atherosclerotic cardiovascular risk prediction. *Biomolecules,* 11**,** 1597.

VAN ROSENDAEL, A. R., MALIAKAL, G., KOLLI, K. K., BEECY, A., AL'AREF, S. J., DWIVEDI, A., SINGH, G., PANDAY, M., KUMAR, A. & MA, X. 2018. Maximization of the usage of coronary CTA derived plaque information using a machine learning based algorithm to improve risk stratification; insights from the CONFIRM registry. *Journal of cardiovascular computed tomography,* 12**,** 204-209.

WANG, X. & ZHU, H. 2024. Artificial Intelligence in Image-based Cardiovascular Disease Analysis: A Comprehensive Survey and Future Outlook. *arXiv preprint arXiv:2402.03394*.

WESTLAND, H., JAARSMA, T., RIEGEL, B., IOVINO, P., OSOKPO, O., MICHAEL, A. S. & ELISE, C. T. 2020. Self-care interventions in patients with coronary artery disease: room for improvement. *European Heart Journal*.

YUSUF, S., JOSEPH, P., RANGARAJAN, S., ISLAM, S., MENTE, A., HYSTAD, P., BRAUER, M., KUTTY, V. R., GUPTA, R. & WIELGOSZ, A. 2020. Modifiable risk factors, cardiovascular disease, and mortality in 155 722 individuals from 21 high-income, middle-income, and low-income countries (PURE): a prospective cohort study. *The Lancet,* 395**,** 795-808.

ZAHEDMANESH, H. & LALLY, C. 2012. A multiscale mechanobiological modelling framework using agent-based models and finite element analysis: application to vascular tissue engineering. *Biomechanics and modeling in mechanobiology,* 11**,** 363-377.

ZHANG, J., XIONG, Y. & MIN, S. 2019. A new hybrid filter/wrapper algorithm for feature selection in classification. *Analytica chimica acta,* 1080**,** 43-54.

Online resources:

Scientist Cindy - Introduction to the circulatory system (2024), Available at: https://www.scientistcindy.com/intro-to-the-circulatory-system.html (Accessed: 10 September 2024.

Radiopaedia - Innervation of the heart (2023), Available at: https://radiopaedia.org/articles/innervation-of-the-heart (Accessed: 10 September 2024)

Dr. Anil Scharma Cardiosurgeon - Coronary artery bypass surgery (2024), Available at: http://dranilsharmacardiacsurgeon.com/Coronaryarterybypasssurgery.html (Accessed: 10 September 2024)

Biography

Dr. Lemana Spahić received her bachelor's degree in Genetics and Bioengineering from the Faculty of Engineering and Natural Sciences, International Burch University, Sarajevo, Bosnia and Herzegovina in 2018, master's degree at the same department in 2020 and gained the title of doctor of philosophy in 2024. As of 2017 until today she had worked as a research trainee at medical device inspection laboratory Verlab, head of laboratory at CH Labs Tuzla, senior teaching assistant at International Burch University and senior expert associate at Research Institute Verlab for Biomedical Engineering, Medical Devices and Artificial Intelligence. She had participated in more than 20 international scientific conferences and published over 80 publications including journal papers, conference papers and book chapters. She had won the best student paper award at CMBEBIH 2019 and the best poster award at IMEKO TC4 2023. Throughout her engagement she has worked as part of the team on implementation of several scientific research projects. Her main fields of interest include biomedical engineering, clinical engineering, medical devices, and artificial intelligence applications in medicine. She has been a part of the local organizing committee of CMBEBIH since 2017 and has established a significant body of experience in organizing international scientific events. She enrolled in a double PhD at the University of Kragujevac, Faculty of Engineering, in the field of applied AI and computational modeling in medicine. Currently she is working as an Early Stage Researcher on Marie Skłodowska-Curie ITN project DECODE (GA No 956470) at BioIRC in Kragujevac, Serbia. She is affiliated with the Society for Medical and Biological Engineering in Bosnia and Herzegovina (DMBIUBIH) that is the country representative in IFMBE (International Federation for Medical and Biological Engineering) as the Secretary General and at IEEE (Institute of Electrical and Electronics Engineers) Standards Association as the Secretary General of 2 working groups for standardization of vocabulary for post-market surveillance of medical devices and post-market surveillance methodology of defibrillators. Her current research interests are focused on application of artificial intelligence on biomedical data analysis with emphasis on diagnostics.

Form 1

AUTHOR'S STATEMENT ON THE ORIGINALITY OF THE DOCTORAL DISSERTATION

I here by declare that the doctoral dissertation entitled:

MULTISCALE MODEL FOR THROMBOSIS / ATHEROSCLEROTIC PLAQUE FORMATION AND PROGRESSION

represents *an original author's work* created as a result of *own research work*.

With this Declaration, I also confirm:

- that I am *the sole author* of the aforementioned doctoral dissertation,
- that *I have not violated* the copyright or other intellectual property rights of other persons in the aforementioned doctoral dissertation,

In Kragujevac, 21.11.2024.,

Lemana Spahić

author's signature

Form 2

AUTHOR'S STATEMENT REGARDING THE CONSISTENCY OF THE PRINTED AND ELECTRONIC VERSIONS OF THE DOCTORAL DISSERTATION

I here by declare that the printed and electronic versions of the doctoral dissertation entitled:

MULTISCALE MODEL FOR THROMBOSIS / ATHEROSCLEROTIC PLAQUE FORMATION AND PROGRESSION

are identical.

In Kragujevac, 21.11.2024.,

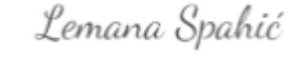

author’s signature

Form 3

AUTHOR'S STATEMENT ON THE USE OF THE DOCTORAL DISSERTATION

I, Lemana Spahic,

[X] permit

[ ] do not permit

the University Library in Kragujevac to create two permanent identical copies in electronic form of the doctoral dissertation entitled:

MULTISCALE MODEL FOR THROMBOSIS / ATHEROSCLEROTIC PLAQUE FORMATION AND PROGRESSION

in its entirety, as well as to create one copy of the duplicated doctoral dissertation permanently available to the public through the digital repository of the University of Kragujevac and the central repository of the competent ministry, so that public can make permanent copies in electronic form of the mentioned doctoral dissertation *by downloading* it.

With this Statement I also

[X] permit

[ ] do not permit[1]

[1] If the author decides not to permit public use of the doctoral dissertation available under the conditions set by one of the Creative Commons licenses, this will not prevent the public from using the mentioned doctoral dissertation in accordance with the provisions of the Law on Copyright and Related Rights.

public members to use the permitted doctoral dissertation under the one of the following Creative Commons licenses:

1) The Authorship

2) The Authorship – to share under the same conditions

3) The Authorship – without rewriting

4) The Authorship - non-commercial

5) The Authorship - non-commercial - to share under the same conditions

6) The Authorship - non-commercial - without rewriting [2]

In Kragujevac, 21.11.2024.

Lemana Spahić

author's signature

[2] We kindly request the authors who have chosen to permit public members to use the doctoral dissertation available under the conditions set by one of the Creative Commons licenses to select one of the licenses offered. The specific details of the mentioned licenses can be found at: http://creativecommons.org.rs/